DOCTORAL DISSERTATION SERIES

TITLE The Analysis of Hipped Plate Structures Considering the Relative Displacements of the Joints

AUTHOR Ibrahim Abdel Samie Gaafar

UNIVERSITY of Michigan DATE 1949

DEGREE Sc. D. PUBLICATION NO. 1256

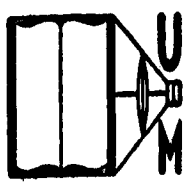

UNIVERSITY MICROFILMS
ANN ARBOR · MICHIGAN

THE ANALYSIS OF HIGH PLATE STRUCTURES CONSIDERING THE RELATIVE DISPLACEMENTS OF THE JOINTS

by

Ibrahim A. Bedair

A dissertation submitted in partial fulfillment of the requirements for the degree of Doctor of Science in the University of Michigan.

Committee in Charge:

Professor L. C. Maugh, Chairman
Associate Professor J. L. Ali
Assistant Professor R.C.F. Bartels
Associate Professor H. M. Hansen
Professor R. H. Sherlock

Ann Arbor, Michigan

February, 1949

ACKNOWLEDGMENTS

The writer wishes to express his appreciation to Professor L. C. Maugh for his valuable advice and suggestions in regard to the conduct of the work, and the time he has kindly given for consultation.

The writer also wishes to express his appreciation to members of his special committee, Professors R. H. Sherlock, G. L. Alt, H. M. Hansen and R. C. E. Bartels.

THE ANALYSIS OF HIPPED PLATE STRUCTURES

TABLE OF CONTENTS

CHAPTER I

CHAPTER II

CHAPTER III

CHAPTER IV

APPENDIX I

APPENDIX II

BEAM ACTION THEORY

APPENDIX III

THE ANALYSIS OF HIPPED PLATE STRUCTURES

CHAPTER I

INTRODUCTION

1. SYNOPSIS:

Both theoretical and experimental investigations on the structural action of hipped plate structures are presented in this dissertation. Tests on a 1/40 scale aluminum model of a hipped plate roof were conducted to check the assumptions and the analytical results. Investigations showed that the change in the shape of the cross-section of such structures under loading, which is usually neglected in the present theory of design, affects the results materially. Discrepancies in the results of solutions that neglected the change in shape of the cross-section of 100% and even up to 200% and more for some cases were obtained.

The more exact theory for this problem as given by E. Gruber is mathematically complicated which may explain the reason for the present adoption of the approximate theory as established by Ehlers and Craemer. However, a more exact, but still practicable method of analysis that considers the change in shape of the cross-section is given here. The results of the different methods are compared with each other and checked against the experimental results.

2. HISTORICAL REVIEW:

A hipped plate structure is a monolithic space structure that is composed of straight plate or slab elements that intersect at an angle as shown in Fig. 1.1. No beams or girders need be used as the plate elements are connected rigidly together to form a structural unit that has some of the characteristics of a shell type structure. The ends of the plate elements are supported by diaphragms and columns. These structures, which carry the loads applied to the plates by a combined slab and beam action, are usually built of reinforced concrete and are particularly applicable to roofs, bins, and bunkers.

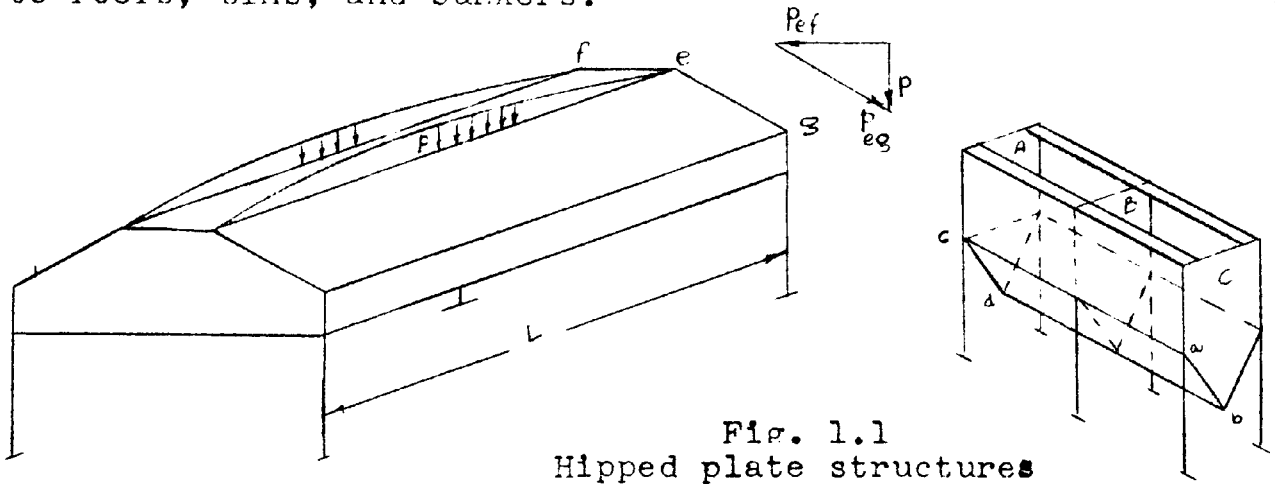

Fig. 1.1
Hipped plate structures

The principle of hipped plate construction was first developed by G. Ehlers in Germany in 1924, who wrote the first technical paper[1] on this subject in 1930. In his method of analysis he considered the different plates a b c d, Fig. 1.1, as beams supported at the cross and end

diaphragms A, B, C. Along the longitudinal edges the plates were assumed as being connected by nonsliding hinged joints. These joints were considered capable of transferring only edge shears T between the contiguous plate elements. Such connections neglected entirely the connecting moments transmitted between the plates due to the rigidity of the joints. To simplify the solution the uniform loads on the plates were transformed to line loads p acting at the joints. These p loads were resolved into two components p_{ef} and p_{fg} parallel to the two adjacent plates as shown in Fig. 1.1. The plates, acting as beams between the diaphragms, carried the loads p. At the same time, edge shear stresses T are created along the edges to maintain equal longitudinal strains along the common edges. This strain condition at each joint was used to determine the magnitude and distribution of the shear stresses T along the edges.

In 1932, however, E. Gruber presented a paper [3] to the International Association for Bridge and Structural Engineering, in which he considered the effect of the rigidity of the joints, the connecting moments acting along the common edges of the plates, and the effect of the relative displacements between the joints. As a first approximation, the hipped roof was assumed to be hinged along the joints. Then, by using this assumed hinged structure as a basic system, he developed his exact solution in the form of simultaneous

differential equations of the fourth order, which could be solved by rapidly converging series. For a hipped roof of r + 1 plates, i.e. r joints, the number of the equations encountered in the solution is 7r + 2. For a roof of five plates this will mean 30 equations. As this solution is complicated even when solved by the use of trigonometric series, it will not be given here. In his solution Gruber showed that the maximum longitudinal stresses on a cross-section and the maximum deflections for a roof with hinged plates were about twice as great as for the rigidly connected plates. He consequently concluded that the influence of the rigid connections ought not to be neglected, as had been the usual practice.

Later the theory was further developed and expanded in many respects by Craemer, Gruber, Ohlig, and others. The European literature on the subject, which is mostly in German, is fairly extensive. All the treatments of the theory by the Germans are developed from elasticity equations in the form of simultaneous algebraic and differential equations which are mathematically involved. With the exception of the paper[3] by E. Gruber, all writers have made the same simplifying assumptions of neglecting the effect of the change of the shape of the cross-section of a hipped structure under loading although some considered the rigidity of the joints and the connecting moments along these joints. In other words,

the effect of the relative deflections of the joints was not considered. The above assumptions which consider the rigidity of the joints but no change in cross-section form the basis of the present simplified theory as established by Craemer and Ehlers.[10]

In January 1947, G. Winter and M. Pei of Cornell University published a paper[12] on Hipped Plate Construction in the Journal of the American Concrete Institute in which they transformed the algebraic solution into a stress distribution method, which has the advantage of numerical simplicity over the other procedures. However, they also made the same simplifying assumption as Craemer and Ehlers, of neglecting the effect of the relative deflection of the joints. In their paper Winter and Pei state that the spreading, which may occur in such structures, and the effect of the relative displacements of the joints is neglegible although they provide no positive proof for this statement.

In a dissertation[13] submitted to the Cornell University in 1948, M. Pei presented a method of analysis considering joint displacements. The method requires the solution of $6n + 1$ simultaneous algebraic equations where n is the number of plates. For a roof of 5 plates as shown in Fig. 1.1, the number of equations is $6 \times 5 + 1 = 31$ equations.

None of the mathematical investigations mentioned above gave any experimental evidence to substantiate the assumptions and analytical procedures that were used. It

appears that no previous experimental evidence from either actual structures or small scale models has been obtained to support the theoretical analysis.

In the development of the analysis which is proposed in this thesis it was found necessary to depend upon a study of the deformations in small scale models to provide information upon which correct assumptions could be made. It will be shown in the following chapters that the translation of the edges of the plate elements materially affects the magnitude and distribution of the internal stresses.

CHAPTER II

PRESENT ANALYTICAL METHOD

1. NOTATIONS:

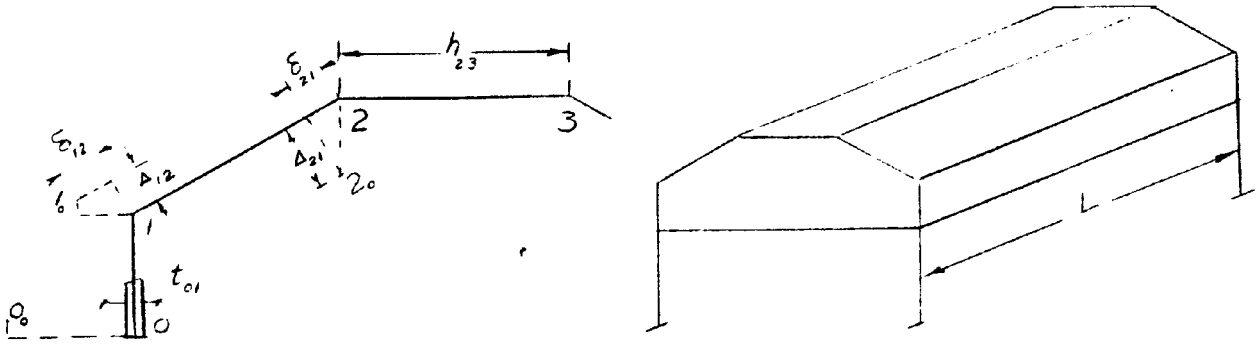

Fig. 2.1

0, 1, 2, ... n, .. = Subscripts used to denote edges and plate elements.

h_{12} = Width of plate 12; or distance between joints 1 and 2 measured along the center line of cross-section of plate.

L = Span of roof between end diaphragms.

t_{12} = Thickness of plate 12.

$A_{12} = h_{12} \times t_{12}$ = Cross-sectional area of plate 12.

$S_{12} = \frac{th^2}{6}$ = Section modulus of plate 12, considered acting as a beam.

Δ_{12} = The component of the displacement of edge 1 perpendicular to plate 12.

Δ_{21} = The component of the displacement of edge 2 perpendicular to plate 12.

δ_{12} = The component of the displacement of edge 1 in the plane of plate 12.

$\delta_{21} = \delta_{12}$

Q_{12} = Shearing force per unit length, acting from joint 1 on plate 12 in the direction parallel to Δ_{12}.

T_1 = Shear stresses per unit length parallel to edge 1 acting from joint 1 along the edges of the adjacent plates.

$N = \int_0^x T\,dx$

Other notations are given where they are used.

N.B.: No particular sign convention was found necessary for the displacements, the forces, or the stresses. Any assumed displacements may be considered positive. A negative value in the result means an opposite sense of displacement to the one first assumed. Consistency in working out the solution, rather than a specified sign convention, is essential.

2. GEOMETRICAL RELATIONS BETWEEN EDGE DISPLACEMENTS IN HIPPED PLATE STRUCTURES

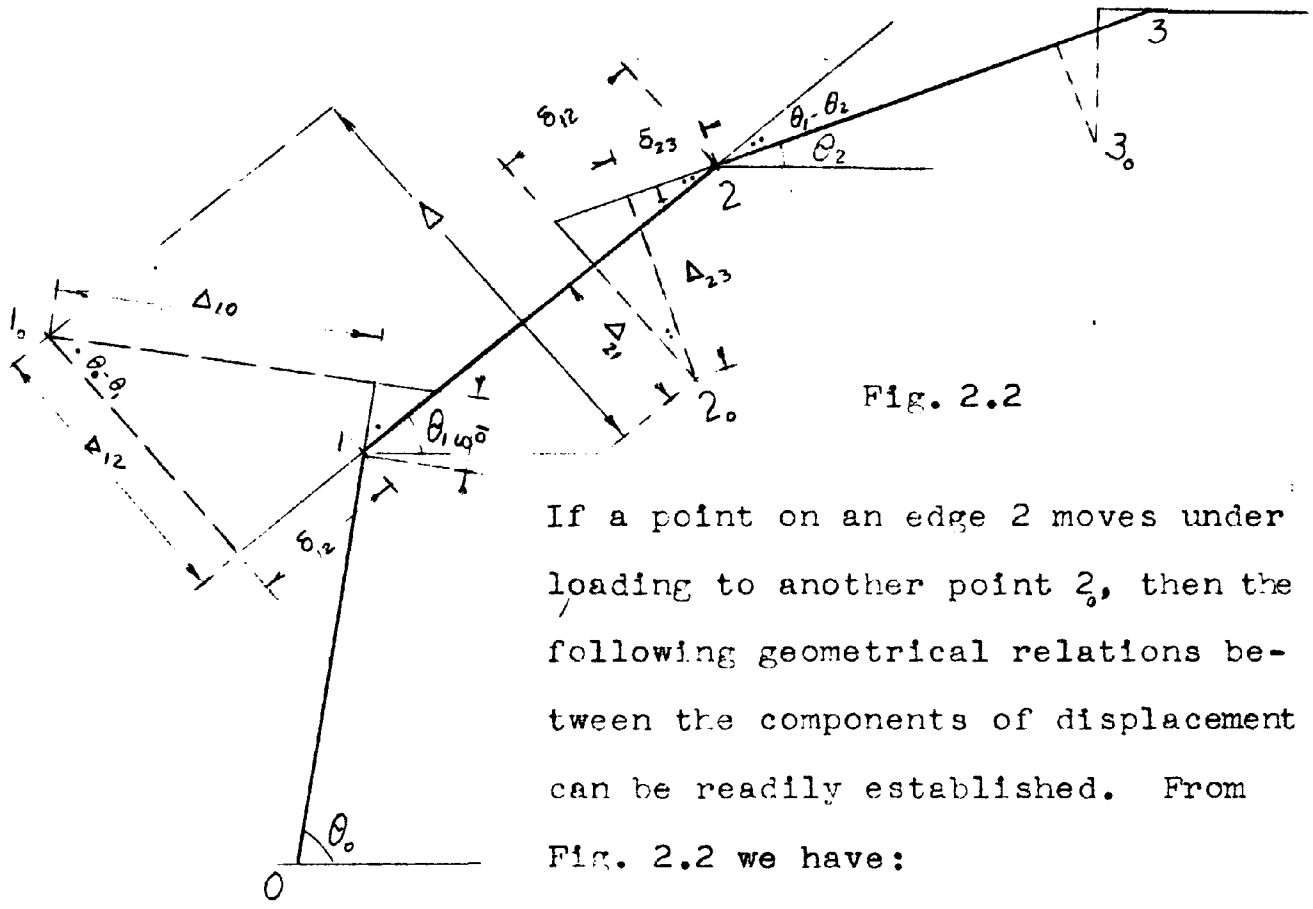

Fig. 2.2

If a point on an edge 2 moves under loading to another point 2_o, then the following geometrical relations between the components of displacement can be readily established. From Fig. 2.2 we have:

$$\Delta_{23} = \left[\frac{\delta_{12}}{\cos(\theta_1-\theta_2)} - \delta_{23}\right] \times \text{Cot}\ (\theta_1-\theta_2) \quad . \quad . \quad . \quad . \quad (1)$$

$$\Delta_{21} = \left[\delta_{12} - \frac{\delta_{23}}{\cos(\theta_1-\theta_2)}\right] \times \text{Cot}\ (\theta_1-\theta_2) \quad . \quad . \quad . \quad . \quad (2)$$

Similarly:

$$\Delta_{12} = \left[\frac{\delta_{01}}{\cos(\theta_o-\theta_1)} + \delta_{12}\right] \times \text{Cot}\ (\theta_o-\theta_1) \quad . \quad . \quad . \quad . \quad (3)$$

and so on.

Adding (2) and (3) we get the relative displacement between edges 1 and 2:

$$\Delta = \Delta_{21} + \Delta_{12} = c_1 \cdot \delta_{12} + c_2 \cdot \delta_{23} + c_3 \cdot \delta_{01} \quad . \quad . \quad (4)$$

where c_1, c_2 and c_3 are constants.

Each of equations (1) and (2) for joints 1 and 2 gives the component Δ of the joint displacement in terms of the two other δ components of the same joint. Two similar equations can be written for every joint. Equation (4) gives the magnitude of the relative displacement between the two joints 1 and 2. Such an equation can be easily obtained for each intermediate plate in the roof. For a roof of 5 plates three such linear algebraic equations can be written. For a roof of 5 plates with symmetrical loading the number of equations can be reduced to one. As mentioned before no particular sign convention for the displacements is necessary but rather only consistency in the successive steps of the analytical solution is desirable. A negative sign of Δ in the final result means an opposite sense to the one first assumed.

3. BASIS OF THE ANALYTICAL APPROACH:

The following limitations that governed the application of the exact solution given by E. Gruber[3] will be discussed and used in the theoretical investigation:

(1) All plates are of rectangular shape.

(2) The length of each plate is more than twice its width.

(3) The structure is monolithically built. All joints are rigid.

(4) Each plate is of uniform thickness.

(5) The material is homogeneous and elastic.

(6) In any plate, plane sections remain plane after deformation.

Ad. (1) E. Gruber gave a theory for plates of near rectangular shapes.[7] The analysis is much more difficult as it requires solutions of simultaneous, linear, nonhomogeneous differential equations of the second order with variable coefficients.

Ad. (2) This limitation makes it possible to treat the plates as one-way slabs, to assume linear distribution of bending stresses, and to neglect the effect of torsional rigidity. Experimental investigations appear to justify this assumption. The resistance to torsion of the lateral beams was taken into account by Ohlig.[9]

Ad. (4) For plates with their thicknesses varying along their lengths, (ref. 8).

Ad. (5) Reinforced concrete is not a homogeneous material. Present statical analysis of reinforced concrete structures assume homogeneity of material and it therefore seems reasonable to make the same assumption here. As to elasticity, it is debatable whether concrete could be treated as an elastic material. This question will be left for investigators on reinforced concrete to decide. The theoretical and experimental investigations given here are applicable to an elastic material. As for application to

reinforced concrete this thesis provides some light on the subject and it is recommended that further experimental and analytical studies be made on reinforced concrete models.

Ad. (6) Experimental investigations given in this thesis show that this assumption is justified. It should be noted that plane cross-sections of the entire structure do not necessarily remain plane after deformation.

4. EQUILIBRIUM CONDITIONS FOR JOINTS AND PLATE ELEMENTS:

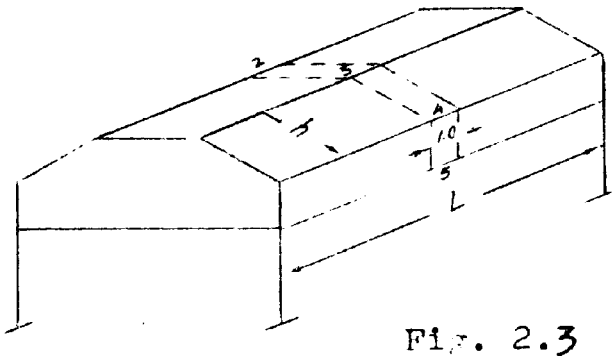

Fig. 2.3

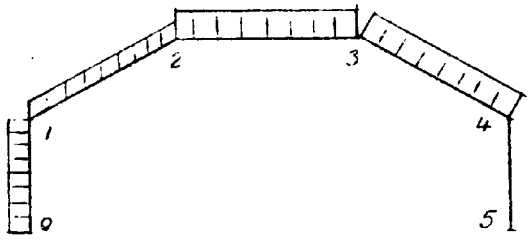

Fig. 2.4

(a) Equilibrium of the joints:

Consider a hipped plate roof as shown in Fig. 2.3, with a span L larger than twice the width h of any plate. Loads on this roof (dead load, snow, wind, etc.) will be assumed arbitrarily, as shown in Fig. 2.4. Since the width h, of any plate, is small compared to its length L, each individual plate, will carry the applied load w, transverse to

the joints. This fact also enables us to ignore the effect of torsional action that takes place in each plate. We can then treat the plates as a one-way slab. Consider any transverse strip (0, 1, 2 ..), of the roof of one unit width, that is some distance away from the supporting end diaphragms. Cut out any joint, j_4 say, from this strip in the manner shown in Figs. 2.5 and 2.6, by two planes R and S perpendicular to the two adjacent plates respectively.

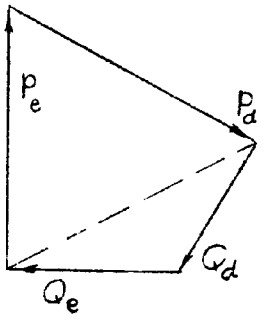

Fig. 2.7

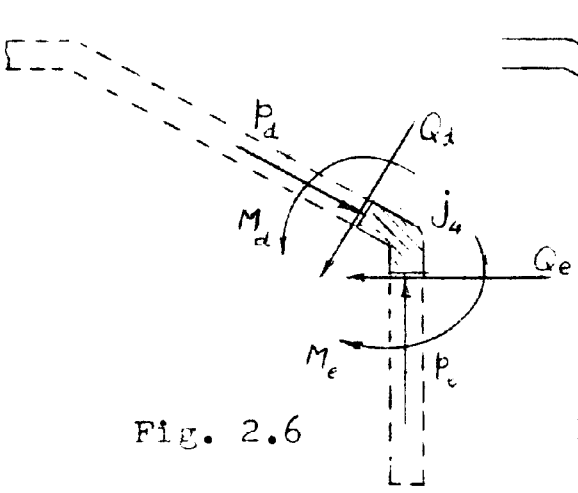

Fig. 2.6

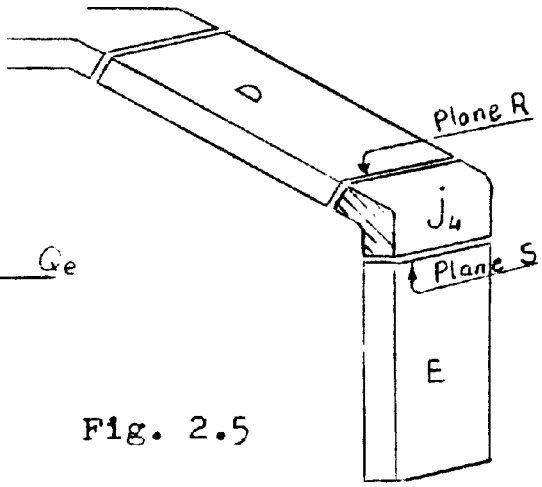

Fig. 2.5

If we now consider the forces acting on this portion of the joint, we find in a vertical cross-sectional plane through the middle of the joint element three kinds of forces acting, namely:

(1) Two forces Q_d and Q_e perpendicular to the two adjacent plates D and E respectively,

(2) Two forces p_d and p_e perpendicular to the Q forces, and

(3) Two bending moments M_d and M_e between the joint and each adjacent plate.

In addition to these forces, shear stresses and torsional stresses will be acting on the vertical sides of the joint element. As the joint element is chosen smaller and smaller by making the planes R and S approach each other, the resultant of these latter stresses becomes smaller and smaller approaching zero as a limit, in which case, M_d and M_e become equal, and the forces Q_d, p_d, Q_e and p_e become concurrent. If we now consider the equilibrium of the joint element in the plane of these forces, and draw the force vectors representing the four mentioned forces, Fig. 2.7, it is evident that the resultant of Q_d and Q_e is equal and opposite to that of p_d and p_e. The forces Q and M represent the action, on the joint, of the adjacent plates, acting as a continuous slab, while the forces p represent the action, on the joint, of the adjacent plates acting as beams between the end diaphragms.

In planes R and S between the joint and each adjacent plate, there also exist shearing stresses T, and on the two transverse planes on both sides of the joint, normal stresses f. However, T and f do not enter into the equilibrium of the forces acting on the joint in a transverse plane as they are perpendicular to that plane.

(b) Equilibrium of a plate element:

Fig. 2.8 shows the forces acting on a plate element. In the figure N represents the resultant of the edge shear

stresses, T acting on the edge of the element at joint n. Otherwise the figure is self-explanatory. The edge shear force acting on the plate in a length x is given by:

$$N = \int_{o}^{x} T.\, dx \qquad \ldots\ldots (1)$$

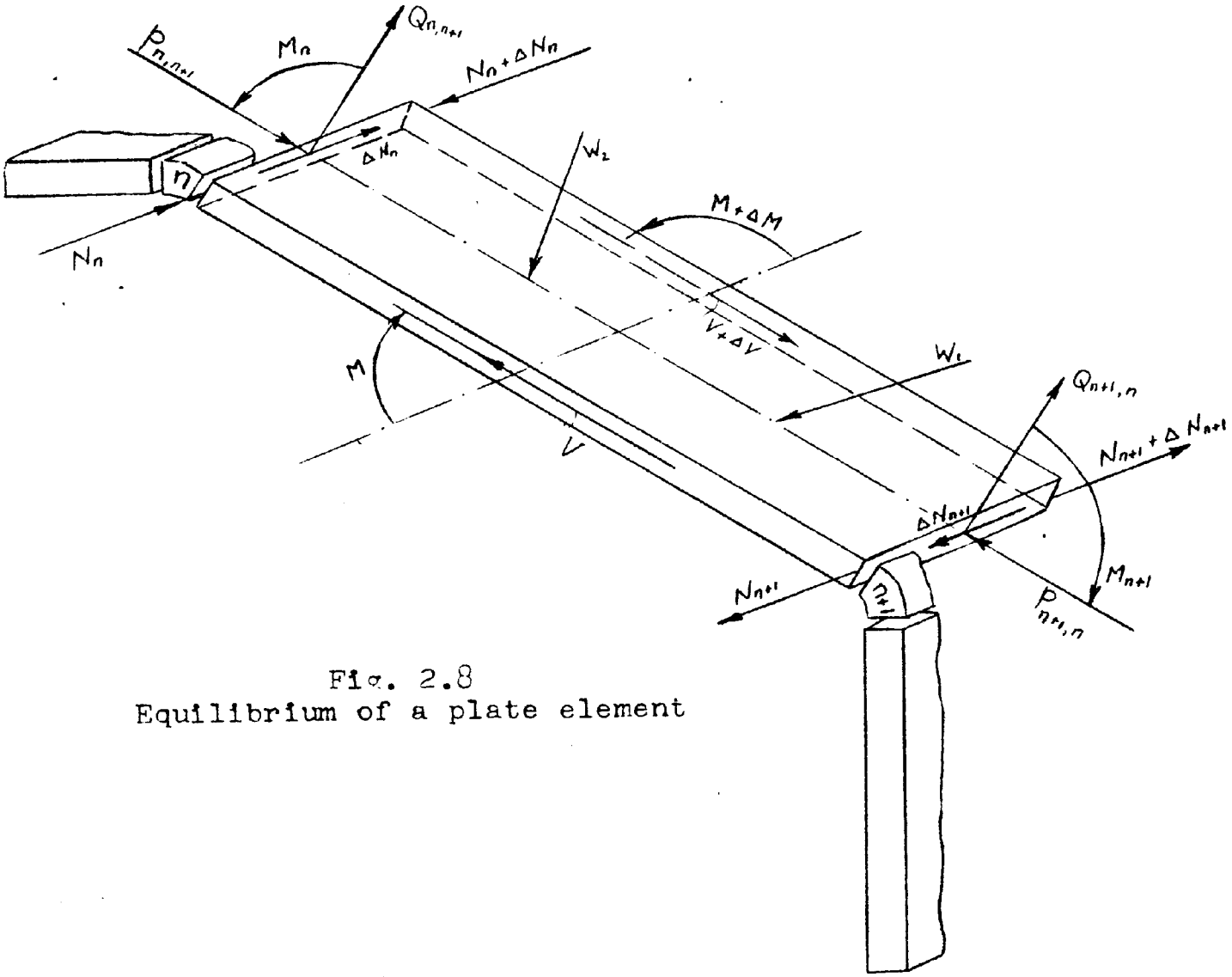

Fig. 2.8
Equilibrium of a plate element

Effect of the edge shear stresses T on shear forces V acting in a transverse vertical plane:

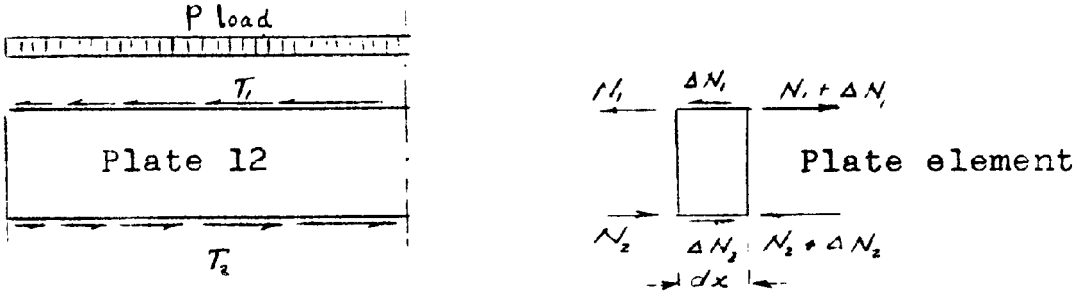

Fig. 2.9

The edge shear stresses T_1 and T_2 on a plate 12 need not be the same. If the edge shear force acting on a length dx of plate is denoted by $\Delta N = T.\ dx$ then the edge shears T will have a resultant on both sides of the element dx of

$$N_1 = \int_0^x T_1\ dx \qquad \ldots\ (1)$$

These forces will produce normal stresses on both vertical sections of the plate element. Since these stresses, acting on opposite vertical sections of the plate element, are not necessarily equal, this will give rise to horizontal and vertical shear stresses acting on the element. However, the resultant of the vertical shear stresses on both vertical sections of the plate element must add up to zero which can be readily seen when the effect of the edge shears T on the element is considered separately. For the plate element shown in Fig. 2.9, if we take moment of the forces shown about any point in the plane of the forces, then it can be seen that the resultants of the shear stresses on each of the

vertical sides must equal zero. From this discussion it can be noted that the shear forces V acting on a vertical side of a plate element, Fig. 2.8, is due only to the p loads since the effect of the edge shears T is zero.

5. STRESS DISTRIBUTION METHOD:

A numerical solution that is based on successive approximations was developed by Winter and Pei[12] as a means of solving the equations that arise in the Craemer and Ehlers method of analysis.[10] This solution is applied in a manner that is almost identical to the Moment Distribution Method that was developed by Professor Cross. In the latter method, an imaginary "locking" or restraint is applied at each support. The moment developed in the restraint is later released and distributed. In the distribution method for Hipped Plate Structures, a "non-shear" joint is first assumed between each two adjacent plates, and edge shear forces N are then gradually added so as to provide the final actual condition of continuity.

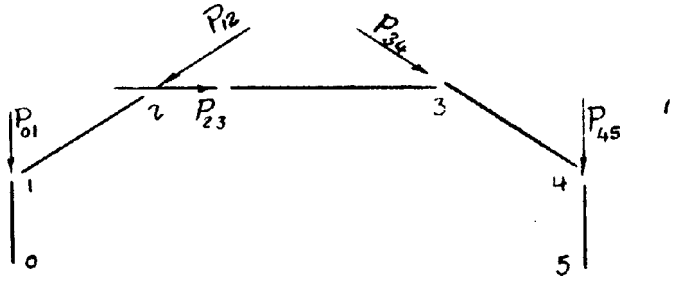

Fig. 2.10 P-forces

Let us assume that the line load $P_{n,n+1}$ acting in the plane of the plate n,n+1, represent the resultant of the p forces transmitted from the joints n and n+1 to the plate n,n+1, (Fig. 2.10). The plate n,n+1 will carry the load $P_{n,n+1}$ as a beam between the end diaphragms, Fig. 2.11.

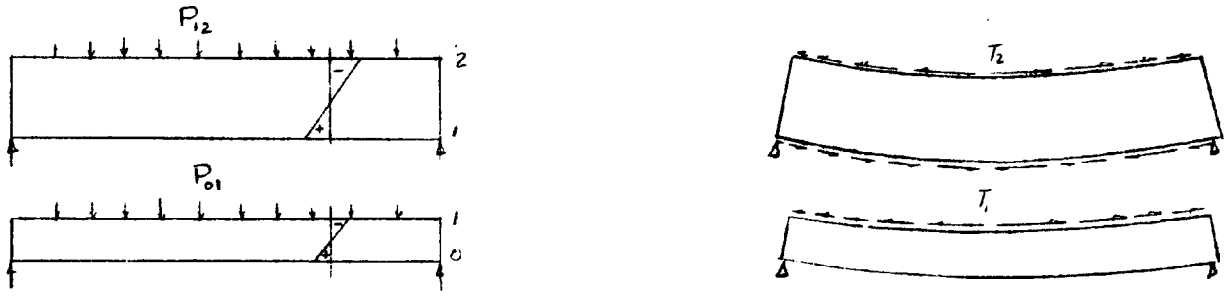

Fig. 2.11
Monolithic action of plates

If the plates were not joined along their common edges they would act as simple beams loaded with their respective P loads. In such a case the normal stresses due to bending in plates 01, 12,.. would be as shown in Fig. 2.11 since with such separate action the plates would deform independently. However, the monolithic action existing at the joints requires equal stress and strain conditions along the common edges. Hence, each of the plates, in addition to its plate load, P, is acted upon along its two edges, by the shear forces T. Although the distribution of these shear forces, at this stage, is not known, it is evident that at any particular section, x, they add up to normal forces N_t and N_b, at top and bottom edge, of magnitude

$$N = \int_0^x T.\, dx \qquad . \; . \; . \; . \; (1)$$

Any section, therefore, will be acted upon by two longitudinal edge-forces, N_t and N_b, in addition to the bending moment M caused by the plate loads P. Since at all points along a common edge, the shear forces T are equal and opposite to each other for the two adjoining plates, from equation (1) the resulting normal forces N are also equal and opposite to each other, in both plates, at all points along the edge. Let us assume that we know the magnitude and distribution of the P-loads acting on each plate, and that each plate acts independently and carries its load as an ordinary beam does. The bending moment is obtained from elementary structural theory. The fiber stresses at the edges corresponding to this bending moment are obtained. In general, $f_{n,n-1}$ and $f_{n,n+1}$ found this way are not equal. Consequently, longitudinal sliding will occur along the joints. To eliminate this sliding, a couple of equal and opposite normal forces is introduced at the joint, Fig. 2.12.

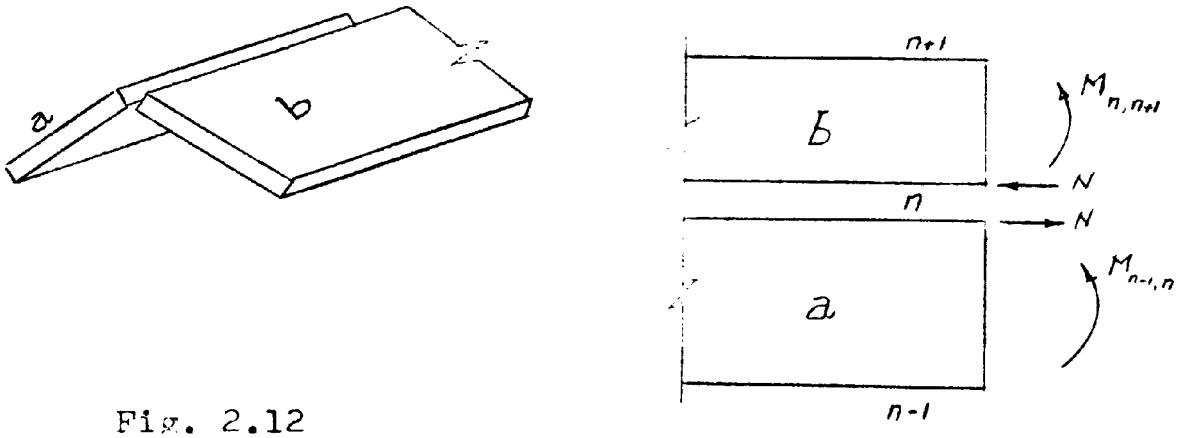

Fig. 2.12

The additional normal stresses f' due to a normal force N acting at the edge n common to two plates a and b, Fig. 2.13, are as follows:

For plate a:

$$f'_{n,n-1} = \frac{N}{A_a} + \frac{N \cdot h_a}{2} \cdot \frac{1}{S_a} \qquad \text{Put } S_a = A_a \times \frac{h_a}{6}$$

$$= \frac{N}{A_a} + 3\,\frac{N}{A_a} = 4\,\frac{N}{A_a} \quad \text{(of the same sense as N)} \quad . \; . \; . \; (2)$$

$$f'_{n-1,n} = \frac{N}{A_a} - 3\,\frac{N}{A_a} = -\,\frac{2N}{A_a} \quad \text{(opposite sense to N)} \quad . \; . \; . \; (3)$$

Similarly the additional normal stresses for plate b are readily obtained (Fig. 2.13).

Stress diagrams due to N:

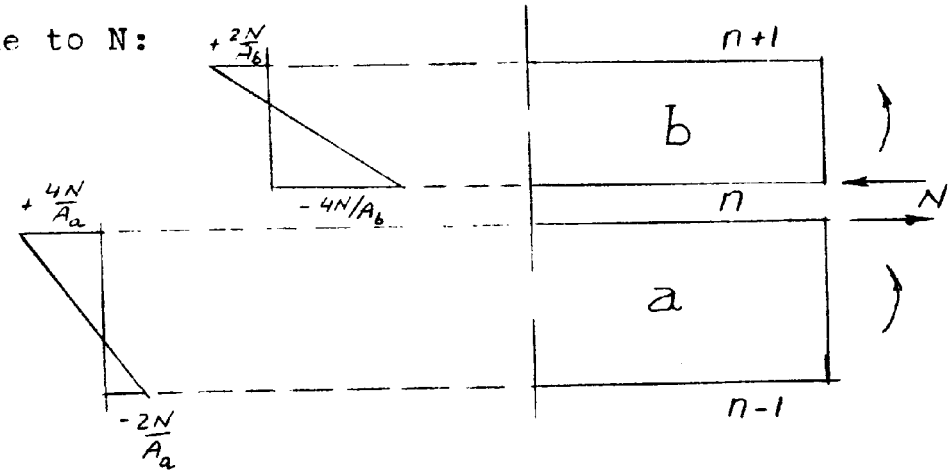

Fig. 2.13

If the original stresses at n in both plates are different by an amount Δf_n, then the correction Δf_n will be distributed on both plates such that:

$$\Delta f_n = f'_{n,n-1} + f'_{n,n+1}$$

$$= 4\,\frac{N}{A_a} + 4\,\frac{N}{A_b} = 4N\left(\frac{1}{A_a} + \frac{1}{A_b}\right) \qquad . \; . \; . \; (4)$$

Distribution factors at joint n:

$$K_a = \frac{4\frac{N}{A_a}}{4N(\frac{1}{A_a} + \frac{1}{A_b})} = \frac{A_b}{A_a + A_b} \quad \ldots (5)$$

$$K_b = \frac{-4\frac{N}{A_b}}{4N(\frac{1}{A_a} + \frac{1}{A_b})} = \frac{-A_a}{A_a + A_b} \quad \ldots (6)$$

Carry-over factors:

From stress diagram due to N in Fig. 2.13, it can be seen that a correction of $4\frac{N}{A_a}$ at edge n in plate 'a' is accompanied by a stress $-2\frac{N}{A_a}$ at the far end of the same plate. Hence the carry-over factor for any plate from end to end is equal to -1/2. Assuming that the magnitude and the distribution of the P-loads on each plate can be determined, the procedure for the stress distribution method is as follows:

(1) Compute the "free edge stresses," by assuming that all edges are free $f = \frac{M}{S}$

(2) Compute the "unbalanced stress"

$$\Delta f_n = f_{n,n-1} - f_{n,n+1}$$

(3) Balance, using distribution factors K

(4) Carry-over. The carry-over factor is -1/2

(5) Repeat the procedure until satisfactory convergence is obtained.

(6) At the end of Step 5, stresses at all joints are balanced and known. In order to find out N at any joint, equation (2) may be used

$$N = \frac{A_a}{4} \cdot f'_{n,n-1} = \frac{A_{n,n-1}}{4} \cdot f'_{n,n-1} \quad . \quad . \quad (2)$$

where $f'_{n,n-1}$ is the correction, i.e., the sum of all distributed stresses at the edge n of the plate n,n-1.

Determination of the P-loads:

The usual procedure for the determination of the magnitude and the distribution of the P-loads, as adopted by Ehlers and Craemer theory,[10] is to consider the plates of the roof in the transverse direction, to be acting as a continuous slab, supported at the joints by nonyielding supports. The shearing forces Q along the joints are readily computed, and from the consideration of equilibrium of the joint element discussed before, the Q forces acting from the adjacent plates on to the joints, are resolved into p-forces parallel to the said plates. The resultant of the p-forces acting on a plate, along its two sides, gives the P-forces for that plate. Consequently, the P-forces obtained will vary along the plate, in the same manner as the external loads applied to the roof. This is also the same procedure used by Winter and Pei.[12]

CHAPTER III

PROPOSED METHOD OF ANALYSIS OF HIPPED PLATE STRUCTURES CONSIDERING THE RELATIVE DISPLACEMENTS OF THE JOINTS

From consideration of the equilibrium of a joint and a plate element discussed in Chapter II, it is clear that the shearing forces Q acting on both sides of a joint are in equilibrium with the p-loads transmitted between the joint and the adjoining plates. Hence the p-loads can be numerically determined once the Q forces are known. The Q forces represent the shearing forces in the roof plates per unit of length along the joints. Referring to Fig. 3.1 representing the vector diagram for the Q and p-forces, it is clear that a small error committed in the computation of the Q forces may result in a considerable error in the evaluation of the p-loads.

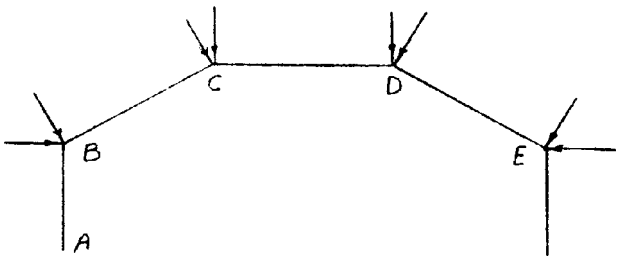

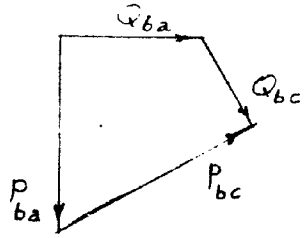

Vector diagram for joint B

Fig. 3.1

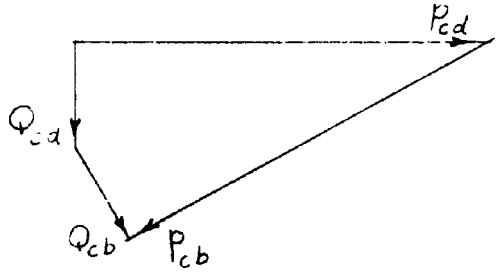

Vector diagram for joint C

1. PROPOSED METHOD OF ANALYSIS:

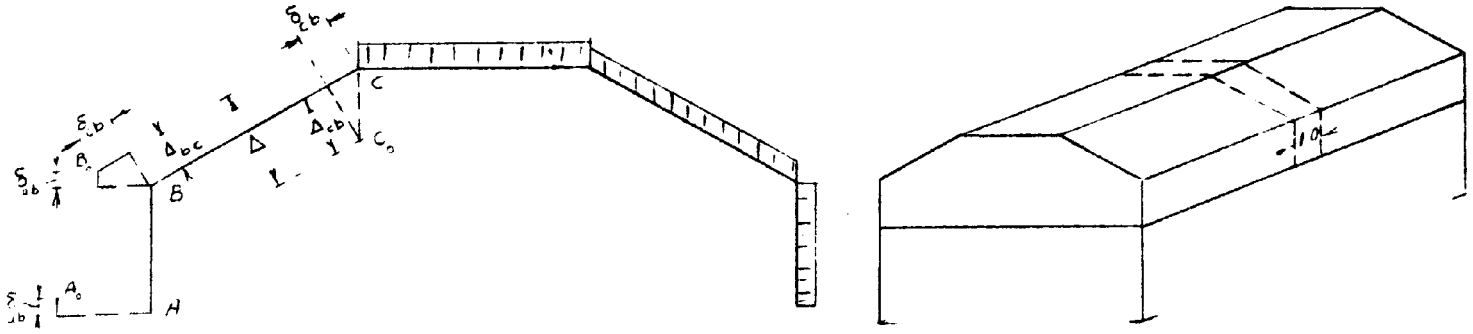

Fig. 3.2

The proposed method of analysis will be discussed in terms of its application to the roof shown above in Fig. 3.2. The displacements of the joints are expressed in terms of their components Δ's perpendicular to the different plates of the roof.

The roof in the transverse direction is treated as a continuous slab with the joints given assigned displacements Δ's. To determine the shearing forces Q acting along the joints of the roof, in its deflected position under loading, we are only interested in the relative displacements Δ's between each two consecutive joints. For this roof we need to work with three unknown values of Δ for unsymmetrical loading, and only one Δ value for symmetrical loading. With the Δ's assumed and the applied load w on the roof given, the shearing forces Q along the joints are obtained in terms of w and the Δ's. The Q forces are then resolved to obtain the P-forces. Using the method of stress distribution dis-

cussed in Chapter II, the final stresses in the roof are obtained in terms of w and the Δ's. Consequently the deflection δ of each plate element, acting as a beam in its plane is obtained in terms of w and the Δ's. Hence we will have the planer deflections δ of the plates in terms of the perpendicular deflections Δ. Substituting the values of the δ's into the geometrical expression for Δ, given in Chapter II, we get the required values of the Δ's.

The steps in the analysis can be summarized as follows:

(1) The first step is the calculation of the forces and the stresses acting at the edges of each element for the assumption of nonyielding supports. The analytical procedure is simplified by using the stress distribution method discussed in Chapter II.

(2) The second step is to express the shearing forces Q and the parallel forces P acting on each element in terms of each Δ value. This operation is most easily accomplished by assigning an arbitrary value to Δ, determining the corresponding fixed-end moments, and then correcting for rotation at the ends of the elements by the moment distribution method. After the end moments are determined the Q and P forces are then calculated in the same manner as in Part (1). This operation must be repeated for each different Δ term. For unsymmetrical loading the number of Δ values for the structure

in Fig. 3.2 is equal to three, but only one unknown for symmetrical loading.

(3) After the Q and P forces are expressed in terms of the Δ's, the corresponding edge stresses are then calculated in the same manner as in Part (1).

(4) From the values of the combined edge stresses from (1) and (3), the displacements δ parallel to the elements are computed. These parallel displacements δ are therefore in terms of the applied load and the transverse movements Δ. It will be found that there are only one set of Δ values that will satisfy the algebraic relations between the Δ's and the δ's that are imposed by the geometrical requirements of the cross-section and the equilibrium conditions. The values of the Δ's can now be calculated from the geometrical relations between the Δ's and δ's since the δ's have already been expressed in terms of Δ's by the calculations in Steps (2) and (3).

(5) After the Δ's have been calculated, the edge stresses, shears, and transverse moments due to these transverse displacements are now known as they have previously been expressed in terms of the Δ's. These values are added algebraically to the corresponding values in Part (1) to give the final results.

The application of the above procedure to a 1/40 scale aluminum model is illustrated in the following pages. This is followed by an example of a reinforced concrete hipped plate roof of seven plates.

2. ILLUSTRATIVE EXAMPLES:

Example 1. The general dimensions of a 1/40 scale aluminum model of a hipped plate roof are given in Fig. 3.3. The model is loaded with a uniform load w p.s.i., distributed all over the top plate CC', and it is required to calculate the maximum longitudinal and maximum transverse stresses in the model, due to this loading.

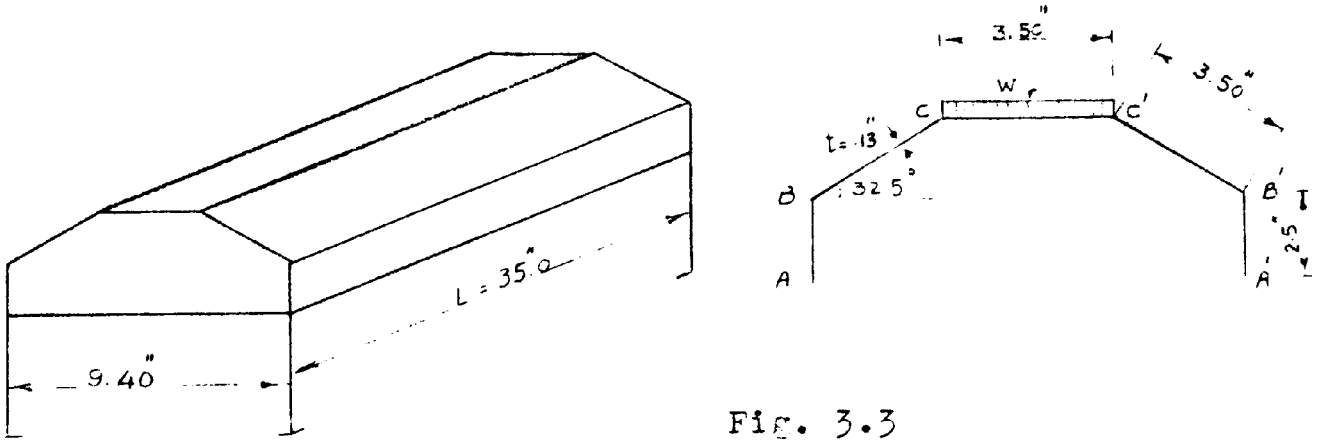

Fig. 3.3

STEP 1. Case of external loads and non-yielding supports: Consider a transverse strip 1.0 inch wide at the middle of the span. This transverse strip will be treated as a continuous slab supported at the joints by non-yielding supports.

Moment Distribution Factors:

Joint C:

Member	c	k	ck	r
CB	3	1	3	.60
CC'	2	1	2	.40
			5	1.00

Fixed end moment at C = $\frac{wh^2}{12}$

The bending moments and shears for this case are given in

Fig. 3.4. The Q-forces, i.e. shear forces acting on the joints per unit length, are given in Fig. 3.5.

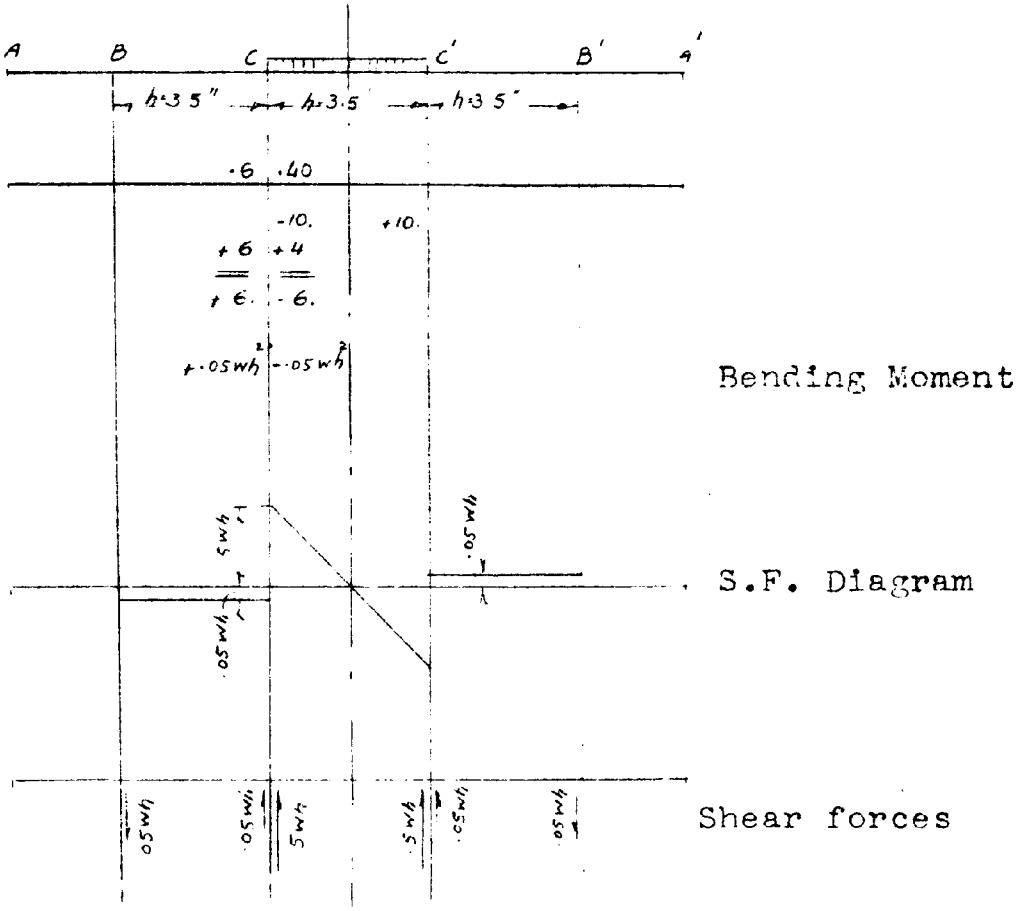

Fig. 3.4
B.M. and Shears

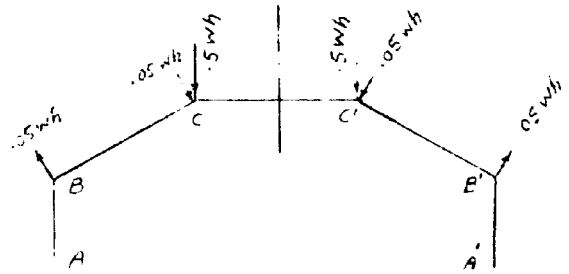

Fig. 3.5
Q-forces acting on joints

Determination of the P-forces acting on the plates:

Let us assume the positive sense for the P-forces be as indicated in Fig. 3.6.

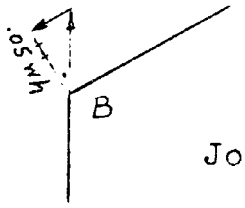

Joint P

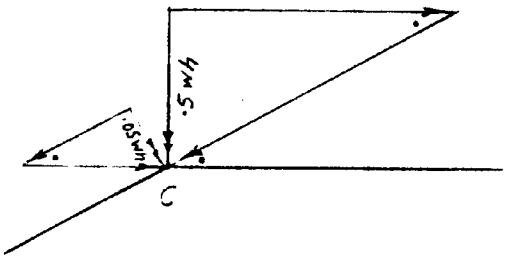

Joint C

Fig. 3.6
Determination of P-forces

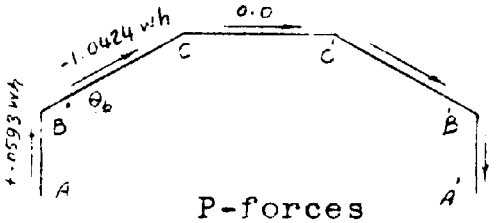

P-forces
on a strip 1.0" wide

$$P_{ab} = +0.05 \text{ wh} \cdot \frac{1}{\cos \theta_b} = +0.05 \text{ wh} \frac{1}{.31434} = +0.0593 \text{ wh}$$

$$P_{bc} = -0.05 \text{ wh} \cdot (\tan \theta_b + \cot \theta_b) - 0.5 \text{ wh} \frac{1}{\sin \theta_b}$$

$$= -0.11014 \text{ wh} - 0.932 \text{ wh} = -1.01424 \text{ wh}$$

$$P_{cc'} = 0.0$$

where h = 3.50 inches

"Free Edge" bending moments and corresponding stresses at the middle section:

Each plate will be treated as a beam carrying the P-loads and spanning between the end diaphragms, with no edge shear T along the joints.

$$M_{ab} = P_{ab} \cdot \frac{L^2}{8} = (+ .0593\ wh) \frac{35.0^2}{8} = +31.80\ w \quad \text{lbs. inch}$$

$$M_{bc} = P_{bc} \cdot \frac{L^2}{8} = (- 1.0424\ wh) \cdot \frac{35^2}{8} = -560.0\ w \quad \text{lbs. inch}$$

$$M_{cc'} = 0.0$$

Corresponding maximum fiber stresses:

Section modulus for plate AB = $S_{ab} = .13 \times \frac{2.50^2}{6} = .1354\ \text{inch}^3$

Section modulus for plate BC = $S_{bc} = .13 \times \frac{3.5^2}{6} = .266\ \text{inch}^3$

$$f_{ab} = \pm \frac{M_{ab}}{S_{ab}} = \pm \frac{31.80}{.1354} w = \pm 235.0\ w \quad \text{p.s.i.}$$

$$f_{bc} = \pm \frac{M_{bc}}{S_{bc}} = \pm \frac{560.0}{.266} w = \pm 2105.0\ w \quad \text{p.s.i.}$$

$$f_{cc'} = 0.0$$

These "free edge" stresses are shown in Fig. 3.7. The signs for the stresses depend upon the sense of the corresponding P-loads.

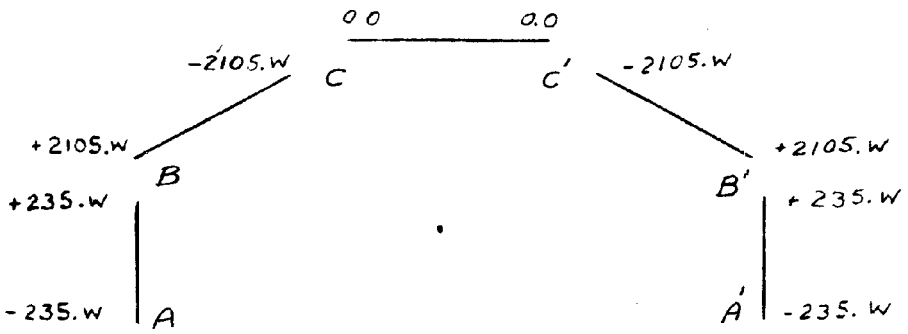

Fig. 3.7
"Free edge" stresses

The "free edge" stresses will be corrected to introduce the effect of shear stresses T acting along the common edges. The stress distribution method discussed in Chapter II will be used here.

Stress Distribution Coefficients:

Joint B:

$$K_{ba} = \frac{A_{bc}}{A_{ba} + A_{bc}} = \frac{3.50}{2.50 + 3.50} = 0.58$$

$$K_{bc} = \frac{A_{ba}}{A_{ba} + A_{bc}} = \frac{2.50}{2.50 + 3.50} = 0.42$$

Joint C:

$$K_{cb} = -K_{cc} = 0.50$$

Carry over factor = $-\frac{1}{2}$

Stress Distribution:

	A		B		C		
		.58	.42		.5	.5	
	-235. w	+ 235.w	+2105.w		-2105.w	0.0	-----(1)
balance:		+ 1085.	- 785.		+1052.	-1052.	
Carry-over balance:	-542.		-526.		+ 392.	+ 526.	
		-305.	+221.		+ 67.	- 67.	
Carry-over balance:	+152		- 33.		- 110.	+ 33.	
		- 19.	+ 14.		+ 72.	- 72.	
	+ 10		- 36.		- 7.	+ 36.	
		- 21.	+ 15.		+ 21.5	- 21.5	
	+ 10		- 11.		- 7.	+ 11.	
		- 6.	+ 5.		+ 9.	- 9.	
	+ 3		- 4.		- 2.	+ 4.	
		- 2.	+ 2.		+ 3.	- 3.	
	+ 1						
	-601.w	+967.w	+967.w		-614.w	- 614.w	-----(2)

The "free edge" stresses are given in line marked (1) in the table, and the stresses, after distribution, are given in line marked (2), and are shown on a section of the model in Fig. 3.8. These stresses represent the stresses at the middle

section for the case of external loads, neglecting the effect of the relative displacements of the joints, which will be considered in the next step.

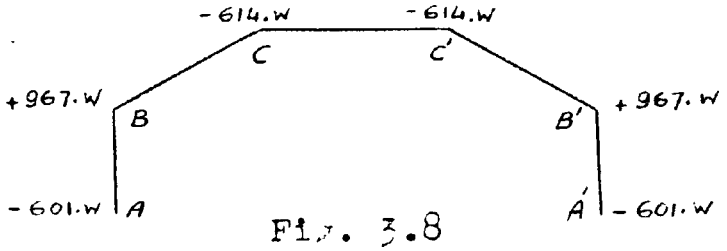

Fig. 3.8

STEP 2. Effect of the relative displacements of the joints: Consider a transverse strip at the middle of the model 1.0 inch wide, and let the relative displacement between edges B and C at the middle of the strip be given by:

$$\Delta = \Delta_{bc} + \Delta_{cb} \qquad \text{(See Fig. 3.9)}$$

Fixed end moment at C, with the edge B free to rotate

$$= 3\,\frac{E\,I}{h} \cdot \frac{\Delta}{h} = 3\alpha$$

where I = moment of inertia of a strip 1.0 inch wide

$$= 1.0 \times \frac{.13^3}{12} = 183 \times 10^{-6} \text{ inch}^4$$

E = modulus of elasticity of aluminum = 10.5×10^6 p.s.i.

h = width of plate BC = 3.50"

$$\alpha = \frac{E\,I}{h} \cdot \frac{\Delta}{h} = E.\ \Delta \times (1/4.90) \times 10^{-6} = 156.5\,\Delta$$

The fixed end moments are distributed, and the moments and the shear forces are given in Fig. 3.10. The Q-forces and the P-loads are given in Fig. 3.11.

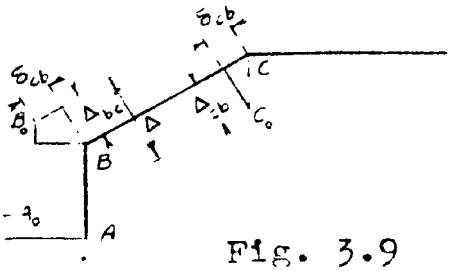

Fig. 3.9

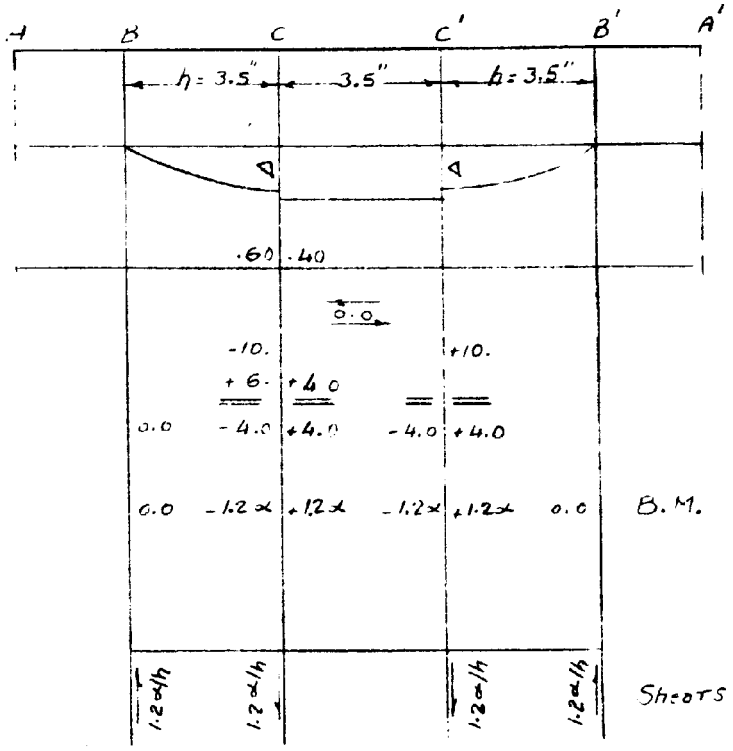

Fig. 3.10
B.M. and shears

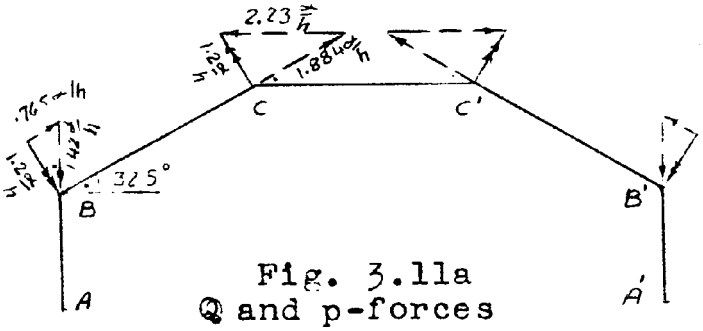

Fig. 3.11a
Q and p-forces

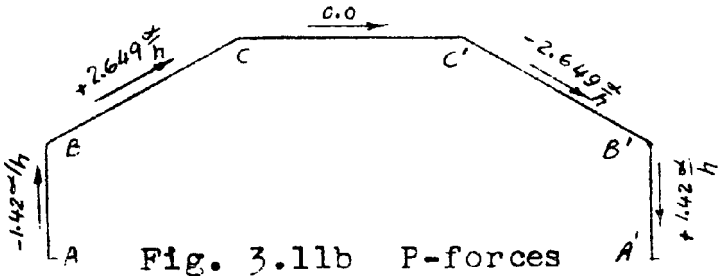

Fig. 3.11b P-forces
on a 1.0" strip at middle

STEP 3. Stresses at the middle section corresponding to the P-loads in Part (2):

The relative deflection Δ between the edges B and C, is assumed to vary as a sine-curve, and hence the corresponding P-loads, bending moments and stresses will vary as a sine-curve.

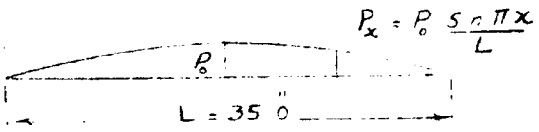

Bending moment at the middle of the span

$$= P_o \frac{L^2}{\pi^2} \qquad \text{(See Appendix II)}$$

$$M_{ab} = P_{ab} \cdot \frac{L^2}{\pi^2} = (-1.42 \frac{\alpha}{h}) \frac{35.0^2}{\pi^2} = -50.40 \alpha$$

$$M_{bc} = P_{bc} \cdot \frac{L^2}{\pi^2} = (+2.649 \frac{\alpha}{h}) \frac{35.0^2}{\pi^2} = +94.10 \alpha$$

$$M_{cc'} = 0.0$$

Corresponding maximum fiber stresses:

$$f_{ab} = \frac{M_{ab}}{S_{ab}} = \pm \frac{50.4 \alpha}{.1354} = \pm 372. \alpha$$

$$f_{bc} = \pm \frac{94.1 \alpha}{0.266} \pm 353. \alpha$$

The "free edge" stresses shown in Fig. 3.12, are then distributed by stress distribution method, to include the effect of the edge shears T. The same coefficients and method used in Step 1 are used to get the stresses shown in Fig. 3.13.

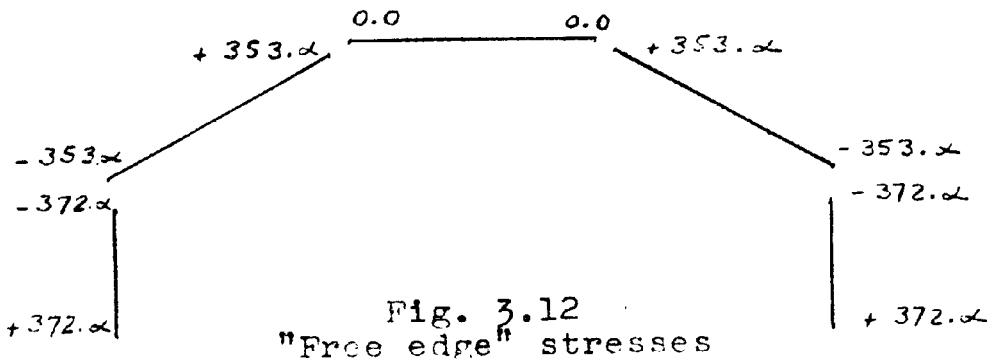

Fig. 3.12
"Free edge" stresses

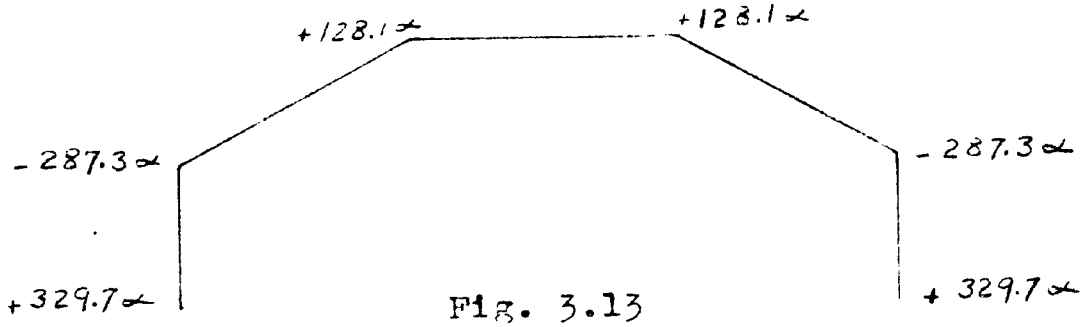

Fig. 3.13
Stresses due to
joints displacement

STEP 4. Determination of the displacements δ parallel to the plate elements:

The deflection at the middle of a beam loaded with a uniform load is given by

$$\delta_o = \frac{f_o}{E\,h} \cdot \frac{5}{48} L^2 \qquad \text{(See Appendix II)}$$

where f_o = difference between maximum fiber stresses at the middle of the span L

h = depth of beam

The deflection at the middle of a beam loaded with a distributed load varying as a half sine wave is given by:

$$\delta_o = \frac{f_o}{E\,h} \cdot \frac{L^2}{\pi^2} \qquad \text{(See Appendix II)}$$

Hence, the deflections δ of the plate elements due to the two cases of loading discussed in Steps 1 and 3 are as follows:

$$\delta_{ab} = \frac{(601. + 967)w}{E \times 2.50} \times \frac{5}{48} \times 35.0^2 - \frac{(329.7 + 287.3)\alpha}{E \times 2.50} \times \frac{35.0^2}{\pi^2}$$

Putting $\alpha = 156.5\,\Delta$ we get:

$$\delta_{ab} = 7.63 \times 10^{-3}\, w - .457\,\Delta \qquad \ldots\ldots (1)$$

$$\delta_{bc} = -\frac{(967. + 614)w}{E \times 3.50} \times \frac{5}{48} \times 35.0^2 + \frac{(287.3 + 128.1)\alpha}{E \times 3.50} \times \frac{35.0^2}{\pi^2}$$

$$= -5.50 \times 10^{-3}\, w + 0.2195\,\Delta \qquad \ldots\ldots (2)$$

Geometrical relations between components of displacements:

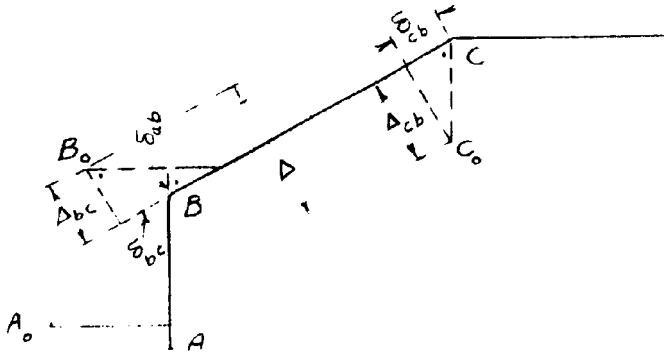

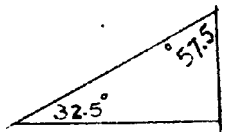

$\cos 57.5^\circ = 0.5373$
$\cot 57.5^\circ = 0.6371$
$\cot 32.5^\circ = 1.571$

Fig. 3.14

$$\Delta_{bc} = (\delta_{bc} + \frac{\delta_{ab}}{\cos 57.5}) \cdot \cot 57.5$$

$$= .6371\ \delta_{bc} + 1.186\ \delta_{ab}$$

$$\Delta_{cb} = \delta_{bc} \times \cot 32.5$$

$$= 1.57\ \delta_{bc}$$

Adding we get: $\Delta = 2.2071\ \delta_{bc} + 1.186\ \delta_{ab}$

Substituting the values given in equations (1) and (2) for δ_{ab} and δ_{bc} we get:

$$\Delta = 10.46 \times 10^{-3}\ w \qquad \text{inches}$$

STEP 5. Edge Stresses:

Substituting the value for Δ in the stresses obtained in Part 3, we get these stresses expressed in terms of the applied load w.

$$\alpha = 156.5\,\Delta = 1.638\ w$$

The maximum longitudinal stresses at the middle section of the model due to:

Case 1. External loads

Case 2. Relative displacements of the joints

Case 3. The above two cases added together are as follows:

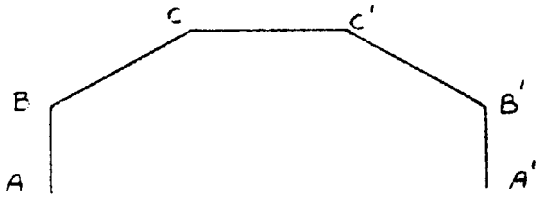

Fig. 3.15

Maximum Longitudinal Stresses p.s.i.

Edge	Case (1)	Case (2)	Case (3)
C	-614.w	+210.w	-404w
B	+967.w	-470.w	+497.w
A	-601.w	+540.w	- 61.w

N.B. Notice how high the longitudinal stresses given in case (1) are, in comparison with those given in case (3).

Bending Moment Diagram on a transverse strip 1.0" wide:

Case (1) Due to external loads and nonyielding supports:

Connecting Moment $M_c = .05\ w\ h^2$

$M_c = .05\ w \times 3.50^2 = 0.612\ w$ lbs. inch.

$\frac{wh^2}{8} = w \times \frac{3.50^2}{8} = 1.530\ w$ lbs. inch.

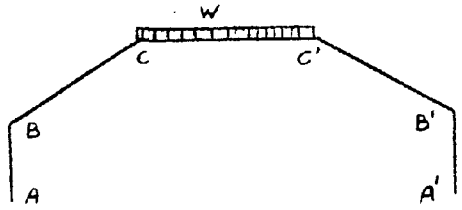

Case (2) Due to Relative Deflection of Joints:

$M_c = 1.2 \times$

$= 1.20 \times 1.638\ w = 1.96\ w$ lbs. inch.

Case (3) The above two cases added together give the resultant Bending Moment Diagram Fig. 3.16.

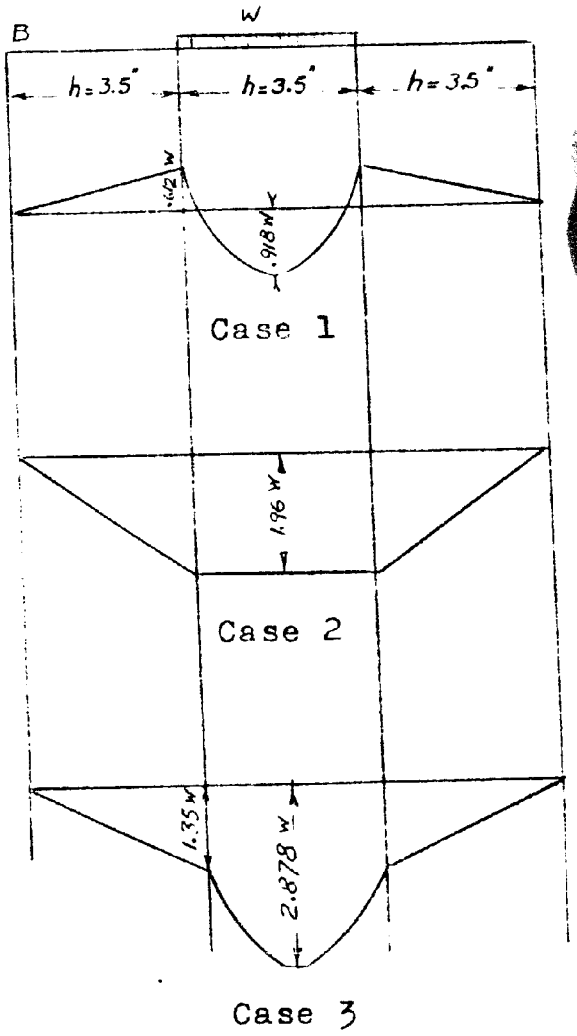

Fig. 3.16

It is important to notice the serious change in the transverse bending moment caused by the relative displacements of the joints, the increase in the value of the bending moment being:

$\frac{1.96}{.918} \times 100 = 213\%$ at the middle of span CC', and

$\frac{-1.96}{.612} \times 100 = -320\%$ at joints C and C'.

Example 2. The same aluminum model of example 1, will be analyzed for the case of four concentrated vertical forces of 58.35 lbs. each, acting on the model as shown in Fig 3.17. The maximum longitudinal and the maximum transverse stresses at the middle of the model will be calculated, and will later be compared with the experimental results obtained for the same case.

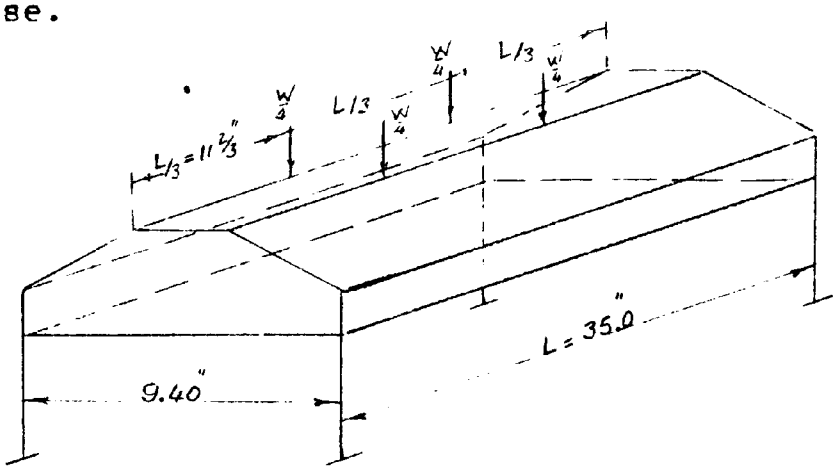

Fig. 3.17

STEP 1. Case of external loads and nonyielding supports: For case of external loads acting at the joints, the loads $\frac{W}{4}$ are resolved in the directions of the two adjacent plates, giving directly, the P- loads acting on the plates. Fig 3.18.

$$P_{ab} = P_{a'b'} = 0.0$$

$$P_{bc} = P_{c'b'} = -0.466\ W$$

$$P_{cc'} = 0.3925\ W - 0.3925\ W = 0.0$$

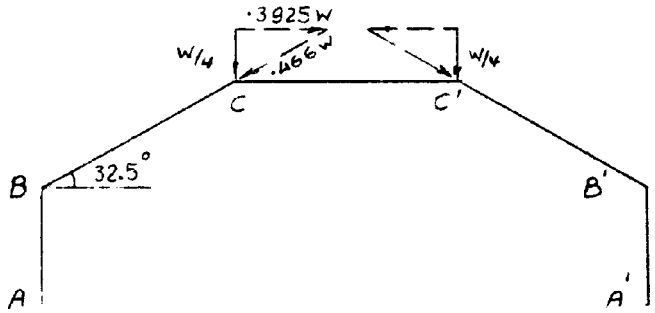

Fig. 3.18 P-loads

"Free Edge" bending moments and corresponding stresses at the middle section:

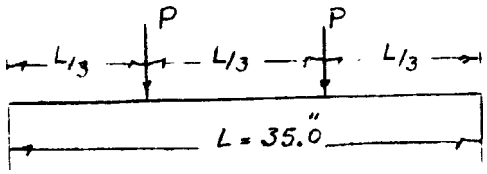

Fig. 3.19

$$M_{ab} = - M_{a'b'} = 0.0$$

$$M_{bc} = - M_{c'b'} = -.466\ W \times \frac{L}{3}$$

$$= - 5.44\ W \quad \text{lbs. inch.}$$

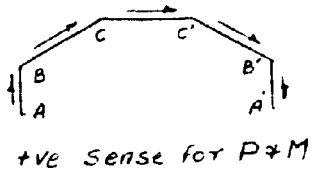

Corresponding maximum fiber stresses:

$$f_{ab} = 0.0$$

$$f_{bc} = \frac{M_{bc}}{S_{bc}} = \frac{-5.44\ W}{.266} = + 20.45\ W$$

$$f_{cc'} = 0$$

These "free edge" stresses are shown in Fig 3.20. Using the same stress distribution procedure and the same coefficients given in example 1, we get the stresses after distribution shown in Fig 3.21.

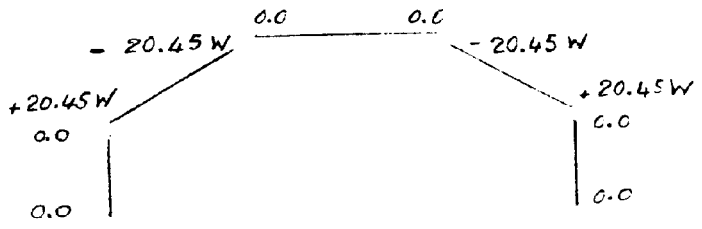

Fig. 3.20
Free edge stresses

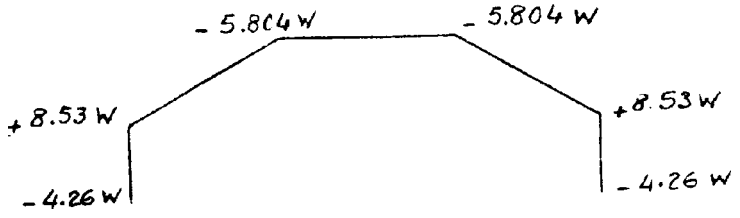

Fig. 3.21
Stresses after distribution (no relative displacements)

STEP 2. Effect of the relative displacements of the joints: The procedure and the results are identicelly the same as for example 1.

STEP 3. Stresses corresponding to the P-loads in Part 2: Results are identical to those of example 1.

STEP 4. Determination of the displacements δ parallel to the plate elements:

The deflection at the middle of a beam loaded with two concentrated loads at $\frac{1}{3}$ of the span, is given by

$$\delta_o = \frac{f_o L^2}{E\ h} \times \frac{23}{216} \qquad \text{(See Appendix II)}$$

where f_o = difference between maximum fiber stresses at the middle of the span L.

h = depth of beam

The deflection at the middle of a beam loaded with a distributed load varying as a half sine wave is given by:

$$\delta_o = \frac{f_o}{E\ h} \cdot \frac{L^2}{\pi^2}$$

Hence the deflections δ of the plate elements due to the two cases of loading discussed in Steps 1 and 3 are as follows:

$$\delta_{ab} = \frac{(4.26 + 8.53)\ W}{E \times 2.50} \times 35.0^2 \times \frac{23}{216} - 0.457\ \Delta$$

$$\delta_{ab} = + \frac{670}{E} W - 0.457 \Delta$$

$$= 0.638 \times 10^{-4} W - .0457 \Delta \quad . \quad . \quad . \quad . \quad (1)$$

$$\delta_{bc} = - \frac{(8.53+5.805)\ W}{E \times 3.50} \times 35.0^2 \times \frac{23}{216} + 0.2195 \Delta$$

$$= - 536 \frac{W}{E} + 0.2195 \Delta$$

$$= - 0.510 \times 10^{-4} W + 0.2195 \Delta \quad . \quad . \quad . \quad (2)$$

Geometrical relation between components of displacements: The geometrical relations between the components of the edge displacements of the model, hold true and are independent of the applied loads. The same geometrical relation of example 1 will be used here, namely:

$$\Delta = 2.2071\ \delta_{bc} + 1.186\ \delta_{ab}$$

Substituting the values given in equations (1) and (2) for δ_{ab} and δ_{bc} respectively, into the geometrical relation, we get

$$\Delta = 0.928 \times 10^{-4} W \quad \text{inches}$$

The positive sign of Δ indicates that Δ is assumed in the correct direction.

STEP 5. Edge stresses: Substituting the value for Δ in the stresses obtained in Part 3, we get these stresses expressed in terms of the applied load W.

$$\alpha = E \Delta (14.90) \times 10^{-6} = 156.5 \Delta$$

$\alpha = 156.5 \times 0.928 \times 10^{-4} \quad W = 0.0145 \quad W$

$W = 4 \times 58.35 = 233.4 \quad \text{lbs.}$

The maximum longitudinal stresses at the middle section of the model due to:

Case 1. External loads and neglecting the relative displacements of the joints.

Case 2. Relative displacements of the joints.

Case 3. The above two cases added together.

are as follows:

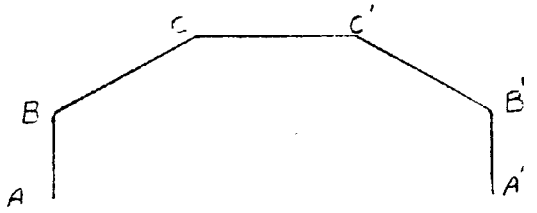

Fig. 3.22

Maximum Longitudinal Stresses p.s.i.

Edge	Case (1)	Case (2)	Case (3)
C	-1360	+435	-925.
B	+2000	-980	+1020.
A	-1000	+1122	+122.

It is important to notice how high the stresses due to Case (1) are, in comparison with the stresses due to Case (3), and that the stress at A in Case (3) has an opposite sign to the stress at A in Case (1).

Bending moment diagram on a transverse strip 1.0 inch wide, at the middle of the model:

Case (1) Due to external loads and no relative displacements between the joints: No transverse bending moment accompanies this case, since the external loads are applied directly at the joints.

Case (2) Due to relative displacements of the joints:

$M_c = 1.2 \alpha$

$= 1.20 \times .0145W$

$= .0174W \times 233.4$

$= 4.065$ lbs. inch.

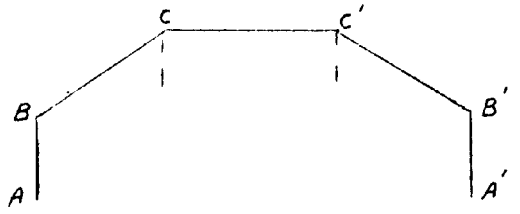

Maximum fiber stresses corresponding to this B.M.:

$$f = \mp \frac{M \cdot Y}{I}$$

$$= \mp \frac{4.065}{183 \times 10^{-6}} \times \frac{.13}{2}$$

$= \mp 1440.$ p.s.i.

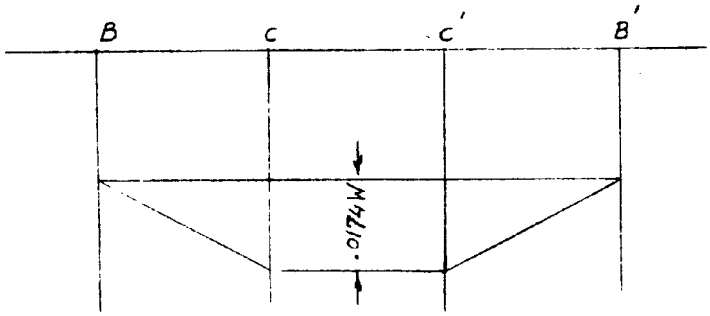

Fig. 3.23 B.M.D. drawn on tension side

Tensile force $p_{cc'}$ in plate CC' due to relative displacements of the joints:

$$p_{cc'} = 2.23 \frac{\alpha}{h} = 2.23 \times \frac{.0145W}{3.5} = .00924W$$

$= .00924 \times 233.4 = 2.16$ lbs./inch run

Corresponding direct stress

$$= \frac{2.16}{1.0 \times .13} = +16.6 \quad \text{p.s.i.} \quad \text{(tension)}$$

In the above example it should be noticed that, although the German theory does not consider any transverse bending stresses due to the joints displacement, yet the maximum value for these stresses is equal to ±1440 p.s.i., i.e. 141% of the maximum value for the longitudinal stresses which is equal to 1020 p.s.i.

A comparison between the analytical results obtained here and the experimental values for the same problem will be given in Chapter IV. For the sake of completion of this comparison, the analytical values for the joints displacements will be worked out here.

Theoretical values for the components of joints displacement:

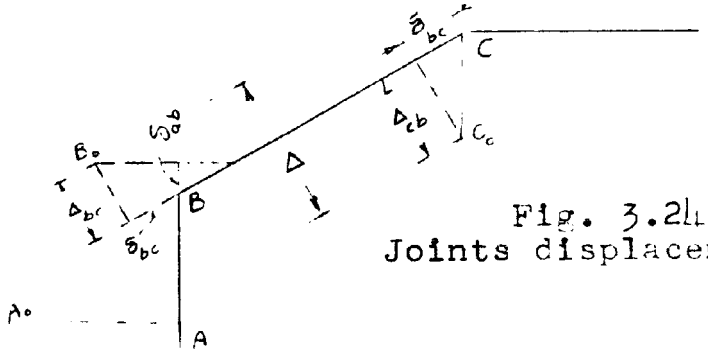

Fig. 3.24
Joints displacement

In part (4) of this example the value of Δ is given by:

$$\Delta = \Delta_{bc} + \Delta_{ch} = 0.928 \times 10^{-4} \, W \quad \text{inches}$$

Equation (1) in part (4) gives:

$$\delta_{ab} = 0.638 \times 10^{-4} \, W - 0.457 \, \Delta$$

$= 0.638 \times 10^{-4} W - 0.424 \times 10^{-4} W$

$= .214 \times 10^{-4} \times 233.4$

$= .00497$ inches (δ_{ab} model = .00412 inches)

Equation (2) in part (4) gives:

$\delta_{bc} = -0.51 \times 10^{-4} W + 0.2195 \Delta$

$= .00713$ inches (δ_{bc} model = .0067 inches)

From geometrical relations between components of displacements we get:

$\Delta_{cb} = 1.57 \delta_{bc} = 1.57 \times .00713$

$= .0112$ inches (Δ_{cb} model = .0111 inches)

$\Delta_{bc} = .6371 \delta_{bc} + 1.186 \delta_{ab}$

$= .0105$ inches (Δ_{bc} model = .0092 inches)

A comparison between analytical and measured values of the components of joints displacement is given on Sheet 8, Appendix I.

Example 3: To illustrate the procedure on a roof of a large number of plates, a seven plate R. C. hipped roof* given in Fig. 3.25 is analyzed. The plates of the roof are tangential to the semi-elliptic curved shell shown dotted. The roof carries a load of 20 lbs. per sq. ft. besides its own weight.

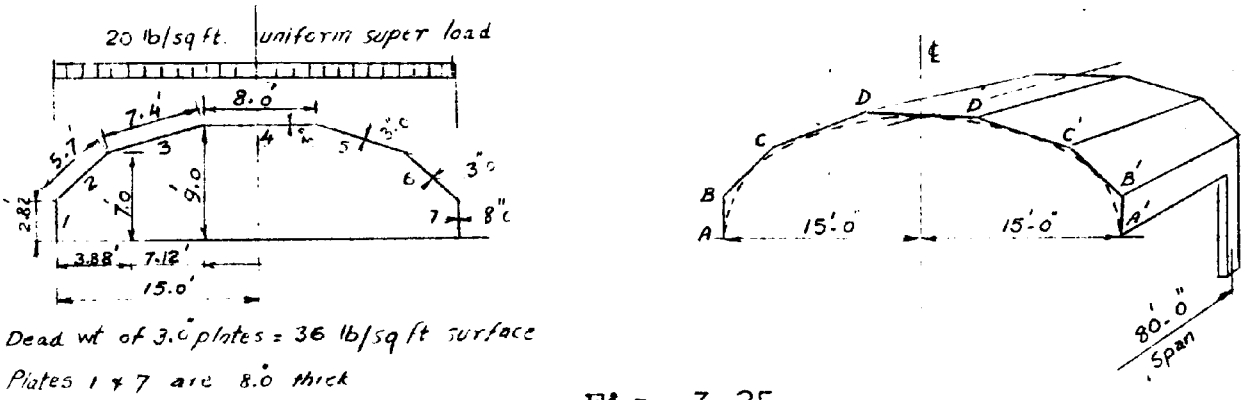

Fig. 3.25

STEP 1. Case of external loads and non-yielding supports: Equivalent uniform load on a horizontal projection

load on plate 2 = $20.0 + 36.0 \times \frac{5.70}{3.88} = 20.0 + 52.9 = 72.90$ lb/sq.ft.

" " " 3 = $20.0 + 36.0 \times \frac{7.40}{7.12} = 20.0 + 37.4 = 57.40$ lb/sq.ft.

" " " 4 = $20.0 + 36.0 = 56.0$ lb/sq.ft.

---

*The analysis of this same roof, on the basis of the approximate theory is given in ref. 14.

Fixed End Moments:

F.E.M. for plate 2 (one end hinged)

$$= \frac{wh^2}{8} = 72.90 \times \frac{3.38^2}{8} = 137.2 \quad \text{lb. ft.}$$

F.E.M. for plate 3

$$= \frac{wh^2}{12} = 57.40 \times \frac{7.12^2}{12} = 242.5 \quad \text{lb. ft.}$$

F.E.M. for plate 4

$$= \frac{wh^2}{12} = 56.0 \times \frac{8.0^2}{12} = 298.5 \quad \text{lb. ft.}$$

Distribution Factors:

Joint C

Member	c	k	ck	r
CB	3	1.40	4.20	.493
CD	4	1.03	4.32	.507
			8.52	1.0

Joint D

Member	c	k	ck	r
DC	4	1.08	4.32	.683
DD'	2	1.0	2.00	.317
			6.32	1.0

The bending moments and shears in a transverse strip 1.0 ft. wide at the middle of the roof for the case of external loads and ignoring the relative displacements of the joints are given in Fig. 3.26.

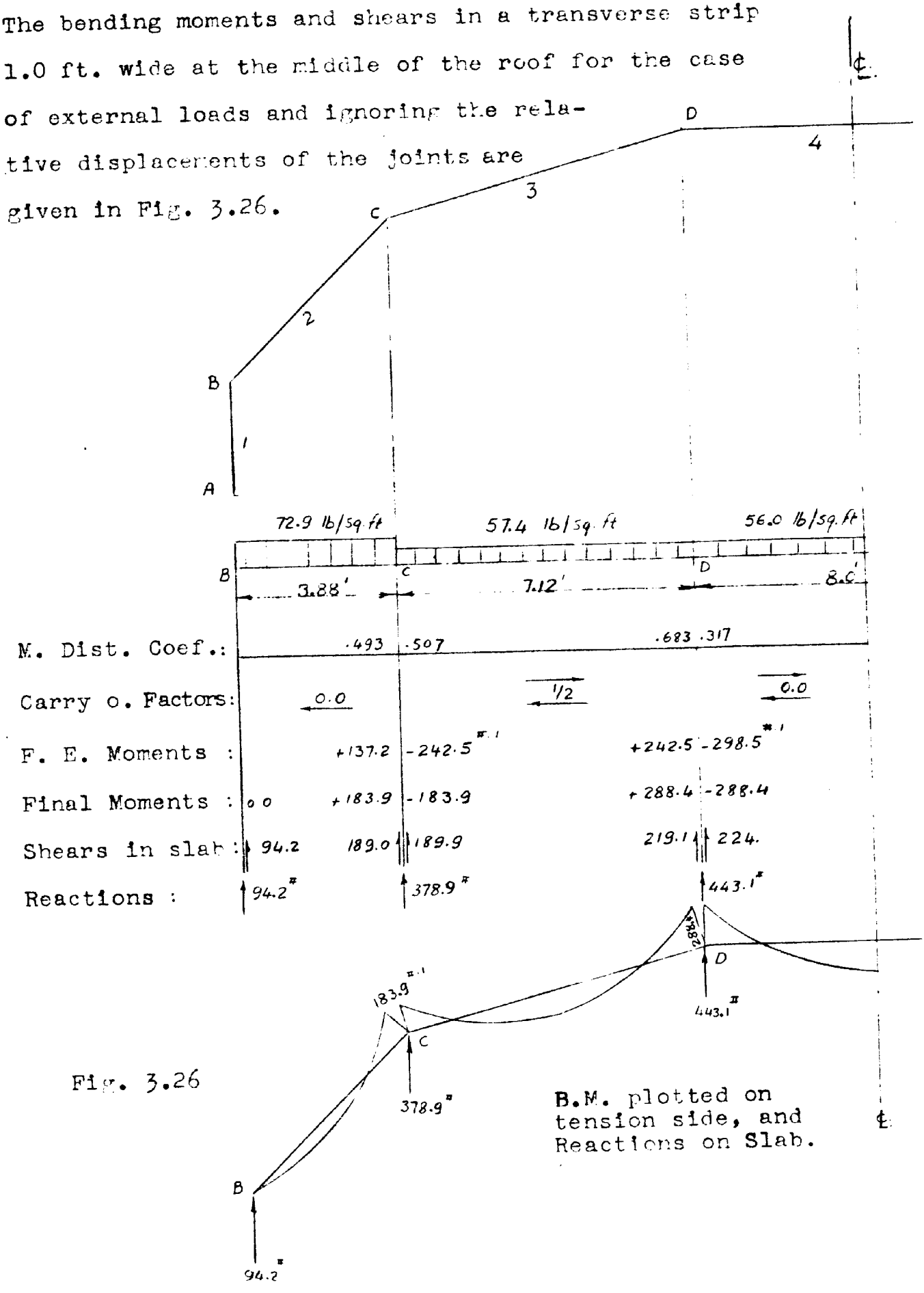

Fig. 3.26

B.M. plotted on tension side, and Reactions on Slab.

STEPS 2 and 3. Bending moments, P-loads and stresses due to relative displacements of the joints:

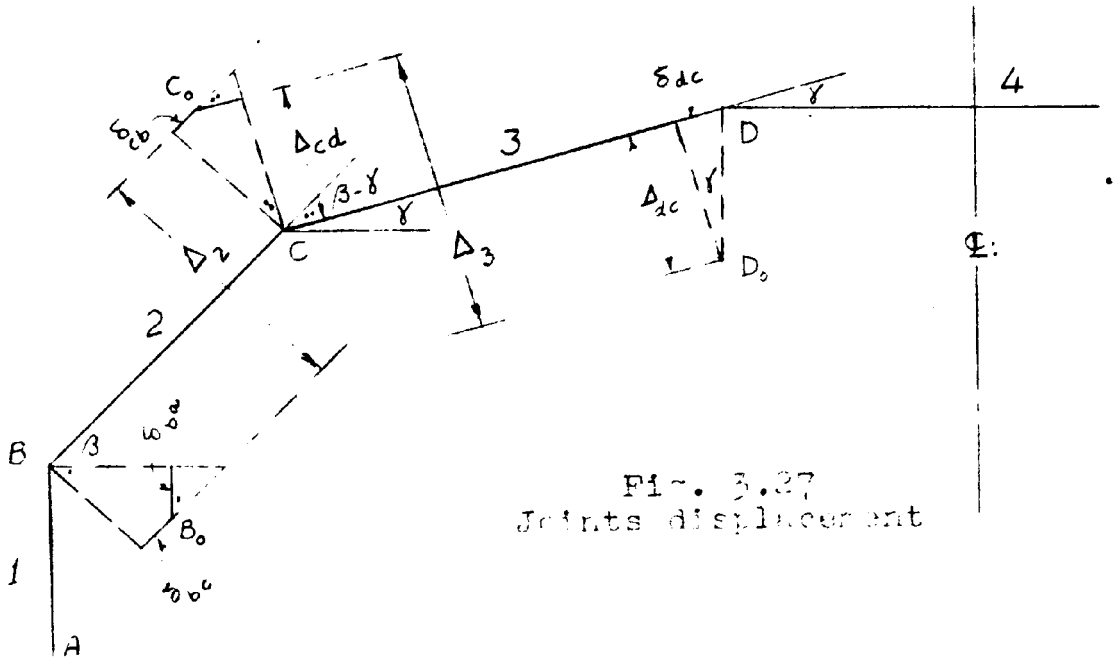

Fig. 3.27
Joints displacement

The transverse displacements Δ's of the joints are assumed arbitrarily as shown in Fig. 3.27. For this roof and with the load symmetrical as given the number of the unknown values is two, namely:

a). Δ_2 for plate 2 and is equal to the relative displacement between the joints B and C at the middle of the roof.

b). Δ_3 for plate 3 and is equal to the relative displacement between the joints C and D at the middle of the roof.

The fixed end moments due to Δ_2 and Δ_3 of plates 2 and 3 respectively, will be corrected for rotation at the joints of the plate elements. After the end moments are determined the Q and P-forces are then calculated. The results of this operation will be given for Δ_2 and Δ_3 on the following pages.

Bending moments and shears in a transverse strip 1.0 ft. wide at the middle of the roof due to Δ_2:

Fixed end moment at joint C with joint B free to rotate=

$$3\frac{EI}{h_2}\cdot\frac{\Delta_2}{h_2} = 3\alpha_2$$

where h_2 = 5.70 ft.

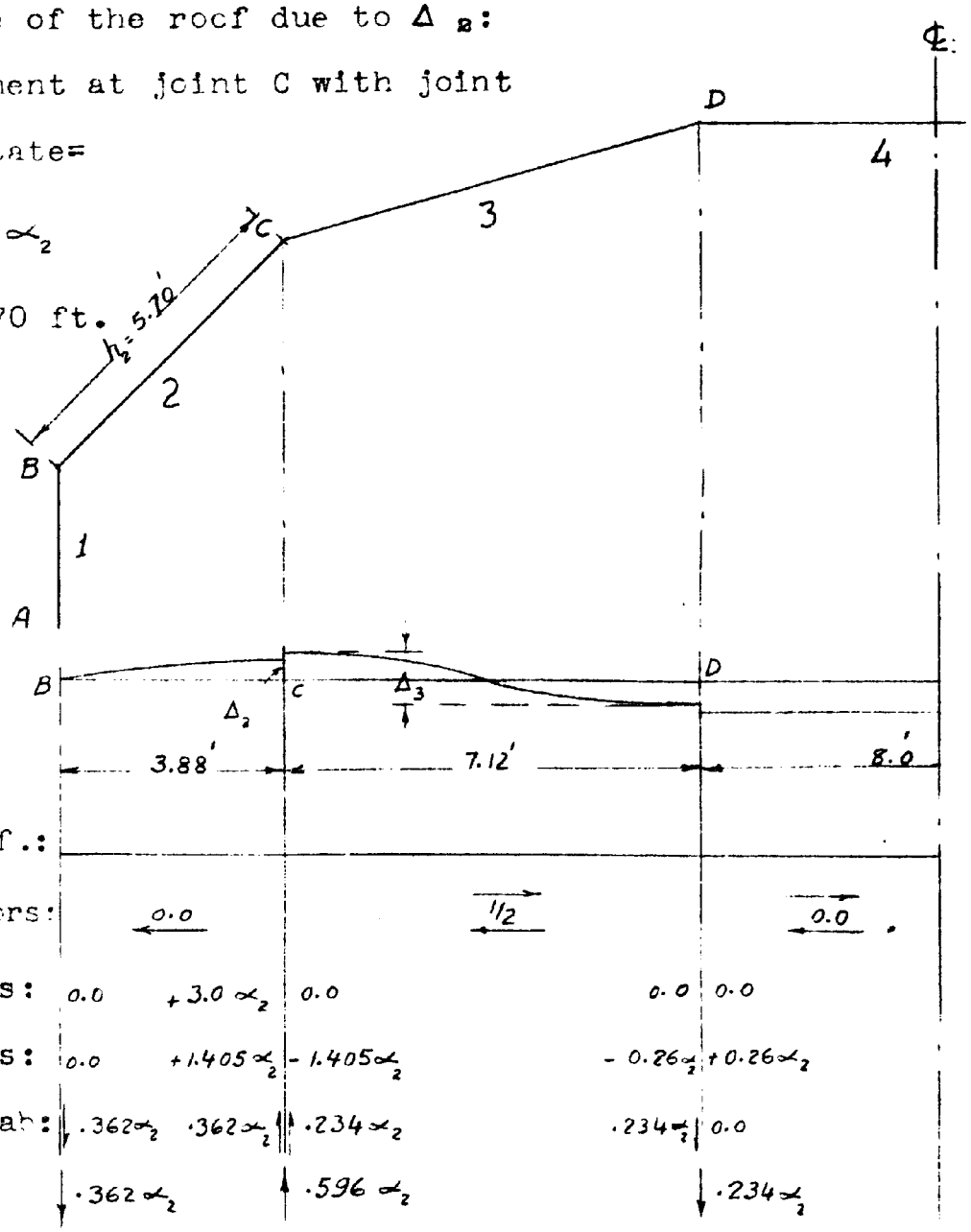

M. Dist. Coef.:					
Carry o. Factors:	0.0 ←		1/2 →		0.0 ←
F. E. Moments:	0.0	$+3.0\alpha_2$	0.0	0.0	0.0
Final Moments:	0.0	$+1.405\alpha_2$	$-1.405\alpha_2$	$-0.26\alpha_2$	$+0.26\alpha_2$
Shears in slab:	$.362\alpha_2$	$.362\alpha_2$	$.234\alpha_2$	$.234\alpha_2$	0.0
Reactions:	$.362\alpha_2$		$.596\alpha_2$	$.234\alpha_2$	

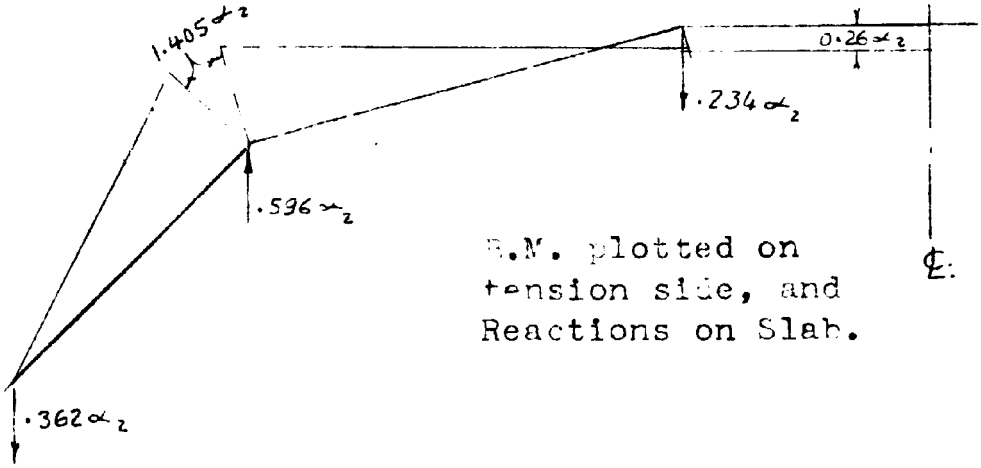

Fig. 3.28

B.M. plotted on tension side, and Reactions on Slab.

Bending moments and shears in a transverse strip 1.0 ft. wide at the middle of the roof due to Δ_3:

Fixed end moment at joints C and D

$$= 6\frac{EI}{h_3} \cdot \frac{\Delta_3}{h_3} = 6\alpha_3$$

$h_3 = 7.40$ ft.

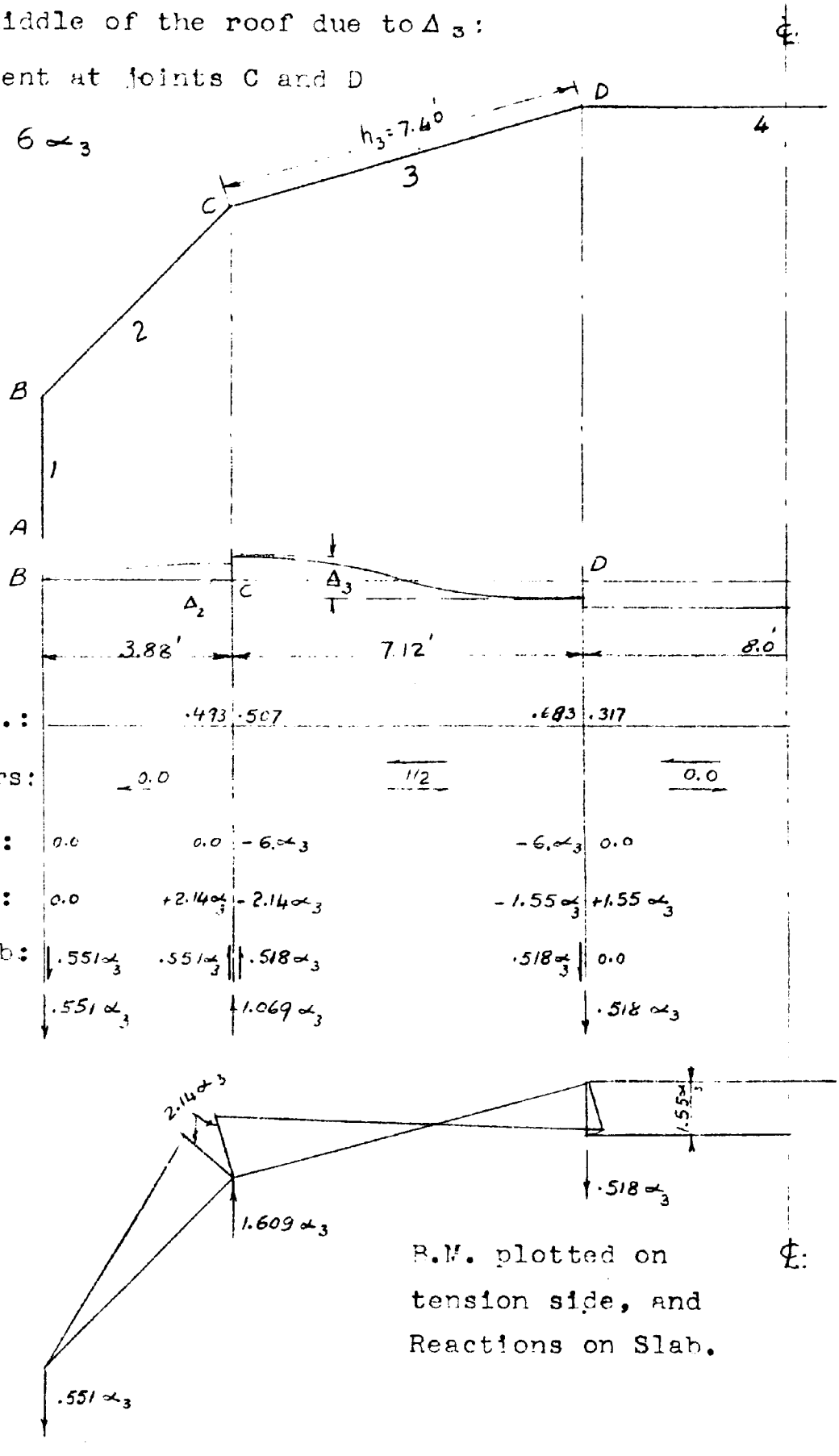

Fig. 3.29

B.M. plotted on tension side, and Reactions on Slab.

Forces acting on joints:

Figures 3.30, 3.31 and 3.32 respectively give the forces* acting at the joints due to

Case (1). External loads and no relative displacement of joints.

Case (2). Relative displacement Δ_2 of plate No. 2.

Case (3). " " Δ_3 " " " 3.

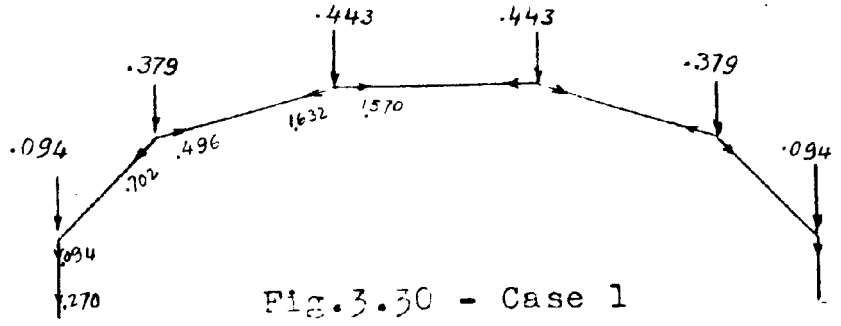

Fig.3.30 - Case 1

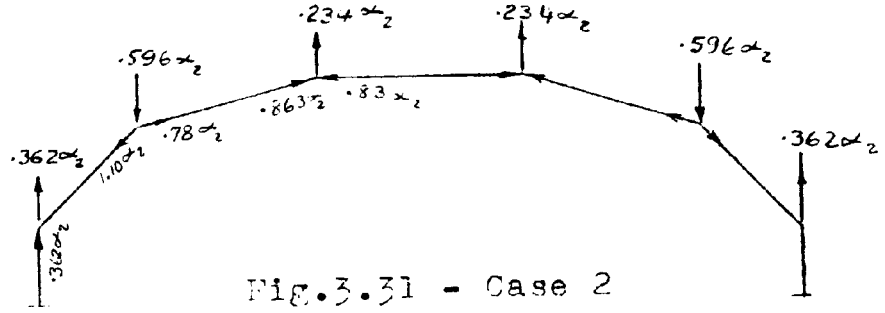

Fig.3.31 - Case 2

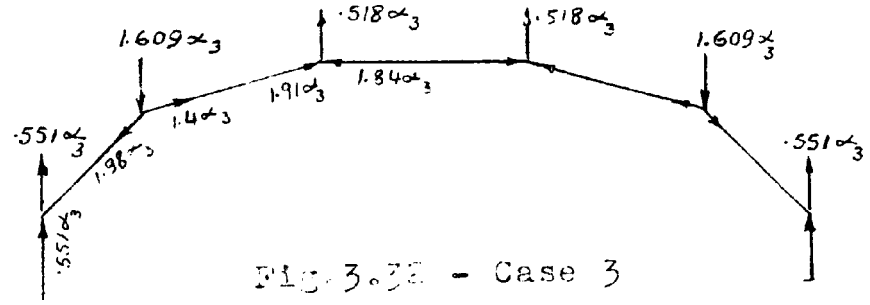

Fig.3.32 - Case 3

*The forces are in kips per ft. of the span, at the middle section of the roof.

P-loads on plates:

Figures 3.33, 3.34 and 3.35 respectively give the P-loads* acting on the plate elements for the three different cases mentioned before.

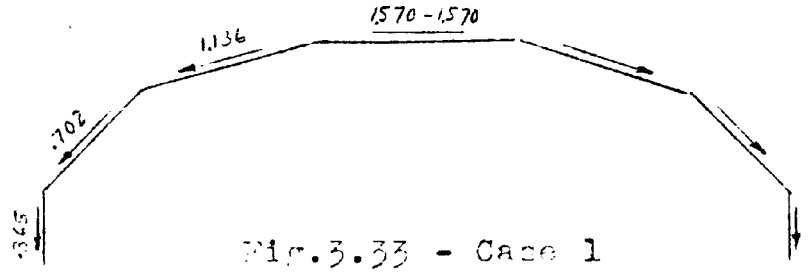

Fig.3.33 - Case 1

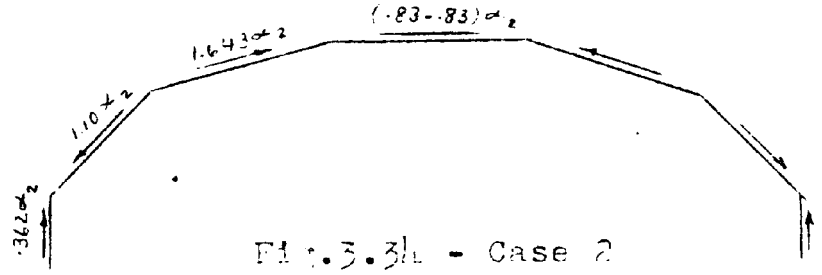

Fig.3.34 - Case 2

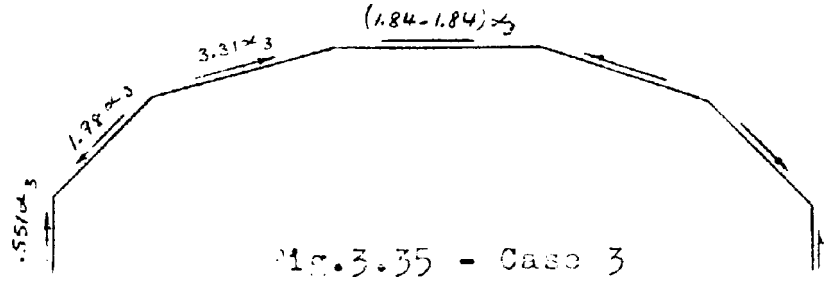

Fig.3.35 - Case 3

*P-loads are in kips per ft. of the span, at the middle section of the roof.

"Free edge" stresses:

The "free edge" stresses in the plate elements for the three different cases of loading are given below.

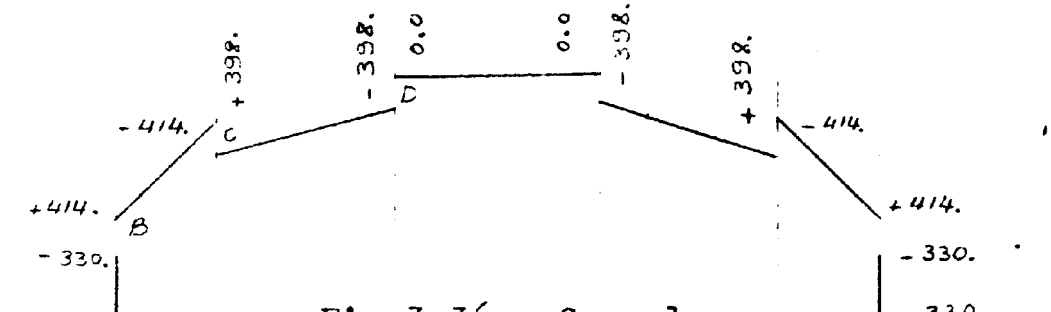

Fig.3.36 - Case 1

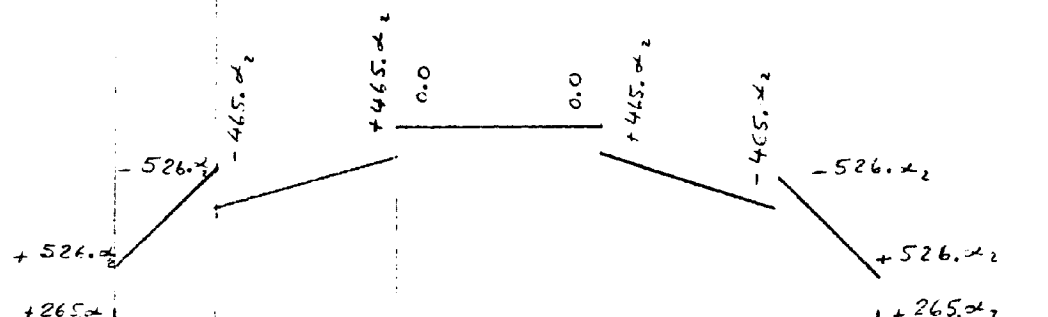

Fig.3.37 - Case 2

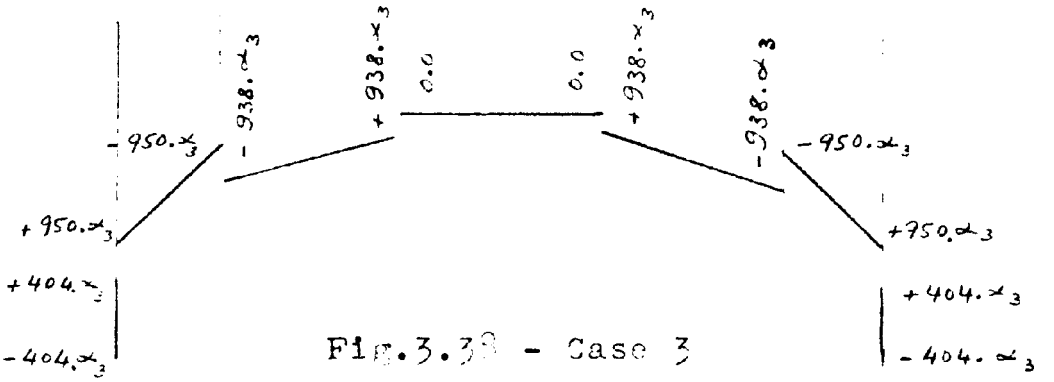

Fig.3.38 - Case 3

Stresses are given in kips per sq. ft. at the middle section of the roof. Plus sign means tension.

The "free edge" stresses are distributed by the stress distribution method to include the effect of the edge shear forces N acting along the joints. The stresses after distribution for the three different cases of loading are given below.

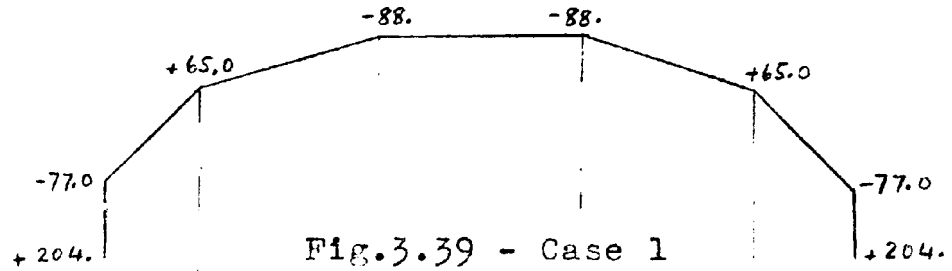

Fig.3.39 - Case 1

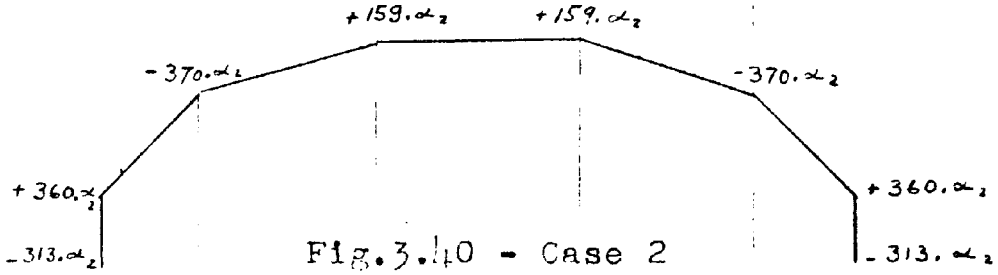

Fig.3.40 - Case 2

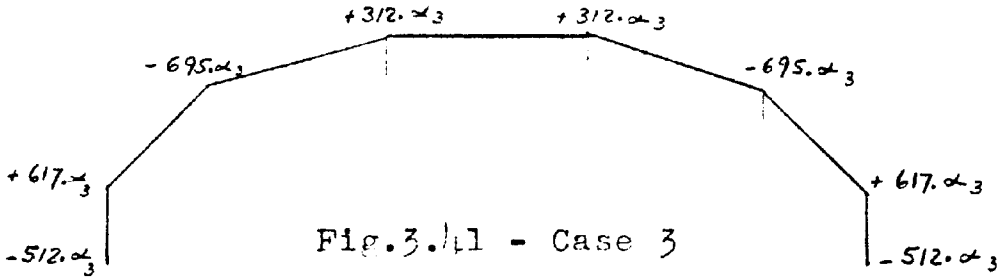

Fig.3.41 - Case 3

Stresses are in kips per sq. ft.

STEP 4: The parallel displacements δ of the plate elements for the three cases of loading are as follows:

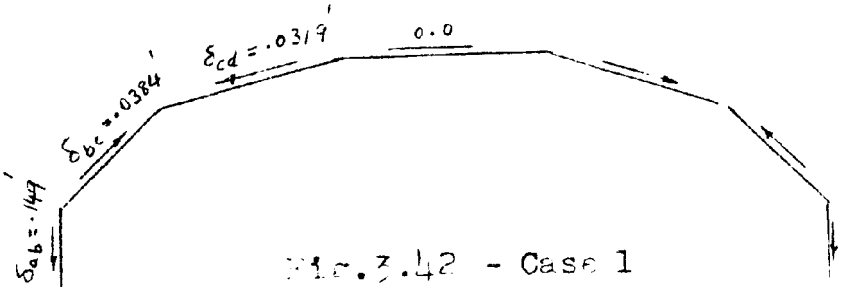

Fig.3.42 - Case 1

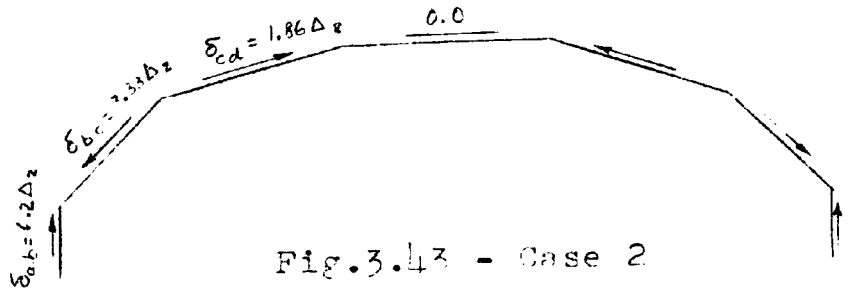

Fig.3.43 - Case 2

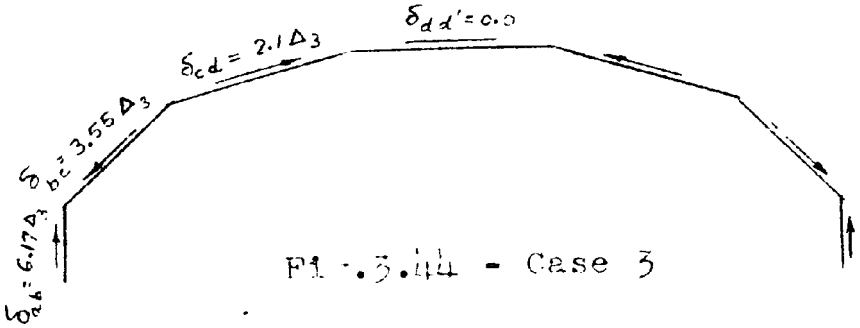

Fig.3.44 - Case 3

Deflections Δ and δ are in ft.

Geometrical relations between components of displacement:

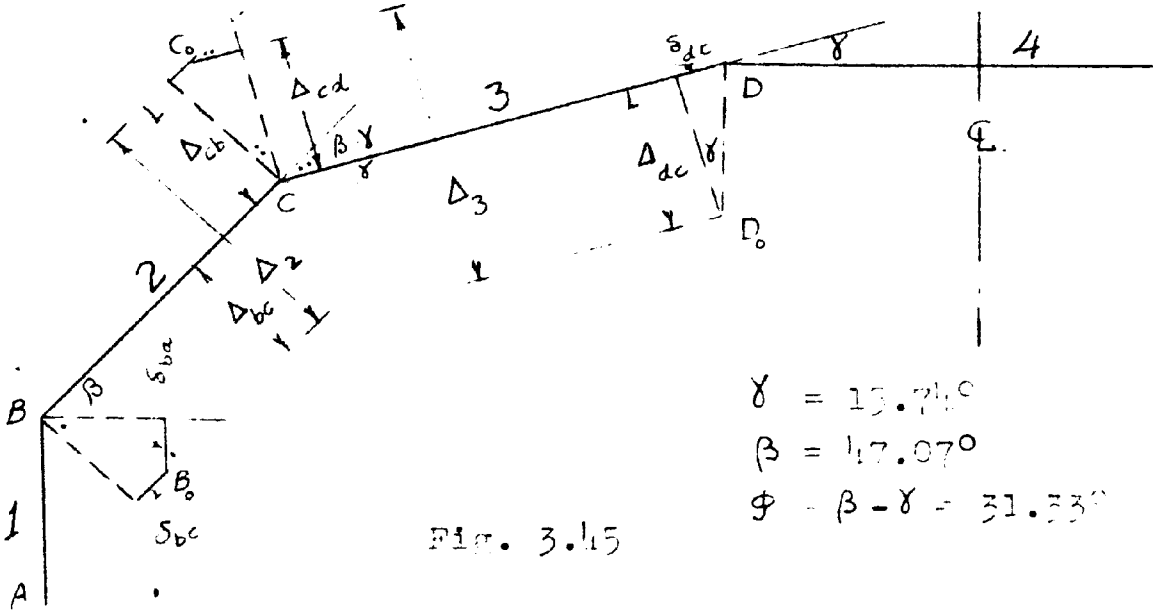

Fig. 3.45

$$\Delta_{bc} = \left[\frac{\delta_{ba}}{\cos(90 - \beta)} + \delta_{bc} \right] \cot(90-\beta)$$

$$= \left[\frac{\delta_{ba}}{.7322} + \delta_{bc} \right] 1.075$$

$$\Delta_{bc} = 1.47\ \delta_{ba} + 1.075\ \delta_{bc} \qquad \ldots\ (1)$$

$$\Delta_{cb} = \left[\delta_{bc} + \frac{\delta_{dc}}{\cos(\beta-\gamma)} \right] \cot(\beta-\gamma)$$

$$= \left[\delta_{bc} + \frac{\delta_{dc}}{.9512} \right] 1.643$$

$$\Delta_{cb} = 1.643\ \delta_{bc} + 1.92\ \delta_{dc} \qquad \ldots\ (2)$$

adding (1) and (2) :

$$\Delta_2 = \Delta_{bc} + \Delta_{cb} = 1.47\ \delta_{ba} + 2.718\ \delta_{bc} + 1.92\ \delta_{dc} \qquad (I)$$

$$\Delta_{cd} = \left[\frac{\delta_{bc}}{\cos(\beta-\gamma)} + \delta_{dc} \right] \cot(\beta-\gamma)$$

$$= \left[\frac{\delta_{bc}}{.5542} + \delta_{dc} \right] 1.643$$

$$\Delta_{cd} = 1.92\ \delta_{bc} + 1.643\ \delta_{dc} \quad . \ . \ . \ . \ (3)$$

$$\Delta_{dc} = \delta_{dc} \cdot \cot(\gamma)$$

$$= 3.543\ \delta_{dc} \quad . \ . \ . \ . \ (4)$$

adding (3) and (4):

$$\Delta_3 = \Delta_{cd} + \Delta_{dc} = 1.92\ \delta_{bc} + 5.191\ \delta_{dc} \quad . \ . \ . \ . \ (II)$$

Equations I and II express the Δ's in terms of the δ's. But our analytical solution gives the δ's in terms of Δ_2 and Δ_3. Hence we have two equations in two unknowns Δ_2 and Δ_3. Solving these two equations we get:

$\Delta_2 = +.099$ ft.

$\Delta_3 = -.082$ ft.

Consequently:

$\alpha_2 = +1.72$ kips and ft. units

$\alpha_3 = -.84$ " " " "

The positive sense for the deflections means that they are in the same sense as were assumed, and the negative means the opposite.

STEP 5. Edge Stresses:

Substituting the values for Δ_2 and Δ_3 in the stresses obtained in part 3, we get these stresses expressed in terms of the applied loads.

$\alpha_2 = +1.72$ kips and ft. units

$\alpha_3 = -0.84$ " " " "

The maximum longitudinal stresses at the middle section of the model due to:

Case (a). External loads and no relative displacements of the joints

Case (b). Relative displacements Δ_2 and Δ_3 between the joints

Case (c). The above two cases added together

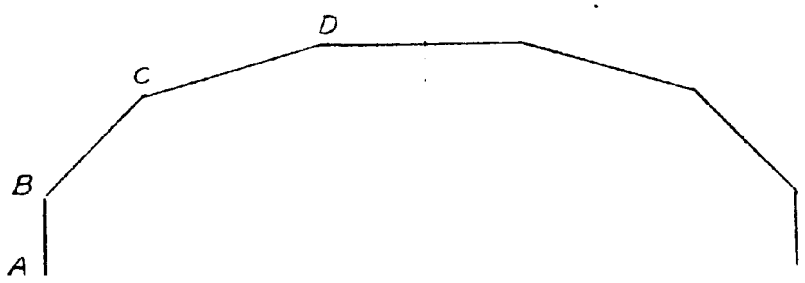

Fig. 3.46

Longitudinal Stresses in kips per sq. ft.

Edge	Case (a)	Case (b)	Case (c)
D	-38.0	+12	-76.0
C	+65.0	-53	+12.0
B	-[illegible].0	+102	+25.0
A	+204.0	-108	+96.0

CHAPTER IV

EXPERIMENTAL INVESTIGATION

1. DESCRIPTION OF THE MODEL:

A 1/40 24 S.T. aluminum model was used for the experimental investigation of the distribution of stresses and strains in a hipped plate structure. The general dimensions of the model are shown in Figure 1a and Figure 1f on Sheet 1, Appendix I. The load was applied at four points on the model as shown by the arrows on the diagrams in Figures 1a and 1b. S.R. 4 resistance gages (Types A1 and A12) were placed to measure the longitudinal strains at sections c, d, and e. (See Figures 1c, 1d, 1e on Sheet 1. These longitudinal gages were placed on both sides of the plate and connected in series to give the average strain. Transverse strains were measured at eight points by means of Type A7 resistance gages. These gages are represented by 1', 2', 3', - - - - 8' as indicated in Figures 1c, and 1d.

Scale relation between model and prototype:

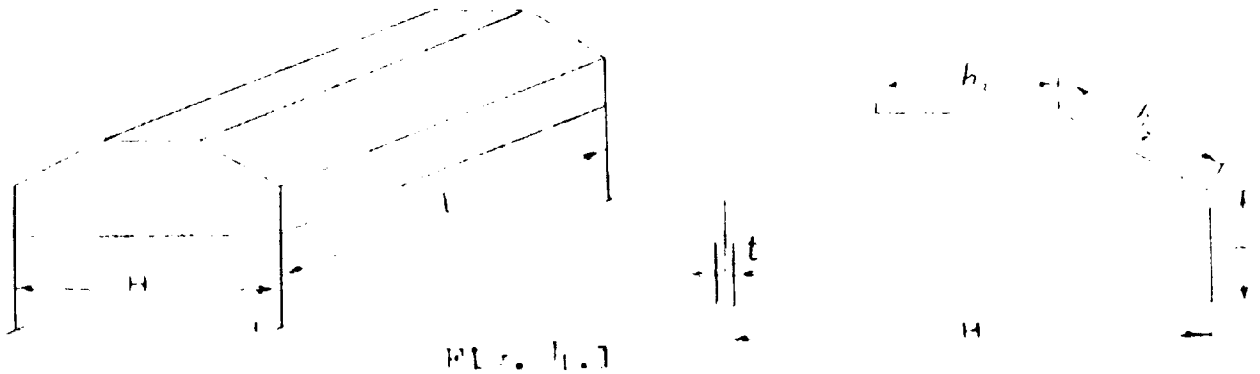

Fig. 4.1

Dimension	Model	Prototype
L	35.0 inches	$\frac{35}{12}$ x 40 = 117 ft.
H	9.4 "	$\frac{9.4}{12}$ x 40 = 31 ft.
h_1	2.5 "	$\frac{2.5}{12}$ x 40 = 8.3 ft.
$h_2 = h_3$	3.5 "	$\frac{3.5}{12}$ x 40 = 11.7 ft.
t	.13 "	.13 x 40 = 5.2 inches

2. RELATIONS BETWEEN STRESSES AND STRAINS IN MODEL AND PROTOTYPE:

Geometrical similarity holds between the model and the prototype, all the dimensions of the prototype being reduced to the same scale 1/40.

(a) Relation between deflections:

$$\text{Scale of Model} = \frac{\text{L model.}}{\text{L prototype}} = \frac{L_m}{L_p} = n = \frac{1}{40}$$

For a beam as shown in Fig. 4.2 the deflection at the middle is given by:

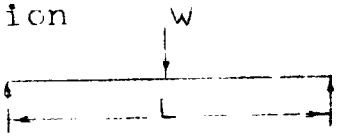

Fig. 4.2

$$\delta = \frac{WL^3}{48EI}$$

$$\frac{\delta \text{ model}}{\delta \text{ prototype}} = \frac{\delta_m}{\delta_p} = \frac{W_m \cdot L^3_m}{W_p \quad L^3_p} \cdot \frac{E_p \cdot I_p}{E_m \cdot I_m}$$

$$\therefore \quad \frac{\delta_m}{\delta_p} = \frac{W_m \cdot E_p}{W_p \cdot E_m} \cdot \frac{1}{n} \qquad \ldots (1)$$

where $n = \frac{L_m}{L_p} = \frac{1}{40}$

To get $\frac{\delta_m}{\delta_p} = n$, we should have:

$$\frac{\delta_m}{\delta_p} = \frac{W_m}{W_p} \cdot \frac{E_p}{E_m} \cdot \frac{1}{n} = n \qquad \ldots\ldots(2)$$

i.e. $$W_m = W_p \cdot \frac{E_m}{E_p} \cdot n^2 \qquad \ldots\ldots(3)$$

Therefore, if we satisfy (3), we will get $\frac{\delta_m}{\delta_p} = n = \frac{1}{40}$

and will have complete geometrical similarity.

(b) Relation between strains:

$$\frac{e_m}{e_p} = \frac{f_m}{E_m} \cdot \frac{E_p}{f_p} = \frac{W_m}{L^2_m} \cdot \frac{L^2_p}{W_p} \cdot \frac{E_p}{E_m}$$

$$= \frac{W_m}{W_p} \cdot \frac{E_p}{E_m} \cdot \frac{1}{n^2} \qquad \ldots\ldots(4)$$

If (3) is satisfied, expression (4) will be equal to unity. This is evident since we have geometrical similarity.

(c) Relation between stresses:

$$\frac{f_m}{f_p} = \frac{W_m}{L^2_m} \cdot \frac{L^2_p}{W_p} = \frac{W_m}{W_p} \cdot \frac{1}{n^2} \qquad \ldots\ldots(5)$$

Substituting the value of W_m from equation (3), we get:

$$\frac{f_m}{f_p} = \frac{E_m}{E_p} \qquad \ldots\ldots(6)$$

Equation (6) gives the relation between the stresses for case of geometrical similarity.

For E_m = E Aluminum = 10.5×10^6 p.s.i.

and E_p = E Concrete = 3.0×10^6 p.s.i.

we get:

$$\frac{f_m}{f_p} = \frac{E_m}{E_p} = \frac{10.5}{3.0} = 3.5 \text{ times}$$

i.e. 3500 p.s.i. in model are = 1000 p.s.i. in prototype.

Writing condition (3) in terms of figures we get:

$$\frac{W_m}{W_p} = \frac{E_m}{E_p} \cdot n^2 = \frac{10.5}{3} \cdot \left(\frac{1}{40}\right)^2 = \frac{1}{457}$$

i.e. 10 lbs. on model are equivalent in terms of equal strain to 4570 lbs. on the prototype.

3. RELATION BETWEEN MEASURED STRAINS AND CORRESPONDING STRESSES IN THE MODEL:

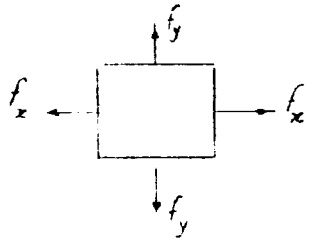

Fig. 4.3

For a plate element of an elastic material under the action of principal stresses as shown in Fig. 4.3, Hooke's Law gives the following relations between stresses and strains:

$$e_x = \frac{f_x}{E} - \mu \cdot \frac{f_y}{E} \qquad \ldots\ldots (1)$$

$$e_y = \frac{f_y}{E} - \mu \cdot \frac{f_x}{E} \qquad \ldots\ldots (2)$$

Multiplying (1) by μ we get:

$$\mu \cdot e_x = \mu \cdot \frac{f_x}{E} - \mu^2 \cdot \frac{f_y}{E} \qquad \ldots\ldots (3)$$

Adding (2) and (3):

$$e_y + \mu \cdot e_x = \frac{f_y}{E} (1 - \mu^2)$$

or

$$f_y = \frac{E}{1-\mu^2} (e_y + \mu \cdot e_x) \qquad \ldots\ldots (4)$$

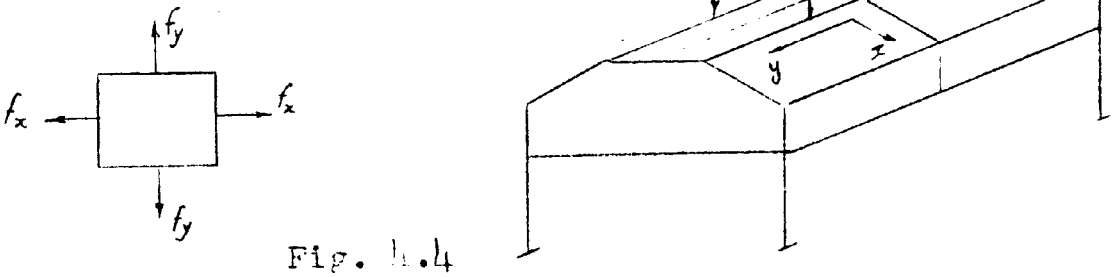

Fig. 4.4

Consider a small rectangular element of a plate at point n, on the middle section of the model Fig. 4.4, with its sides parallel to the two axes of symmetry of the model. Due to symmetry, such an element will have no shear stresses acting on its sides, and consequently its sides will be parallel to the two principal axes of stresses at that point. If we denote the longitudinal fiber stress at the top of the plate element by f_{y_1}, and that at the bottom by f_{y_2}, and write down equation (4) for both sides, we get:

$$f_{y_1} = \frac{E}{1-\mu^2} (e_{y_1} + \mu \cdot e_{x_1})$$

$$f_{y_2} = \frac{E}{1-\mu^2} (e_{y_2} + \mu \cdot e_{x_2})$$

Adding and dividing by 2 we get:

$$1/2(f_{y_1} + f_{y_2}) = \frac{E}{1-\mu^2} \left[1/2(e_{y_1} + e_{y_2}) + \frac{\mu}{2} (e_{x_1} + e_{x_2}) \right] \qquad (5)$$

In these equations tensile stresses and strains are considered positive. Equation (5) will be put in a simpler and more convenient form for use in experimental investigation after the following discussion:

The forces causing direct stresses, which act on the plate element at point n, are shown on Fig. 4.5.

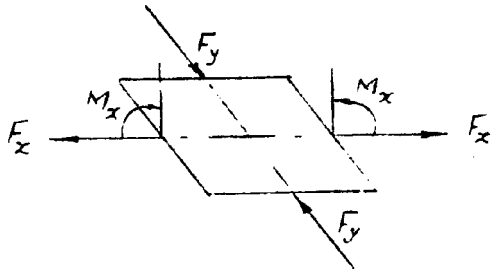

Fig. 4.5

F_y : is the longitudinal direct force due to the external bending moment acting on the middle section of the model. It causes uniform compression across the entire thickness of the element considered.

F_x : is the transverse direct force due to the tensile or compressive forces acting from the joints, on the plates in the transverse direction.

M_x : represents the bending moment acting on the roof slab in the transverse direction, and caused in this case by the relative deflection of the joints.

Referring back to the analytical solution of the same problem in example 2, it is useful here to indicate that:

(1) The longitudinal direct stress f_y at the middle plane of the top plate, due to F_y, is equal to -925 p.s.i.

(2) The portions of the transverse direct stresses f_{x_1} and f_{x_2} at n caused by the direct transverse force F_x, are equal to:

$$f'_{x_1} = +16.60 \text{ p.s.i.}$$

$$f'_{x_2} = +16.60 \text{ p.s.i.}$$

(3) The portions of the transverse direct stresses f_{x_1} and f_{x_2}, caused by the transverse bending moment M_x, are equal and of opposite signs:

$$f''_{x_1} = -1440 \text{ p.s.i.}$$

$$f''_{x_2} = +1440 \text{ p.s.i.}$$

(4) The ratio of $\frac{f'_x}{f''_x} = \pm \frac{16.6}{1440} = \pm 1.15\%$

This indicates the very small effect that the direct force F_x has on the stresses, compared to the effect of M_x or F_y.

In equation (5) each of the strains e_{x_1} and e_{x_2} can be split up into three parts as shown in Fig. 4.6.

Strains due to:

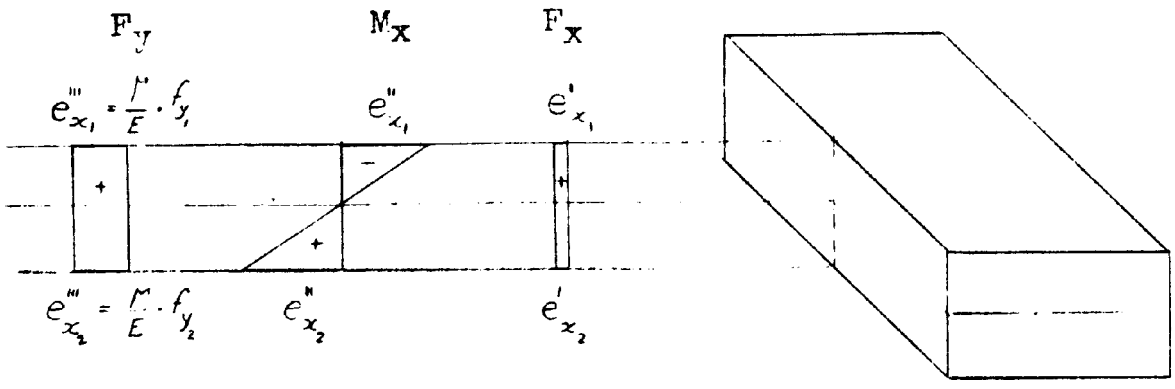

Fig. 4.6
Transverse strain

Now it can be easily noticed that:

(1) The portion e'_x due to direct transverse forces F_x is negligible compared to the other two components e''_x and e'''_x due to M_x and F_y respectively.

(2) The strains e''_{x_1} and e''_{x_2} due to M_x are equal and opposite.

Therefore the term $(e_{x_1} + e_{x_2})$ in equation (5) can be put equal to:

$$e_{x_1} + e_{x_2} = (e'_{x_1} + e'_{x_2}) + (e''_{x_1} + e''_{x_2}) + (e'''_{x_1} + e'''_{x_2})$$

$$= e'''_{x_1} + e'''_{x_2}$$

$$= \frac{\mu}{E} (f_{y_1} + f_{y_2})$$

Substituting this in equation (5) we get:

$$1/2(f_{y_1} + f_{y_2}) = E/2(e_{y_1} + e_{y_2}) \quad \ldots\ldots (6)$$

The left hand side of equation (6) represents the longitudinal stress at the middle plane of the plate. The right hand

side represents the average of the longitudinal strains measured at the top and at the bottom surfaces of the plate. Equation (6) can also be obtained directly if we put $f_x = 0$ in equations (1) and (2).

In our investigation, as far as the longitudinal direction is concerned, we are interested in the longitudinal stresses f_y acting at the middle plane of each plate. As for the transverse direction, we are interested in both f_{x_1} and f_{x_2}, i.e. the maximum positive and negative fiber stresses. For this reason the longitudinal strain gages, used to measure the longitudinal strain at a point, were fixed on the model, one on each side of the plate, and then coupled together in series. The reading of the strain indicator, therefore, gave the average strain $1/2(e_{y_1} + e_{y_2})$. Using equation (6), f_y (average) $= 1/2(f_{y_1} + f_{y_2})$ is readily obtained. In the transverse direction the gages on both sides of a plate were wired independently, and thus giving the transverse strains at the outer and inner surface of the roof separately.

4. SUMMARY OF EXPERIMENTAL RESULTS AND COMPARISON WITH THEORETICAL VALUES:

The distribution of longitudinal strains at the middle section of the model, for a total load of 233.4 lbs. (58.35 lbs. at each point) is shown in Figure 2a. on Sheet 2, Appendix I. The corresponding transverse strains -82, -96,

+140 and +143 micro-inches are recorded in Figure 2b. The difference between the readings on the top and bottom of the plate are due to the transverse effect of the longitudinal strains. The true value of the transverse strain is the average or

$$\frac{82 + 140}{2} = \pm 111 \text{ and } \frac{96 + 143}{2} = \pm 119.$$

This checks quite closely with:

$$(-82) - (1/3)(78) = -108 \text{ micro-inches/inch}$$
$$(+140) - (1/3)(78) = +114 \quad " \quad " \quad "$$
$$(-96) - (1/3)(78) = -122 \quad " \quad " \quad "$$
$$(+143) - (1/3)(78) = +117 \quad " \quad " \quad "$$

where (1/3)(78) is Poisson's ratio (1/3) times the longitudinal strain -78 micro-inches.

The longitudinal strains at sections d - d and e - e (see Figures 1d and 1e) are shown in Figures 3a and 3b on Sheet 3. Transverse strains at section d - d are also shown in Figure 3c. These diagrams show that the action at section d - d is similar to that at the middle section c - c. In fact the strains at these sections are nearly proportional to the bending moments. At section e - e, however, where the translation of the edges is small, the distribution of strain approaches more nearly to that for ordinary beam action although some effect of change of shape of the cross-section is apparent.

The vertical displacements of the edges are shown in Figure 4 and the horizontal movements in Figure 5 (see Sheets 4 and 5.) It is interesting to note that the vertical movement of the elements AB and A'B' is upward which agrees with the theoretical value that was obtained. This motion is comparatively small, but nevertheless, it is very significant. The horizontal movements of edges B and B' are of the same order of magnitude as the vertical movement of C and C'. As shown on the diagrams, the calculated values of the displacements (see illustrative example 2, Chapter III) agreed quite well with the measured values.

The theoretical and experimental values of the longitudinal and transverse stresses are shown in Figures 6 and 7 on Sheets 6 and 7. It should be noted that the experimental values indicate clearly that the structure does not behave as a unit according to the ordinary beam theory. The actual measured longitudinal stresses as shown in Figure 6 are fairly linear across each plate element, but are not proportional to the distances from the centroid of the entire cross-section. On the other hand, the longitudinal stresses obtained from consideration of plate action without involving the effect of the translation of the edges, as discussed by Winter and Pei,[12] are considerably higher than the measured values. The measured stresses at edges A and A' are opposite in sign from the computed values for plate action when no translation is considered.

However, when the relative displacements of the edges, as shown in Figure 8, were considered in the solution proposed in this thesis the calculated stresses and displacements agreed much better with the experimental results. A graphical comparison of the stresses for the different assumptions is shown in Figure 6. A comparison of the theoretical and measured edge translations is shown in Figure 8 on Sheet 8.

The correction diagram for the effect of translation is shown separately in Figure 6. It can be shown that if these values are multiplied by a proper constant and subtracted algebraically from the values obtained by the ordinary beam theory for the entire cross-section, the results will agree closely with the experimental values. On the other hand, if the stresses due to translation are multiplied by a proper constant and added algebraically to the results obtained from plate action which neglects the edge displacements, the combined effect agrees closely with the experimental results. This comparison, therefore, brings up the question as to which analytical approach may be desirable, a question which will be discussed in the next article.

The effect of translation of the edges has also been checked from the transverse stresses. The theoretical distribution of maximum flexural stress in the transverse direction at sections c - c and d - d is shown in Figure 7. The measured values of the stresses are indicated by circles. It can be

seen that the agreement is quite satisfactory and confirms the remarks previously made as to the importance of relative translation of the edges.

5. DIFFERENCE BETWEEN HIPPED PLATE STRUCTURES AND ORDINARY BEAMS:

In case of hipped plate structures the thickness of each plate element is relatively small compared to the other dimensions of the cross-section of the structure. Consequently the section of the structure changes its shape under loading, and the part of the load carried by each plate element varies according to the position of the load on the cross-section. We also have forces and bending moments acting in the transverse direction. The idea of plane before deformation remaining plane after deformation does not hold for the cross-section as a whole, except under very special cases of loading, but it holds fairly well for each individual plate element, especially for cross-sections away from the diaphragm. See the measured longitudinal strains given on Sheets 2 and 3.

When we speak of a member behaving under load as a beam, we are actually putting on it several restrictions. The thickness of the member should be large enough compared to the other dimensions of the cross-section so as to keep the cross-section from changing its shape when the member is deflected longitudinally under loading. The section will

just move parallel to itself and the whole cross-sectional plane before bending will remain plane after it. No transverse bending or deflection can exist under the limitations for beam action, otherwise the section will change its shape. The longitudinal stress distribution over the cross-section is not affected by the manner in which the load is applied, or its point of application, so long as the load is symmetrical with respect to the axis of the cross-section, Fig. 4.7.

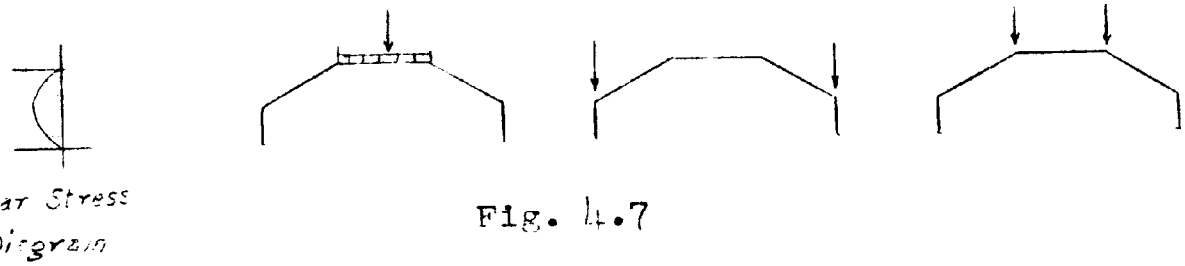

Fig. 4.7

The share of each plate element of the member from the applied load is a constant ratio of the total load, a ratio which is defined by the share of the same plate element from the total shear stress diagram on the cross-section. Beam action can be a very special case of a hipped plate structure under the following conditions:

External forces are either line loads or concentrated loads acting only at the edges or distributed loads which are tangential to the plates, and distributed in a special manner such that the resultant P-load on each individual plate is proportional to its corresponding share of the shear stress diagram on the whole section, assumed to act as a beam. Any distributed load or concentrated load

acting in between the joints will result in transverse bending, and consequently, a change in the shape of the cross-section.

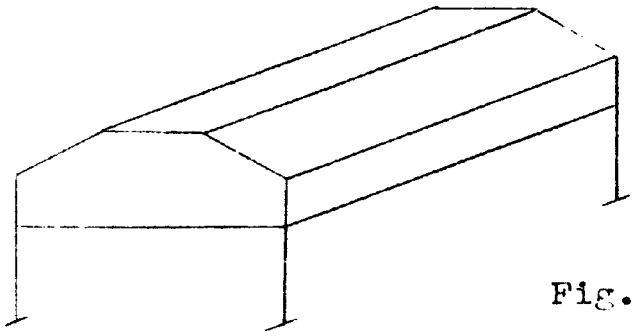

Fig. 4.8

From this discussion it is evident that, if we try to solve a hipped plate roof similar to that of Fig. 4.8, by beginning from the preliminary assumption of a beam action and trying to correct it to arrive at the stresses of a hipped plate structure, then we will have to apply two corrections for the stresses got from beam action, namely:

1. Stresses due to the difference between the plate loads P included in the assumption of beam action, and the plate loads P got from the actual external loads. Under the preliminary assumption of beam action a certain portion of the total loads will have to be carried by each plate element which is not necessarily the case. However, beam action can be acquired by applying certain restraining line loads along the joints, which must be removed by means of the first correction. The analytical work for carrying out this correction is very similar to that used in correcting for the relative displacements of the joints.

2. Stresses corresponding to the change in the P-loads due to the relative deflections of the joints must be determined, since the beam action does not take care of the transverse deflections. The procedure for this correction has already been discussed before.

It can be seen from the above discussion that the amount of the analytical work will be increased by trying to solve the problem from the beam action approach, in as much as we cannot escape the necessary correction for the relative displacements of the joints.

6. CONCLUSIONS:

The results presented in this dissertation illustrate and emphasize the importance of a careful examination of the basic assumptions of any theory by experimental tests before developing an analytical solution. The experimental study of a hipped plate structure by means of a model provided the following conclusions:

(a) A (24S.T.) aluminum model is both convenient and satisfactory for studying the structural action of hipped plate roofs.

(b) The results obtained from tests on a 1/40 scale aluminum model show that the change in shape of the cross-section due to translation of the edges is important. It appears to dominate the structural action over the middle 2/3 of the span.

(c) An analysis by the Ehlers and Craemer theory as proposed by Winter and Pei, or by beam action, does not agree with the test results unless the values obtained by such assumptions are corrected for the effect of relative edge translation. The longitudinal stresses obtained from the Ehlers and Craemer theory are considerably higher than the measured values. The following table gives the maximum longitudinal stresses at the middle section of the model according to:

Case 1. The Ehlers and Craemer theory which neglects the effect of change of shape of the cross-section.

Case 2. The experimental values obtained from tests on the model.

Case 3. The method of analysis proposed in this thesis which considers the effect of the change in shape of the cross-section.

Case 4. Beam action theory.

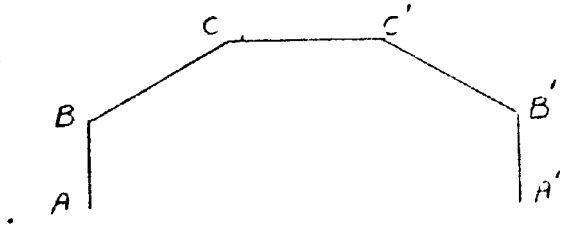

Fig. 4.9

Maximum Longitudinal Stresses p.s.i.

Edge	Case (1)	Case (2)	Case (3)	Case (4)
C	-1360	-820	-925	-537
B	+2000	+740	+1020	+166
A	-1000	+378	+122	+1102

(d) The stresses in the transverse direction which rule for the design of the plates as a continuous slab, are even more seriously affected by edge translation. The values obtained from the German theory are considerably lower than the measured values. The necessary correction for such stresses may be up to 320% (see example 1, Chapter III). In a case of concentrated loads at the joints (example 2, Chapter III),

while the German theory does not consider any transverse stresses due to the joints displacement, the maximum transverse stresses were experimentally found to be 15$\frac{1}{4}$% of the maximum longitudinal stresses. The following table gives the maximum fiber stresses due to transverse bending in a strip 1.0 inch wide at the middle of the model according to:

Case 1. The Ehlers and Craemer theory.

Case 2. The experimental values obtained from tests on the model.

Case 3. The method of analysis proposed in this thesis.

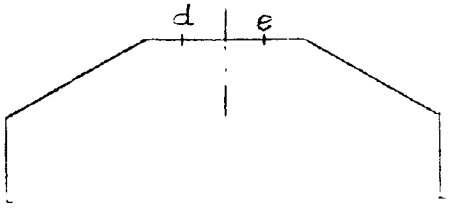

Fig. 4.10

Maximum Transverse Stresses p.s.i.

Point	Case 1	Case 2	Case 3
d	0.0	∓1170	∓1440
e	0.0	∓1260	∓1440

Similarly, the above discussion holds true for the case of distributed loads applied tangentially to the plates.

(e) It is recommended that more extended investigations be made by similar model studies. Some of the points that are worth investigating are:

1. Effect of intermediate diaphragms.

2. Behavior of models just before failure.
3. Effect of change of thickness t, width h, and span L of plate elements, on the behavior of the model.
4. Effect of the shape of the cross-section of a roof on the behavior of the model.
5. Study of reinforced concrete models.
6. Deep beam action.
7. Effect of additional spans in both directions.

APPENDIX I

1. DIAGRAMS AND EXPERIMENTAL DATA.

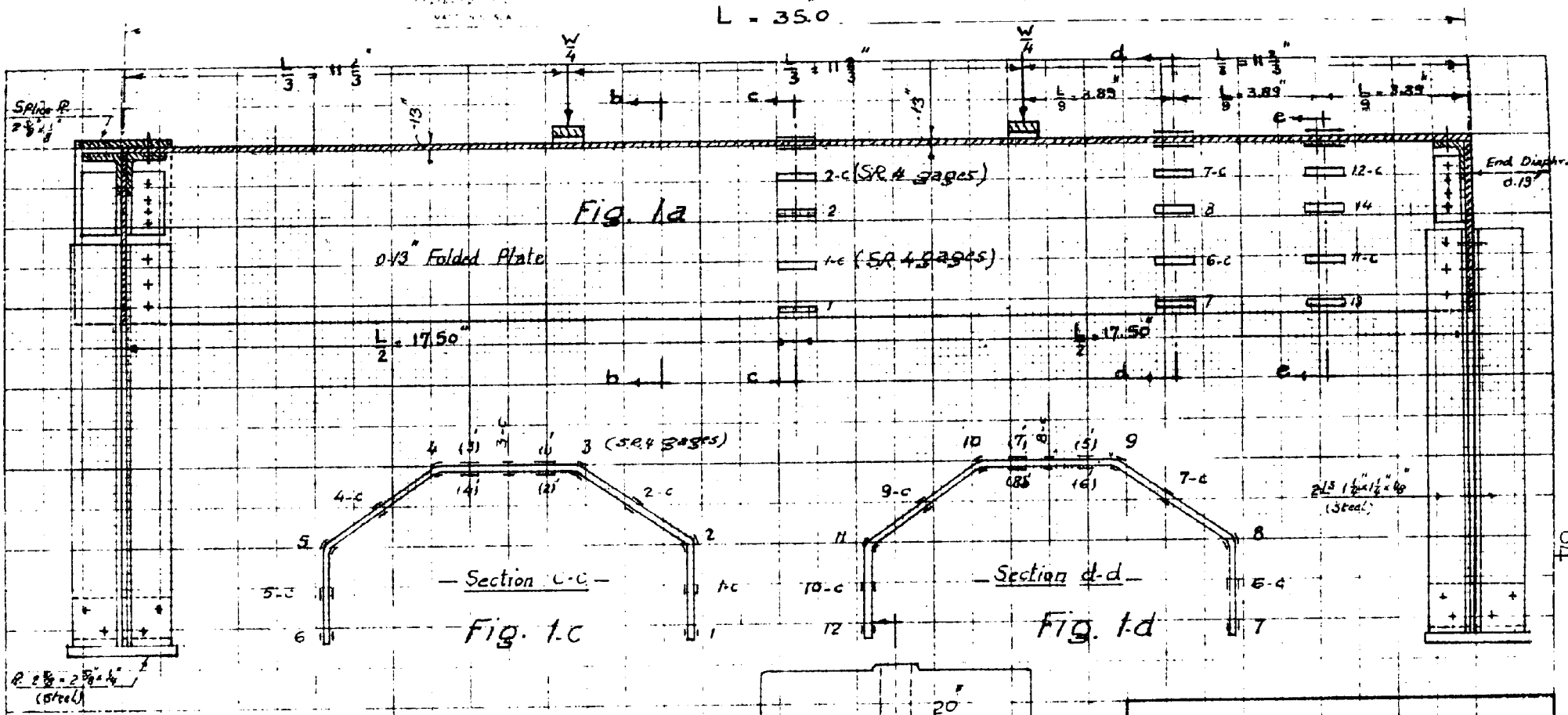

Fig. 1a

Fig. 1c

Fig. 1d

Fig. 1e

Fig. 1f

Fig. 1b

University of Michigan
Structural Models Lab

Aluminum Model of Flipped-plate Roof

Scale of Model 1/40

Scale of Drawing 1:4

Material 24ST Alum. Unless noted

U. of Mich.	I. A. GAMFAR	12.27.68

Sheet 1

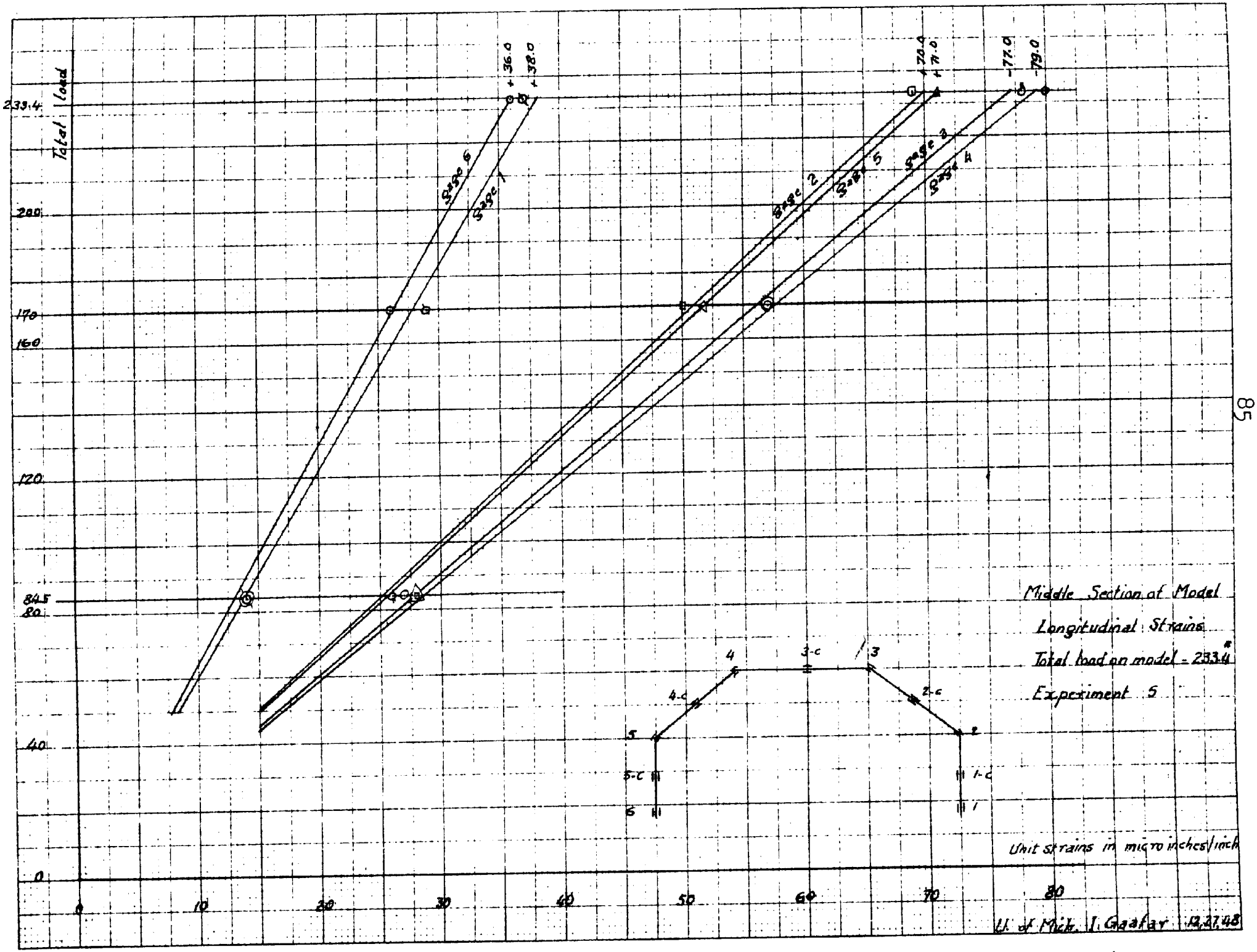
Total load
233.4
200
170
160
120
84.5
80
40
0
0
10
20
30
40
50
60
70
80
+36.0
+38.0
+70.0
+74.0
-77.0
-80.0
S 39 c 6
S 39 c 5
S 39 c 2
S 39 c 3
S 39 c 4
4
3-c
3
4-c
2-c
5
5-c
6
1-c
1
Middle Section of Model
Longitudinal Strains
Total load on model - 233.4#
Experiment 5
Unit strains in micro inches/inch
U. of Mich. I. Gaafar 12.27.48

85

Sheet 1.

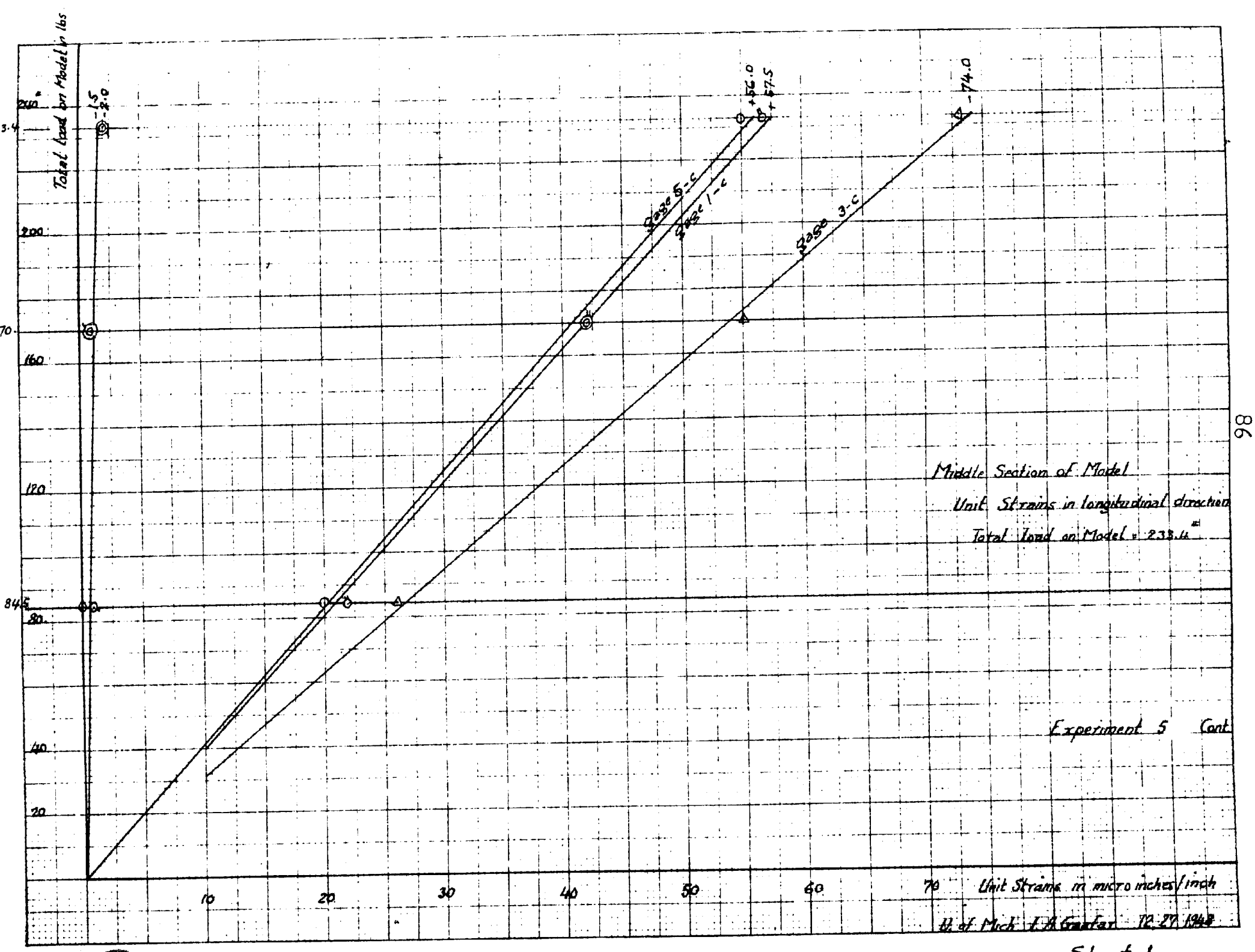
Total load on Model in lbs
240
200
160
120
80
40
20
3.4
70
84.5
-1.5
-2.0
+56.0
+67.5
-74.0
Gage 5-C
Gage 1-C
Gage 3-C
Middle Section of Model
Unit Strains in longitudinal direction
Total load on Model = 238.4
Experiment 5 Cont
10
20
30
40
50
60
70
Unit Strains in micro inches/inch
U. of Mich. J.B. Gratfar 12.27.1944

86

Sheet 100

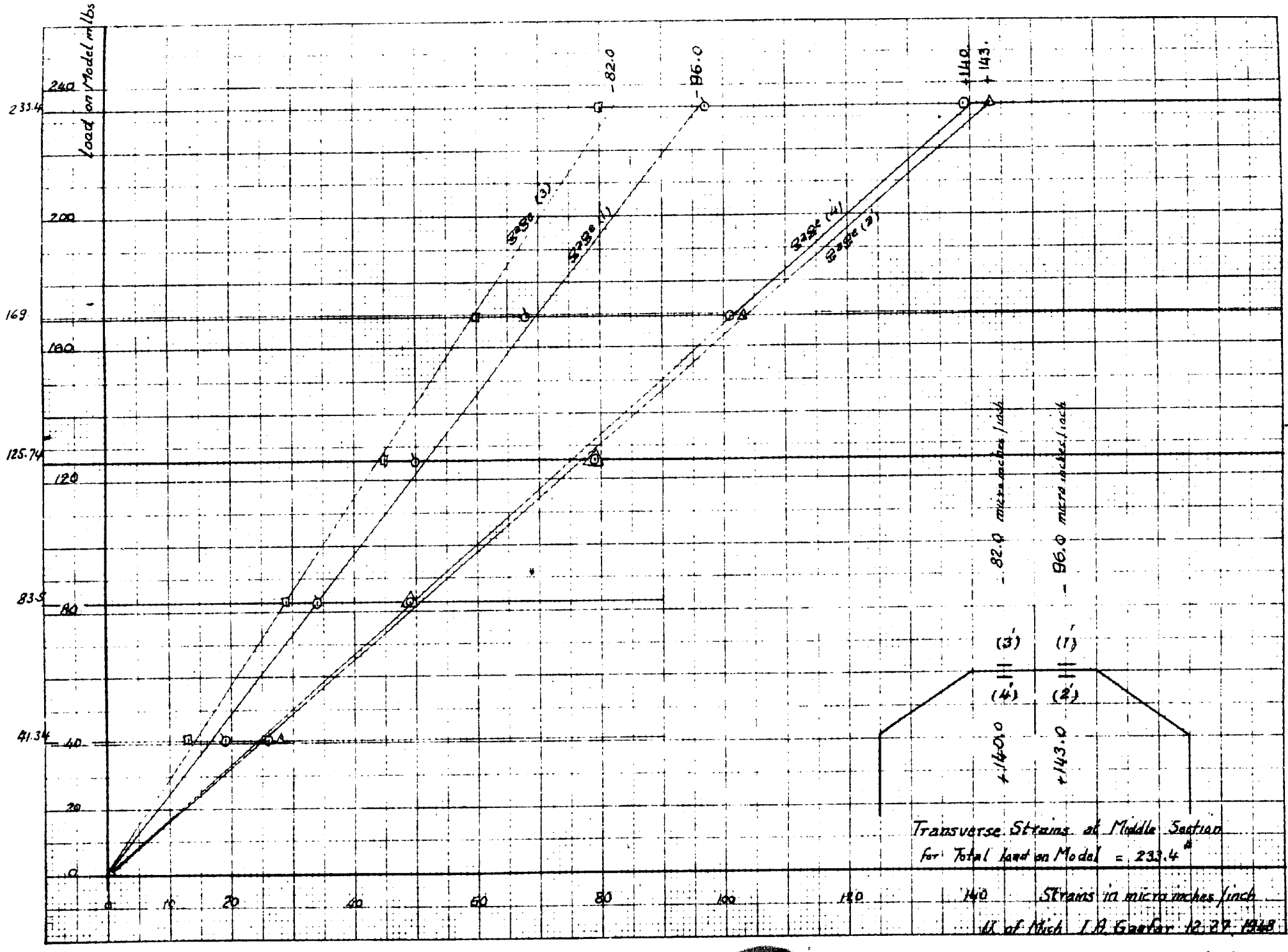
Load on Model in lbs
240
233.4
200
169
125.74
120
83.5
80
41.34
40
20
0
-82.0
-86.0
+140
+143.
S22S (3)
S22S (1)
S22S (4)
S22S (2)
0
10
20
40
60
80
100
120
140
- 82.0 micro inches / inch
- 86.0 micro inches / inch
(3')
(1')
(4')
(2')
+140.0
+143.0
Transverse Strains at Middle Section
for Total Load on Model = 233.4#
Strains in micro inches / inch
U of Mich I.A. Gaertner 12-27-1948

Sheet 1000

N.B.: Total load on Model = 233.4 #

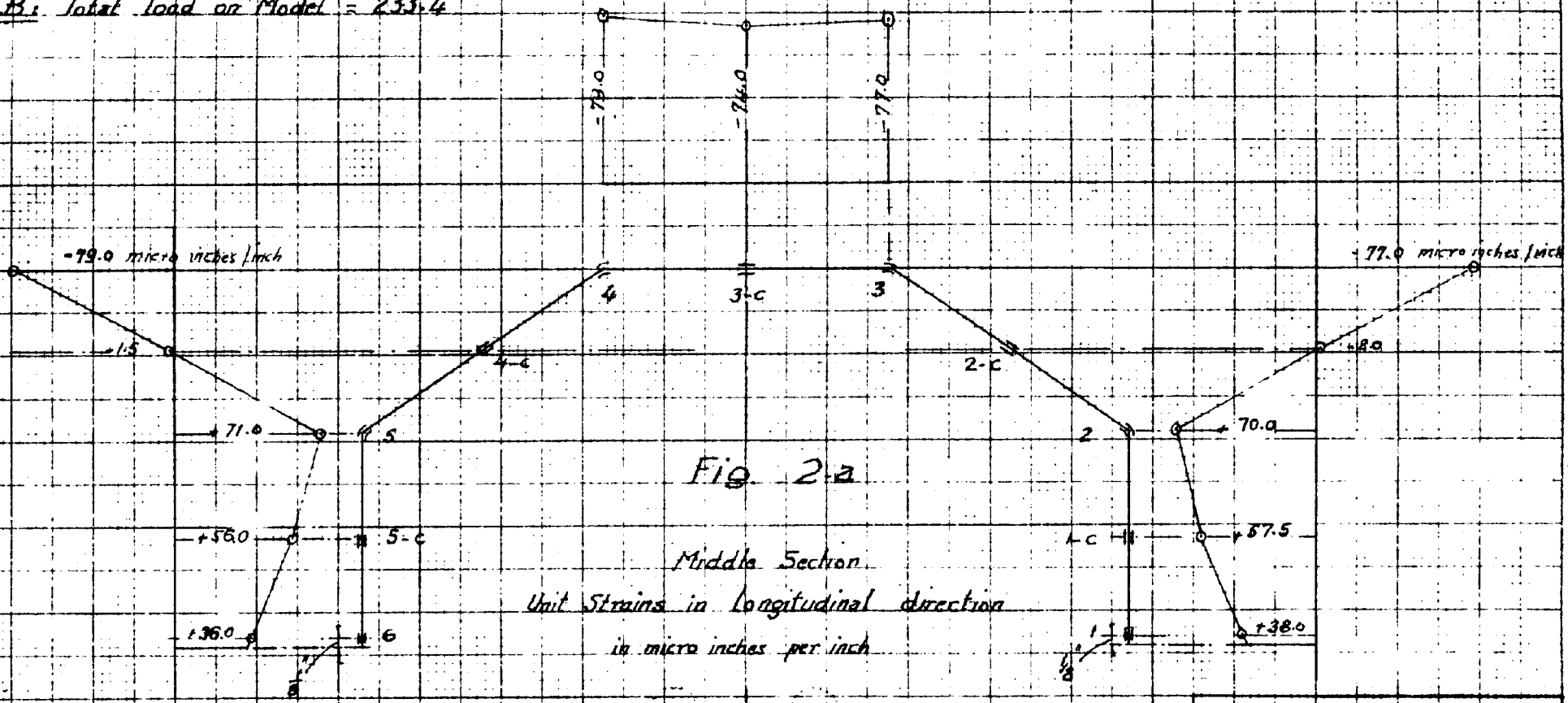

Fig. 2-a

Middle Section

Unit Strains in Longitudinal direction

in micro inches per inch

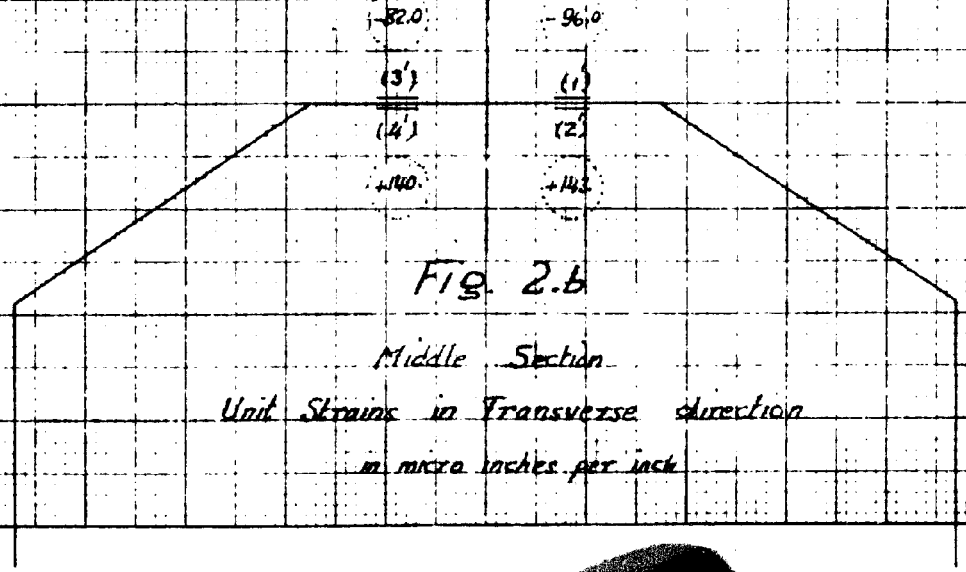

Fig. 2-b

Middle Section

Unit Strains in Transverse direction

in micro inches per inch

University of Michigan

Structural Models Lab.

Aluminum Model

of

Hipped-plate Roof

Unit Strains at Middle Section

Scale: 1"=2" x 1"-80 micro inches/inch

U of Mich. | I. A. GARFAR | 12.28.1948

Sheet 2

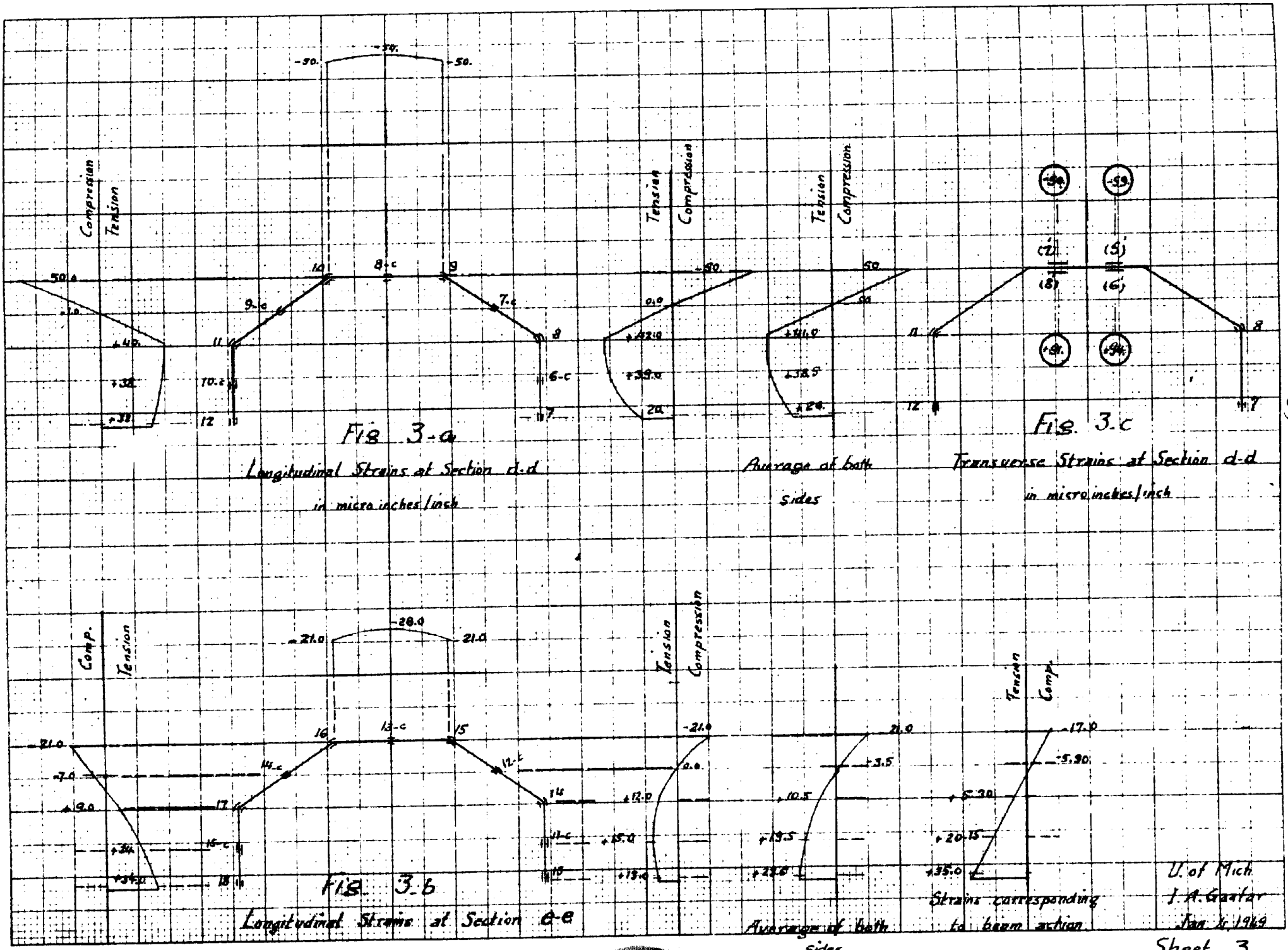

Fig 3-a

Longitudinal Strains at Section d-d

in micro inches/inch

Average of both sides

Fig. 3.c

Transverse Strains at Section d-d

in micro inches/inch

Fig. 3.b

Longitudinal Strains at Section e-e

Average of both sides

Strains corresponding to beam action

U. of Mich

J. A. Gaafar

Jan 6, 1949

Sheet 3

89

Vertical Displacements of The Edges:

+ = Downwards

− = Upwards

Unit of Displacements is = 1/1000 "

Scale 1" = .020"

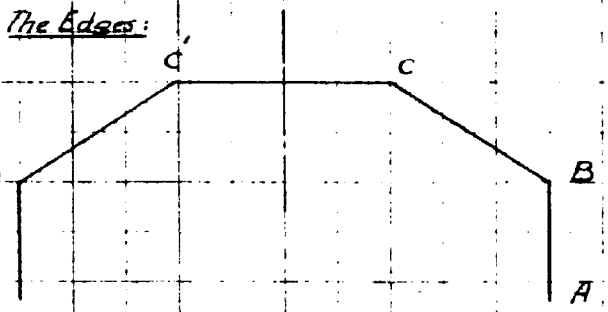

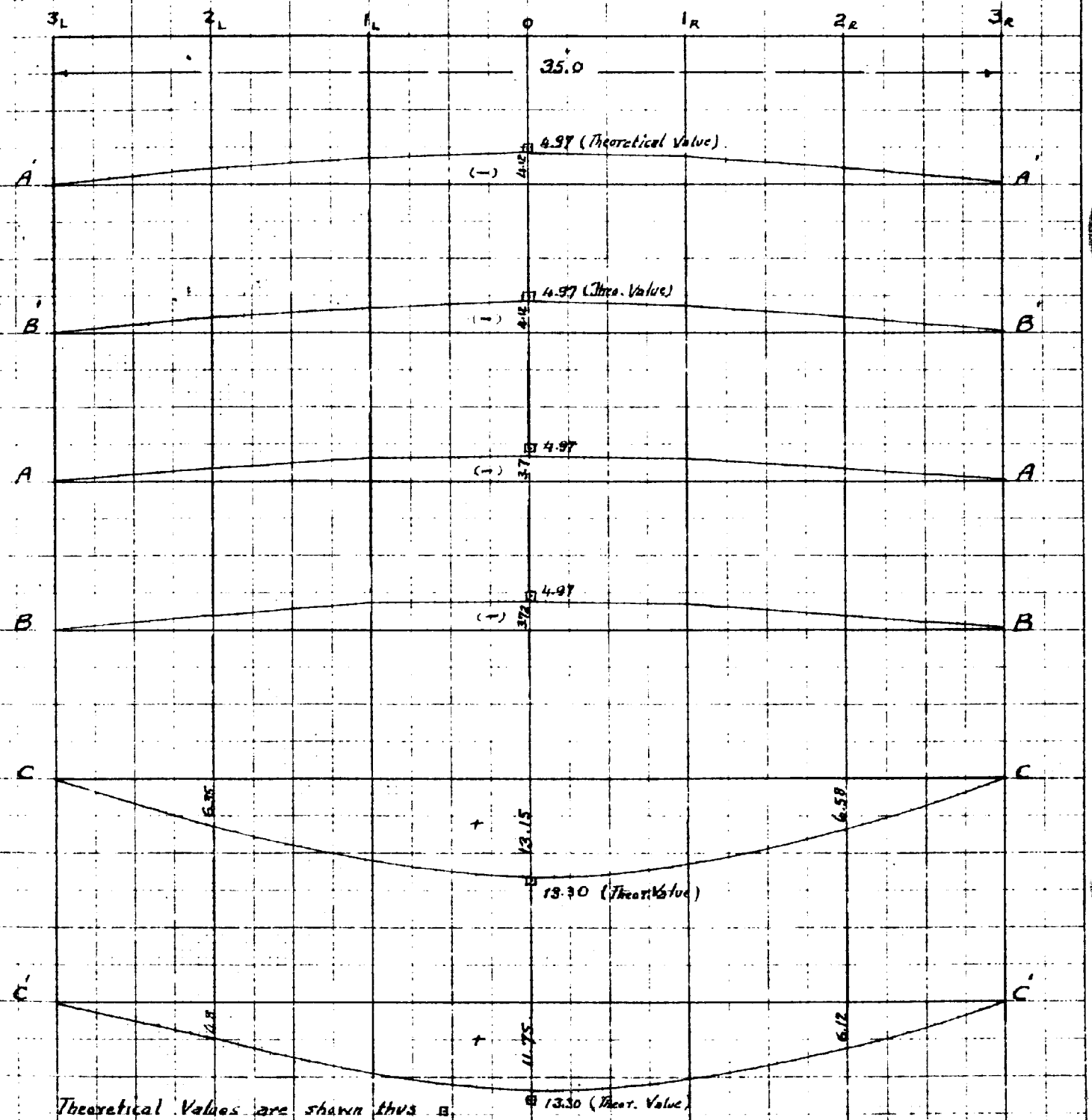

Theoretical Values are shown thus ⊡

Total load on Model = 233.4 lbs

U. of Mich. I. A. GAAFAR Jan. 4, 1942

Sheet 4

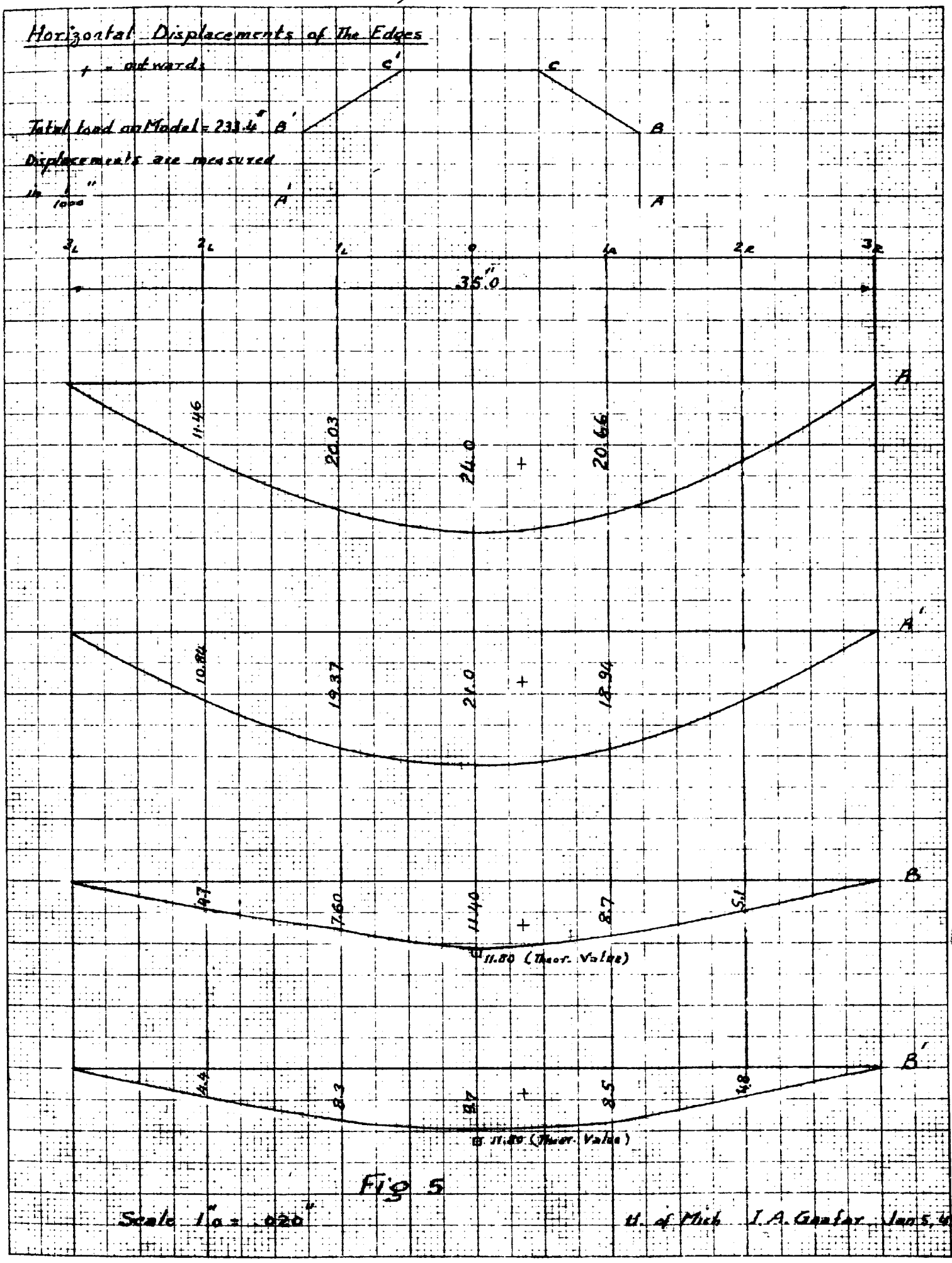

Fig 5

Scale 1" = .020"

U. of Mich I.A. Glaser Jan 5, 47

Sheet 5

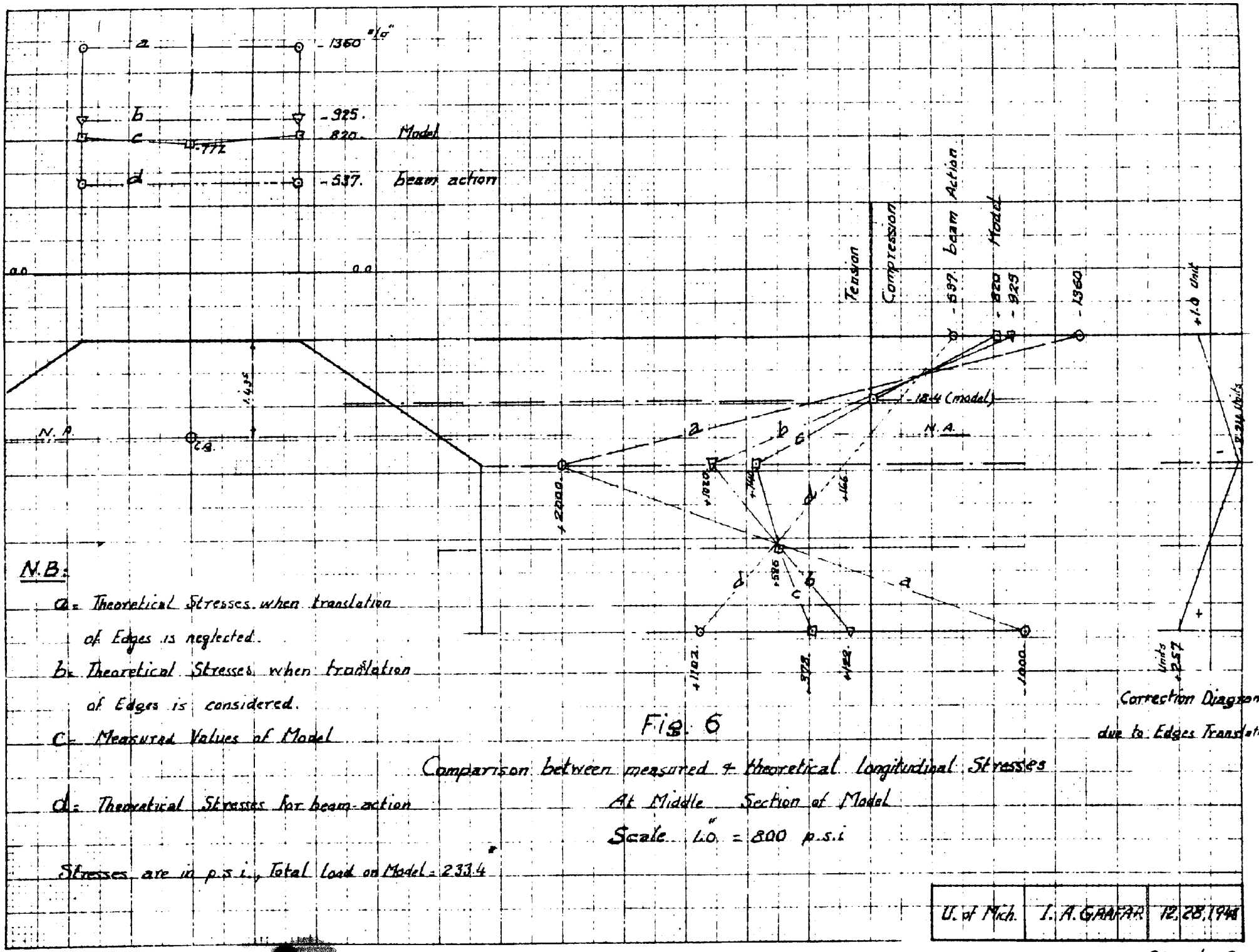

N.B:

a = Theoretical Stresses when translation of Edges is neglected.

b = Theoretical Stresses when translation of Edges is considered.

c = Measured Values of Model

d = Theoretical Stresses for beam-action

Stresses are in p.s.i, Total load on Model = 233.4

Fig. 6

Comparison between measured & theoretical longitudinal Stresses

At Middle Section of Model

Scale 1.0" = 800 p.s.i

U. of Mich.	I. A. GAAFAR	12.28.1948

Sheet 6

92

N.B. Total load on model = 2333.4 lbs

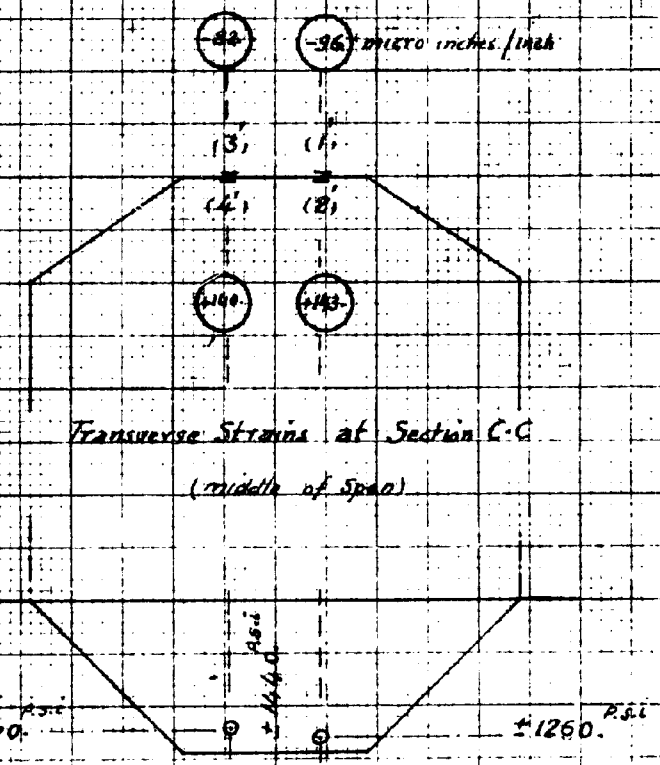

Transverse Strains at Section C-C
(middle of Span)

Theoretical Transverse Flexural Stress
at Section C-C

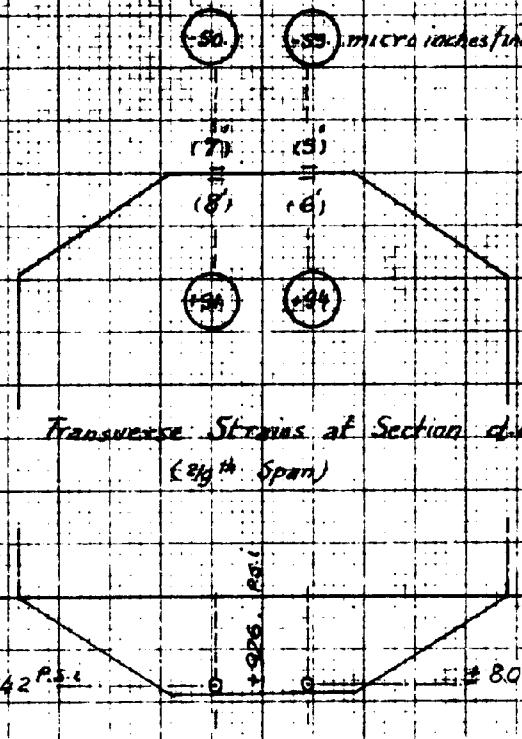

Transverse Strains at Section d-d
(2/9th Span)

Theoretical Transverse Flexural Stress
at Section d-d

Scale 1" = 2000 P.S.i

Experimental Values are indicated by ⊙

Fig 7

U. of Mich. I. Gamlen Jan. 1935

Sheet 7

93

Theoretical and Experimental Values of Edge Deflections

Total Load on Model = 233.4 lbs.

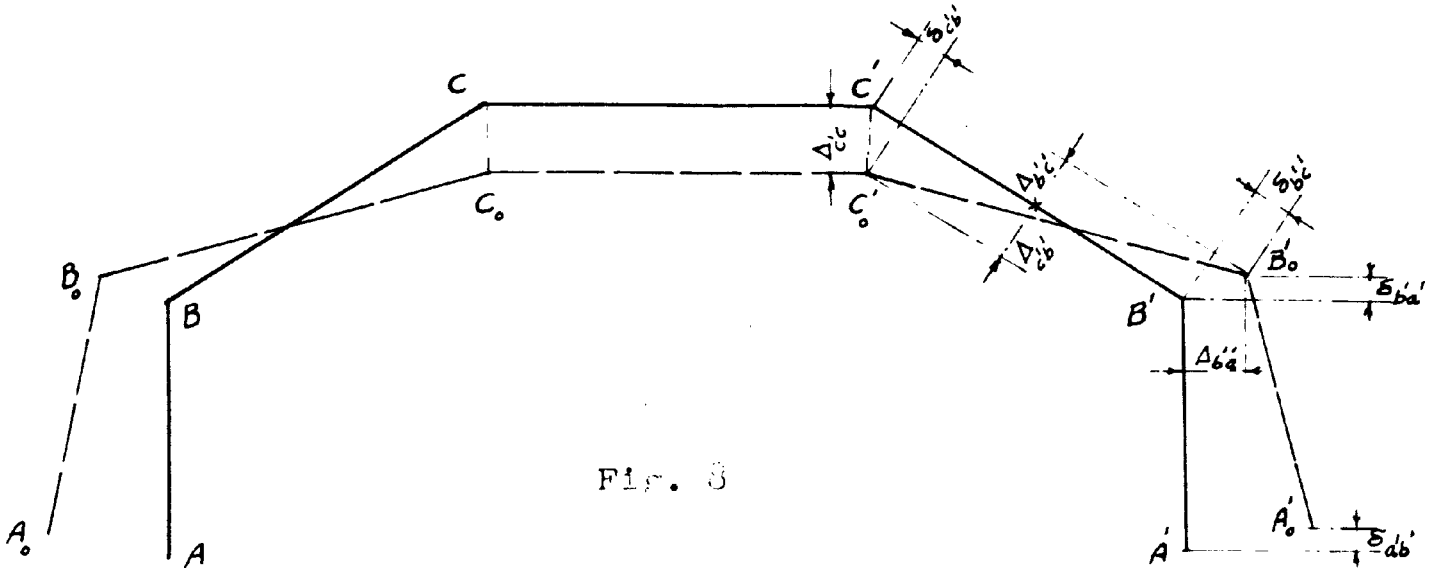

Fig. 8

Deflections at the Middle of the Model

Deflections	Theoretical Values in inches	Experimental Values in inches
$\delta_{a'a'}$	.00497	.00412
$\delta_{a'a'}$	.00497	.00412
$\Delta_{a'a'}$	.0117	.0097
$\Delta_{aa'}$	.0113	.0114
$\Delta_{b'c'}$	.0105	.0092
$\Delta_{c'b'}$	.0112	.0099
Δ_{cb}	.0112	.0111
$\Delta_{cc'}$	.0133	.0131

U. of Mich. I. Gaafar
1, 4, 49
Sheet 8

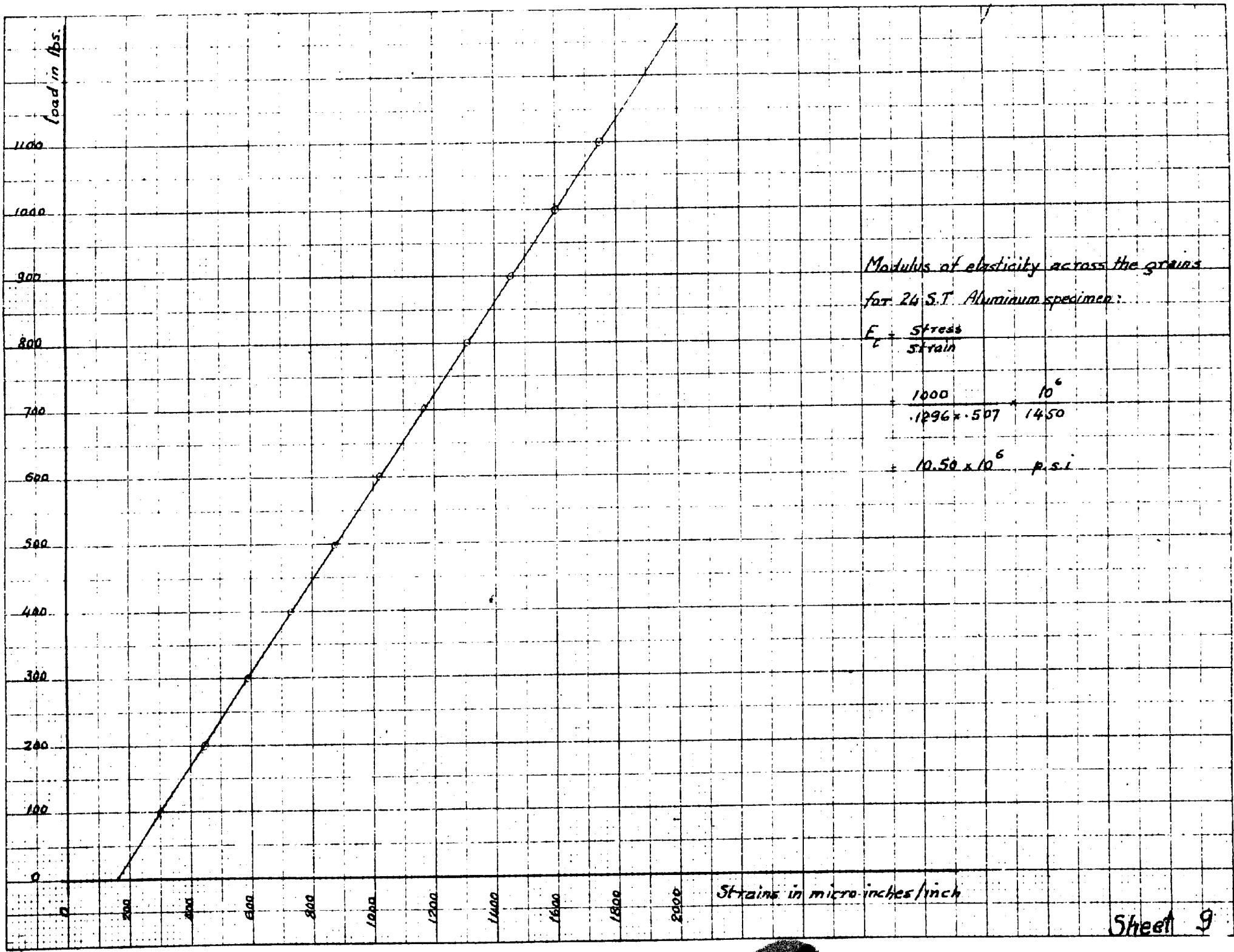

Modulus of elasticity across the grains for 24 S.T Aluminum specimen:

$E_t = \frac{\text{Stress}}{\text{Strain}}$

$= \frac{1000}{.1296 \times .507} \times \frac{10^6}{1450}$

$= 10.50 \times 10^6$ p.s.i

Sheet 9

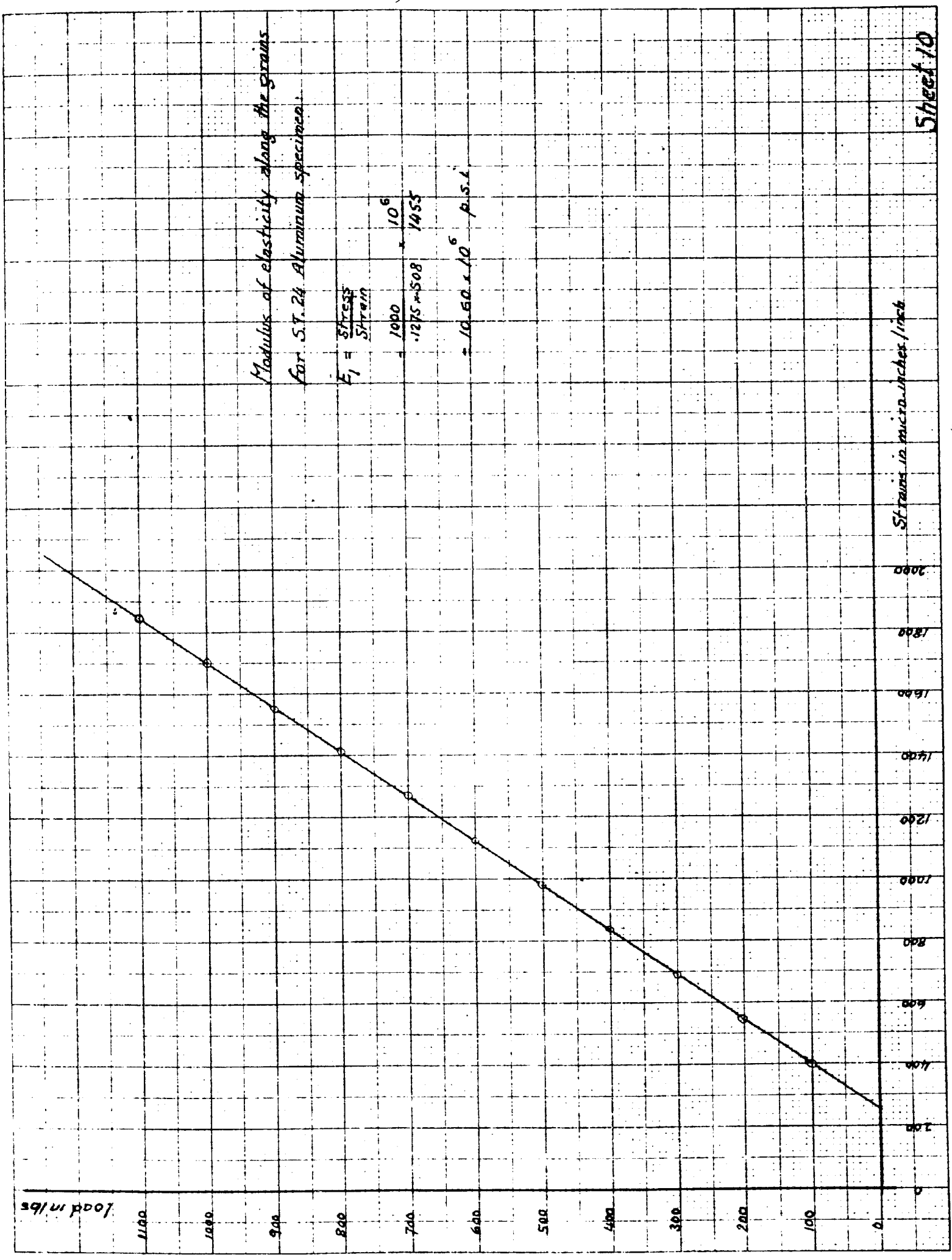
Sheet 10
Modulus of elasticity along the grains
for S.T.24 Aluminum specimen.
$E_1 = \frac{\text{Stress}}{\text{Strain}}$
$= \frac{1000}{.1275 \times 508} \times \frac{10^6}{1455}$
$= 10.60 \times 10^6$ p.s.i.
Load in lbs
Strains in micro-inches/inch
0
100
200
300
400
500
600
700
800
900
1000
1100
200
400
600
800
1000
1200
1400
1600
1800
2000

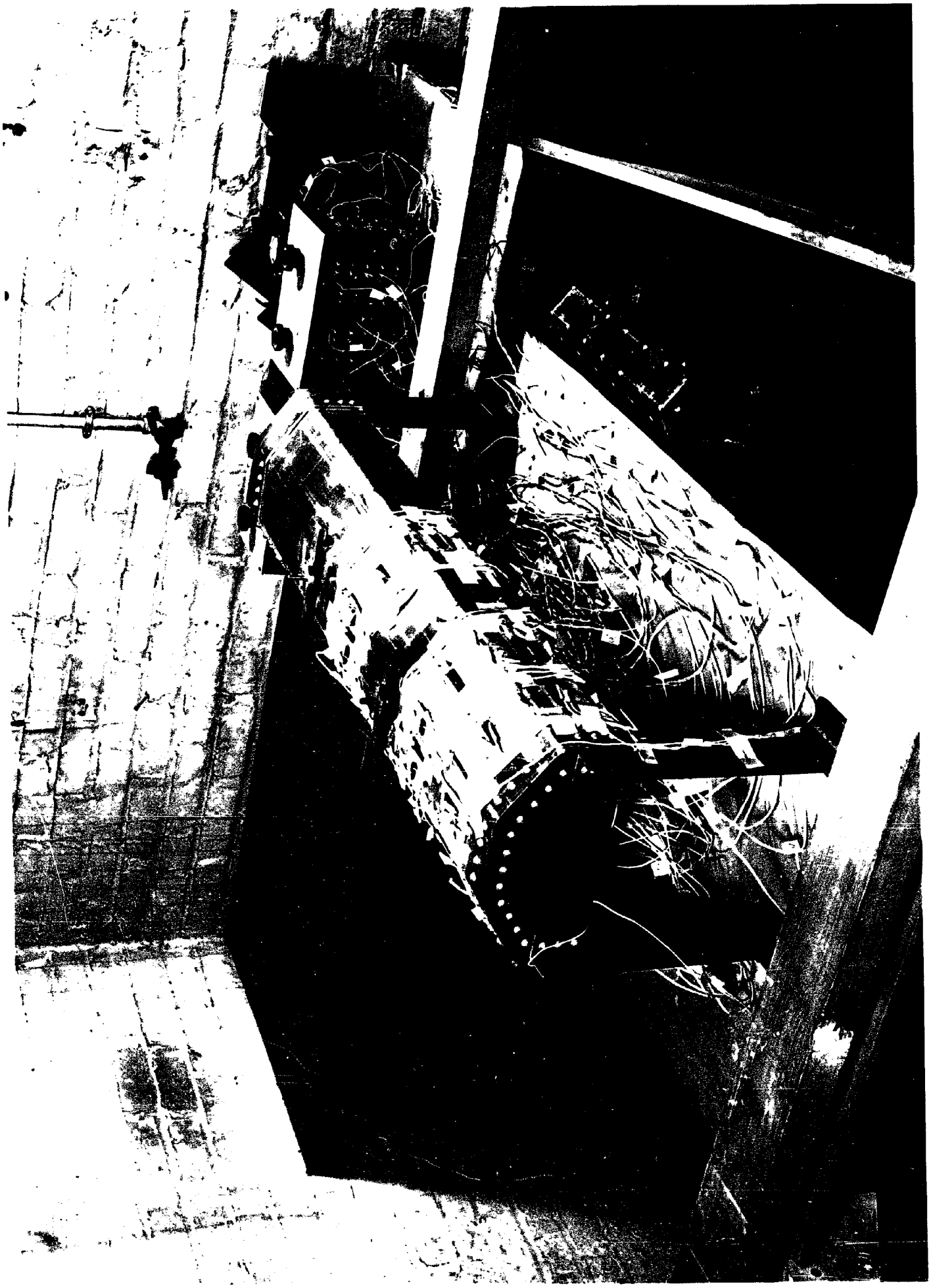

The Aluminum Model,
Strain Gages, and Strain Indicator

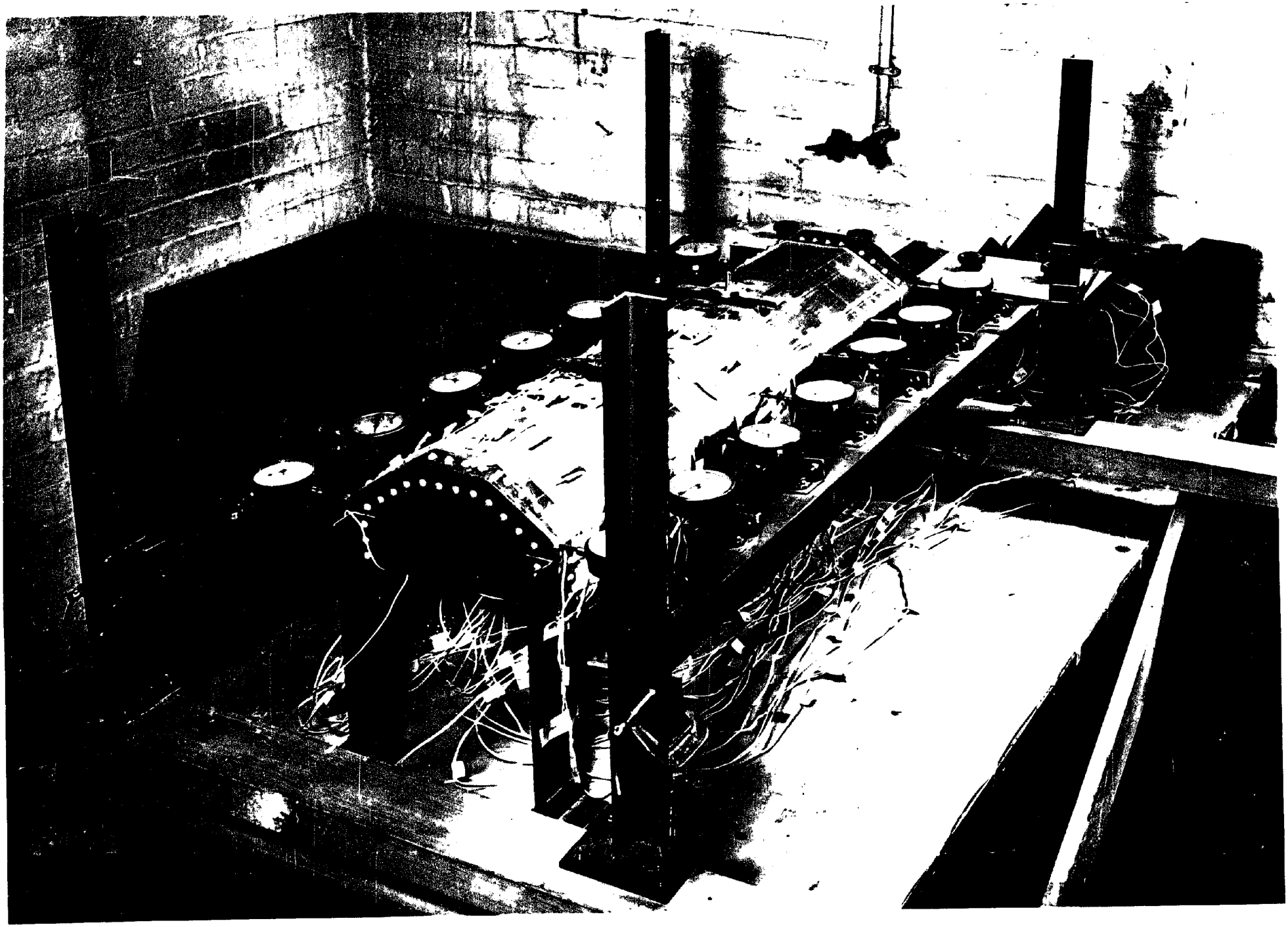

The Model and Dial Gages
for Measuring Displacements

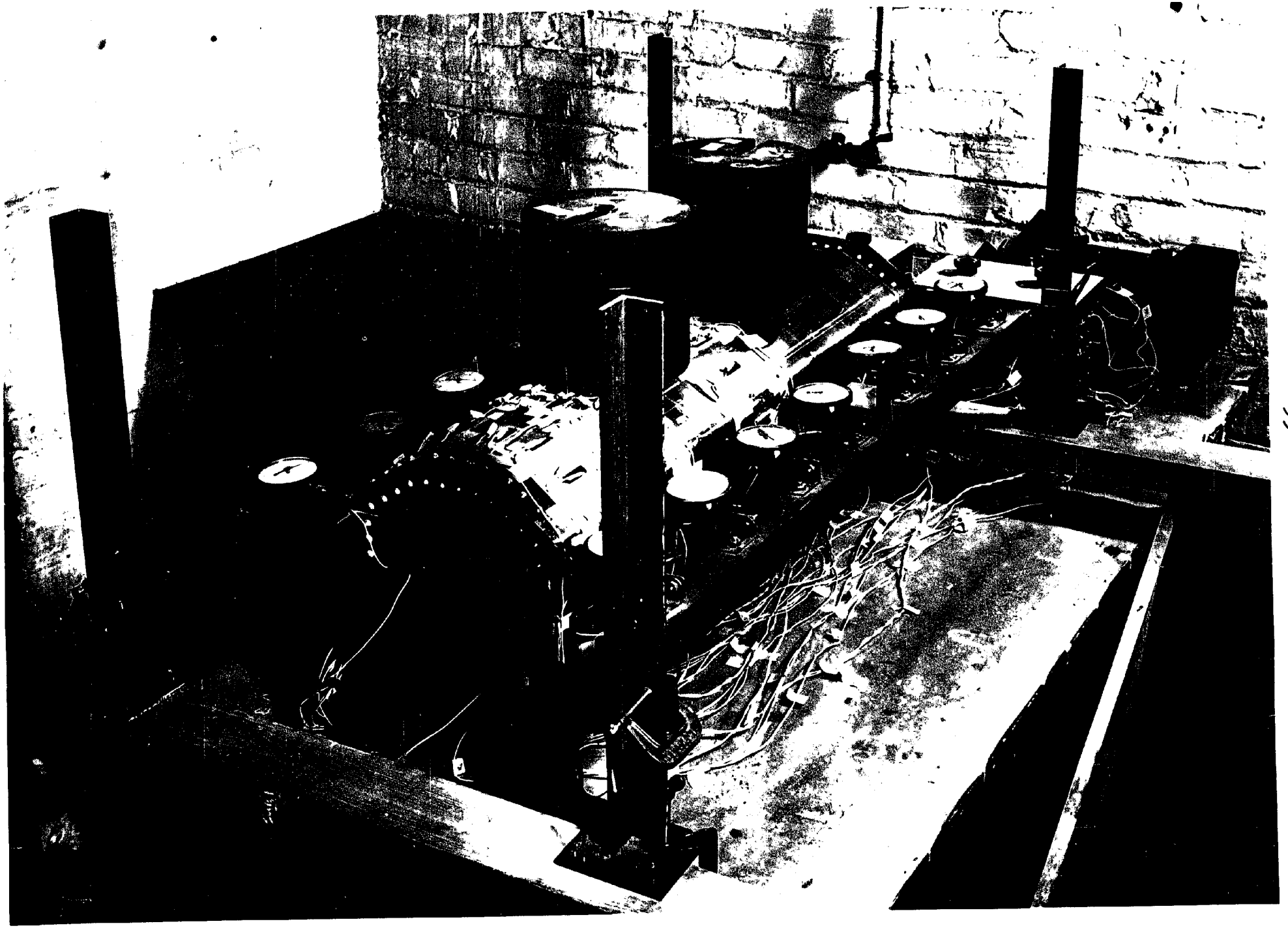

Loading the Model

2. BIBLIOGRAPHY:

(1) G. Ehlers, "Ein neues Konstruktionsprinzip," Bauingenieur, V. 9, 1930, p. 125.

(2) H. Craemer, "Theorie der Faltwerke," Beton und Eisen, V. 29, 1930; p. 276.

(3) E. Gruber, "Berechnung Prismatischer Scheibenwerke," Intern. Assoc. Bridge and Struct. Engg. Memoires, V. 1, 1932, p. 225, (with English summary).

(4) G. Gruening, "Die Nebenspannungen in Prismatischen Faltenwerken," Ingenieur-Archiv. V. 3, No. 4, 1932.

(5) W. Petry, "Scheiben und Schalen im Eisenbetonbau," Intern. Assoc. Bridge and Struct. Engg. 1st Congress, Final Report, p. 209, 1932.

(6) J. Goldenblatt and E. Ratz, "Berechnung von Faltwerken welche aus Scheiben mit verschiedenen statischen Systemen bestehen," Beton und Eisen, V. 33, 1934, p. 369.

(7) E. Gruber, "Die Berechnung pyramidenartiger Scheibenwerke und ihre Anwendug auf Kaminkuehler," Intern. Assoc. Bridge and Struct. Engg. Memoires, V. 2, 1933-34, p. 206, (with English summary).

(8) E. Gruber, "Die Berechnung aeusserlich statisch unbestimmter prismatischer Scheibenwerke," Intern. Assoc. Bridge and Struc. Engg., Memoires,

V. 3, 1935, p. 134, (with English summary).

(9) Ohlig, "Beitrag zur Theorie der prismatischen Faltwerke," Ingenieur-Archiv, V. 6, No. 5, p. 346.

(10) H. Craemer, "Der heutige Stand der Theorie der Scheibentraeger und Faltwerke in Eisenbeton," Beton und Eisen, V. 36, 1937, pp. 264 and 297.

(11) E. Gruber, "Hohltraeger als Faltwerke," Intern. Assoc. Bridge and Struc. Engg., Memoires, V. 7, 1943-44, p. 139.

(12) G. Winter and M. Pei, "Hipped Plate Construction," Journ. of the American Conc. Inst. January 1947.

(13) M. Pei, "Hipped Plate Structures," a doctoral dissertation, Cornell University, 1948.

(14) E. Sheepley, "Approximate Design of Thin Vault Roofs," Civil Engineering and Public Works Review, V. 43, No. 509, Nov. 1948, p.574.

(15) A. J. Ashdown, "Prismatic Thin-slab Structures," Concrete and Constructional Engineering, V. 43, No. 11, Nov. 1948, pp. 347-352, and V. 44, No. 1, Jan. 1949, pp. 3-7.

APPENDIX II

BEAM ACTION THEORY

1. DISTRIBUTION OF EXTERNAL LOADS TO THE ELEMENTS OF A SECTION OF A BEAM:

Consider the forces acting on a small length dx of a beam, which is loaded with a load w per unit of length. The cross-section of the beam may be of any shape as shown in Fig. 6.1, and it is required to determine the amount of the vertical shear force V' acting on a certain portion of the whole cross-sectional area. If V is the vertical shearing force acting on the whole cross-sectional area, then the ratio $\frac{V'}{V}$ will provide a measure for the amount of the external load carried by that certain portion of the section of the beam.

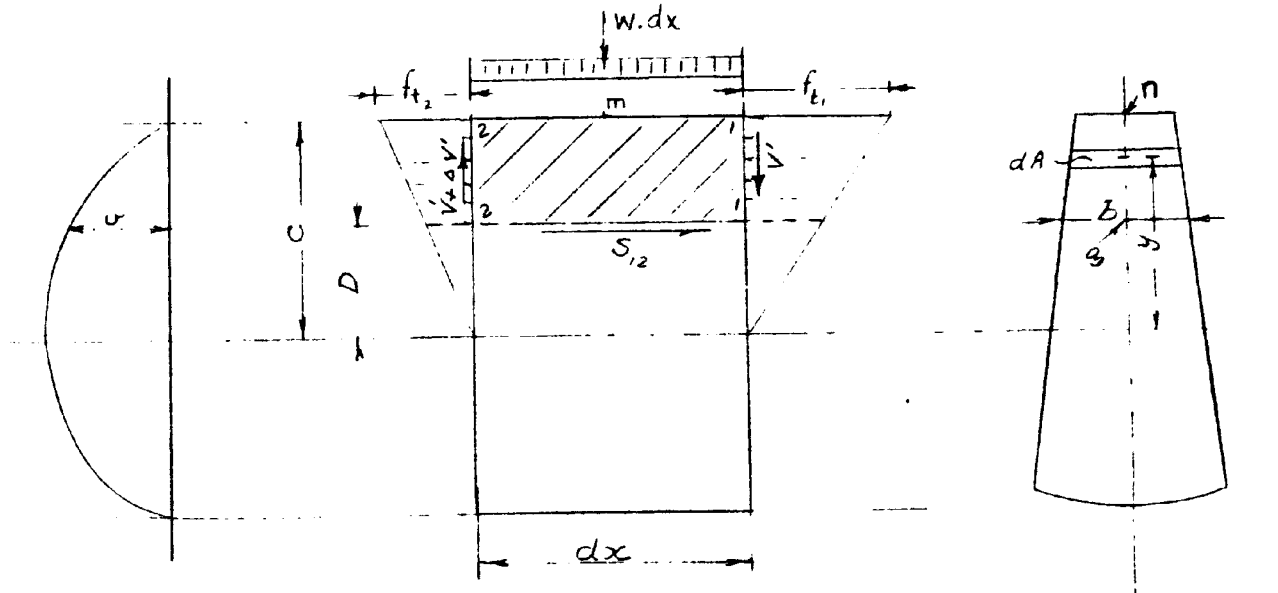

Fig. 6.1

The following notations will be used here:

v = The intensity of the vertical or horizontal shear stress at a point g in the cross-section.

γ = Statical moment of area, about the neutral axis, of the portion of the cross-section beyond the horizontal layer containing the point g.

b = Width of the layer containing the point g.

I = Moment of inertia of the whole cross-section about the neutral axis.

S_{12} = Total horizontal shearing force acting on side 12 on an area equal to b.dx.

Other notations are shown on Fig. 6.1.

Consider the forces acting on the element 1122, and denote the moment of the normal stresses acting on both sides 11 and 22 about point m by λ say.

$$\lambda = \int_g^n (f_1 - f_2)\, dA \,.\, (c - y)$$

$$= (f_{t_1} - f_{t_2}) \cdot \frac{y}{c} \cdot dA \,.\, (c - y)$$

$$= \frac{1}{c} (f_{t_1} - f_{t_2}) \cdot \left[c \int_g^n y.dA - \int_g^n y^2 \,.\, dA \right]$$

put $\quad \frac{1}{c}(f_{t_1} - f_{t_2}) = \frac{M_1 - M_2}{I} = \frac{dM}{I}$

$$\int_g^n y.dA = Q$$

and $\int_g^n y^2.dA = I'$ = moment of inertia of hatched area only about the neutral axis

$$\therefore \lambda = \frac{dM}{I} (c \cdot q - I') \qquad \ldots (1)$$

Taking moment of all the forces acting on the element 1122 about point m, and dropping terms of smaller magnitude, we get:

$$S_{12} \cdot (c - D) - \lambda = V' \cdot dx \qquad \ldots (2)$$

but

$$S_{12} = v \cdot b \cdot dx = \frac{V}{I} \frac{Q}{b} \cdot b \cdot dx$$

$$= \frac{V}{I} q \cdot dx$$

Dividing equation (2) by dx and substituting for the values of λ and S_{12} we get:

$$\frac{V}{I} q(c - D) - \frac{V}{I} (c \cdot q - I') = V'$$

or

$$V' = \frac{V}{I} (I' - qD) \qquad \ldots (3)$$

Equation (3) gives the magnitude of the vertical shearing force V' acting on the cross-sectional area of the element 1122.

2. DISTRIBUTION OF EXTERNAL LOADS TO THE PLATE ELEMENTS OF THE MODEL UNDER THE ASSUMPTION OF BEAM ACTION

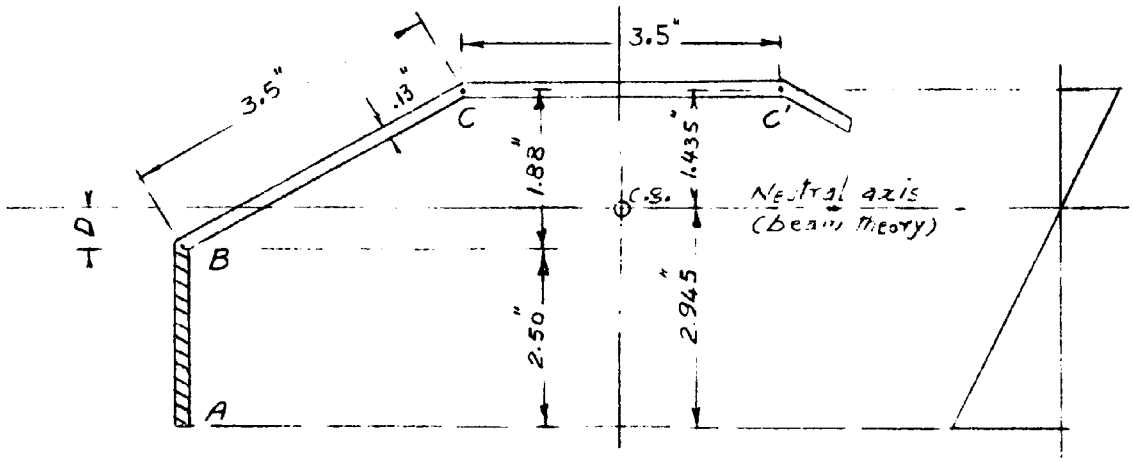

Fig. 6.2

Area of cross-section:

$$= 2 \times .325 + 3 \times .455 = 2.015 \text{ inch}^2$$

Moment of area about CC':

$$= .455 \times 1.88 + .325 \times 3.13 = 2.89 \text{ inch}^3$$

Center of gravity:

$$\bar{y} = \frac{2.89}{2.015} = 1.435 \text{ inch}$$

Moment of inertia:

$$I_{xx} = \left(3.5 \times \frac{.13^3}{12} + .455 \times 1.435^2\right)$$

$$+ 2\left(.242 \times \frac{1.88^3}{12} + .455 \times .495^2\right)$$

$$+ 2\left(.13 \times \frac{2.50^3}{12} + .325 \times 1.695^2\right)$$

$$= 3.637 \text{ inch}^4$$

Portion of vertical load carried by side plates AB and A'B':

Statical moment of hatched area about the neutral axis

$$Q = 2(2.5 \times .130) \times 1.695 = 1.103 \text{ inch}^3$$

Moment of inertia of hatched area about N. axis

$$I' = 2(.13 \times \frac{2.50^3}{12} + .13 \times 2.50 \times 1.695^2)$$

$$= 2.208 \text{ inch}^4$$

$$Q.D = 1.103 \times .445 = .491 \text{ inch}^4$$

Portion V' of shear carried by side plates AB and A'B', from total shear V carried by the whole cross-section

$$V' = \frac{V}{I} (I' - QD) \qquad \ldots (3)$$

$$= \frac{V}{3.637} \times (2.208 - .491)$$

$$V' = 0.472 \text{ V}$$

i.e. under the assumption of beam action, plates AB and A'B' carry o.472 W, where W is the total load on the model.

3. LONGITUDINAL STRESSES AT THE MIDDLE OF THE MODEL ON THE BASIS OF BEAM ACTION:

These stresses are computed for comparison with stresses due to other analytical procedures as shown in Fig. 6 on sheet 6, Appendix I. The total load on model is 233.4 lbs. applied as shown in Figs. 1a and 1b, on sheet 1.

B.M. at middle section of model

$$= \frac{233.4}{2} \times \frac{35}{3} = 1360 \text{ lbs. inch}$$

Moment of inertia of cross section

$$I_{xx} = 3.637 \text{ inch}^4$$

Stresses at edges A, B and C:

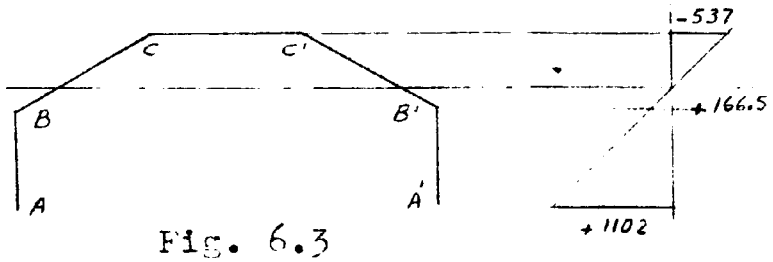

Fig. 6.3

$$f_A = \frac{M}{I} \cdot c = +\frac{1360}{3.637} \times 2.945 = +1102 \text{ p.s.i.}$$

$$f_B = +\frac{1360}{3.637} \times .445 = +166.5 \text{ p.s.i.}$$

$$f_C = \frac{1360}{3.637} \times 1.435 = -537. \text{ p.s.i.}$$

4. SOME RELATIONS BETWEEN FIBER STRESSES AND DEFLECTIONS IN BEAMS:

From the theoretical discussions given in Chapter II, it is evident that the edge forces N acting along the edges of any plate element vary along the span in the same manner as the "free edge" moments due to the P-loads vary. Therefore, if the P-loads acting on a given plate element vary as a sine curve, the corresponding "free edge" bending moments and

edge forces N will vary as a sine curve. Consequently, for this case the longitudinal stresses along the edges of the plate element will vary as a sine curve. Similarly, in the case of a uniform load w over the whole span of the plate element, the "free edge" bending moment, the edge forces N, and the longitudinal stresses along the edges of the plate will vary as a parabola. In general, the longitudinal stresses along the edges of a plate will vary in the same way as the "free edge" bending moment diagram due to the P-loads. The deflection δ at the middle of a plate element in its plane due to the P-loads and the corresponding edge forces N acting on the said plate, will be given here for three kinds of P-loads.

Case 1. P-loads vary as a half wave of a sine curve:

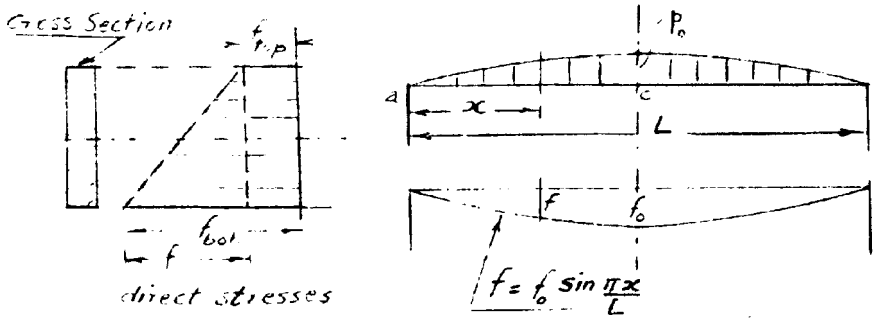

Fig. 6.4

For a simple beam loaded as shown in Fig. 6.4 with a distributed load varying as a half wave of a sine curve, the bending moment and consequently the maximum fiber stresses due to bending will also vary as such.

Deflection at the middle is given by:

$$\delta_o = \int_a^c x \cdot d\phi$$

$$d\phi = \frac{f \cdot dx}{Eh}$$

where f = difference between fiber stresses at top and bottom of any section $x = f_o \sin \frac{\pi x}{L}$

f_o = difference between maximum fiber stresses at middle section.

L = span of each plate element acting as a beam between the end diaphragms.

h = depth of the beam.

$$\therefore \delta_o = \int_a^c \frac{f \cdot dx}{Eh} \cdot x$$

$$\delta_o = \frac{f_o}{Eh} \int_0^{\frac{L}{2}} x \sin \frac{\pi x}{L} \cdot dx$$

$$= \frac{f_o}{Eh} \cdot \frac{L^2}{\pi^2} \left[\sin \frac{\pi x}{L} - \frac{\pi x}{L} \cos \frac{\pi x}{L} \right]_0^{\frac{L}{2}}$$

$$= \frac{f_o}{Eh} \cdot \frac{L^2}{\pi^2} \qquad \ldots (1)$$

Case 2. Uniform P-loads over the whole span:

Maximum fiber stresses vary as a parabola for this case.

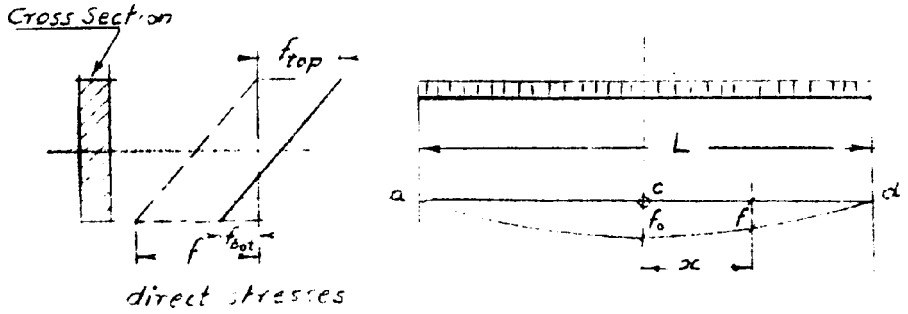

Fig. 6.5

Considering Fig. 6.5 above the difference between the top and bottom fiber stresses at any section is given by

$$f = f_o \left(1 - \frac{4}{L^2} \cdot x^2\right)$$

Deflection at the middle is given by

$$\delta_o = \int_c^d \left(\frac{L}{2} - x\right) d\phi$$

$$d\phi = f \cdot \frac{dx}{Eh}$$

Working out the above integral we get:

$$\delta_o = \frac{f_o}{Eh} \cdot \frac{L^2}{\pi^2} \qquad \ldots\ldots (2)$$

Case 3. Two concentrated loads at one third points of the span:

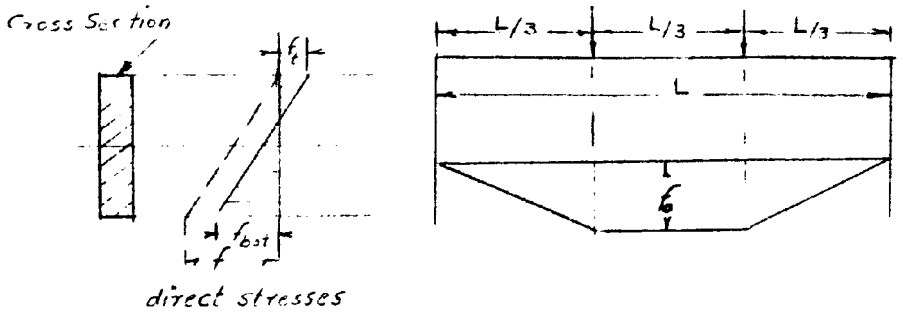

Fig. 6.6

$$\delta_o = \int_a^b x \cdot d\varphi + \int_b^c x \cdot d\varphi$$

$$= \int_0^{\frac{L}{2}} x \cdot \frac{3f_o}{L} \cdot x \cdot \frac{dx}{Eh} + \int_0^{\frac{L}{2}} \frac{x \cdot f_o \, dx}{Eh}$$

$$= \frac{f_o}{Eh} L^2 \cdot \frac{27}{216} \qquad \ldots \quad (3)$$

APPENDIX III

COMPARISON OF THE THEORETICAL AND EXPERIMENTAL STRESSES AND STRAINS IN THE MODEL, WITH THE BASIC EQUATIONS OF EQUILIBRIUM

1. CORRECTION DIAGRAM FOR STRESSES DOES NOT DISTURB THE EQUILIBRIUM CONDITIONS:

The correction diagram for longitudinal stresses, for the effect of joints translation, is shown separately in Fig. 6 on Sheet 6, Appendix I. This diagram represents the necessary correction in the longitudinal stresses, due to the relative translations of the joints, which should be added to the values obtained from the Craemer and Ehlers theory to obtain the longitudinal stresses given by the theory proposed in this thesis. It can be noticed further, that the latter values could be obtained if the values of the correction diagram are multiplied by a proper constant and subtracted algebraically from the values obtained by the ordinary beam theory for the entire cross-section. In fact every one of the above analytical solutions satisfies the equilibrium conditions, and the correction diagram gives only the readjustment in the distribution of the longitudinal stresses as we change from one solution to the other. It should be noticed that the relative translations of the joints change the forces acting on a plate element but do not change the resultant shear

force or bending moment acting on the entire section which are determined by the initial equilibrium conditions. In other words the total resisting moment or the resisting shear force at any section of the entire structure due to the relative translations of the joints is always zero. The correction diagram given on sheet 6 will be checked here for this condition:

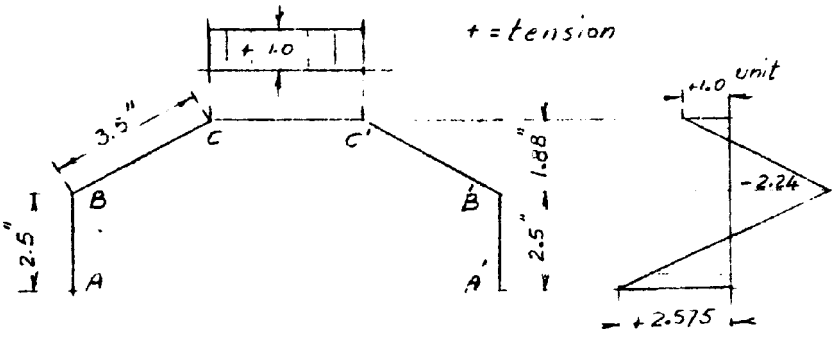

Fig. 7.1. Correction diagram for longitudinal stresses

Area of plate elements:

$$A_{ab} = .13 \times 2.50 = .325 \text{ inch}^2$$

$$A_{bc} = A_{cc'} = .13 \times 3.5 = .455 \text{ inch}^2$$

Summation of longitudinal stresses:

$$\Sigma f.dA = 1.0 \times .455 + 2\left[.455\frac{(1.0-2.24)}{2} + 3.25\frac{(2.575-2.24)}{2} \right]$$

$$= .455 - .564 + .109$$

$$= .564 - .564$$

$$= 0.0$$

Summation of moments about any axis CC', Fig. 7.1:

$$\Sigma M_{cc'} = \frac{1.0}{2} \times .455 \times \frac{1.88}{3} - \frac{2.24}{2} \times .455 \times \frac{1.88}{3} \times 2$$

$$- \frac{2.24}{2} \times .325 \times 2.713 + \frac{2.575}{2} \times .325 \times 3.547$$

$$= 1.62 - 1.62$$

$$= 0.0$$

$\therefore$ correction diagram does not distrub the equilibrum conditions.

2. CHECK OF PROPOSED THEORETICAL STRESS DIAGRAM AT THE MIDDLE OF THE MODEL BY EQUILIBRIUM CONDITIONS

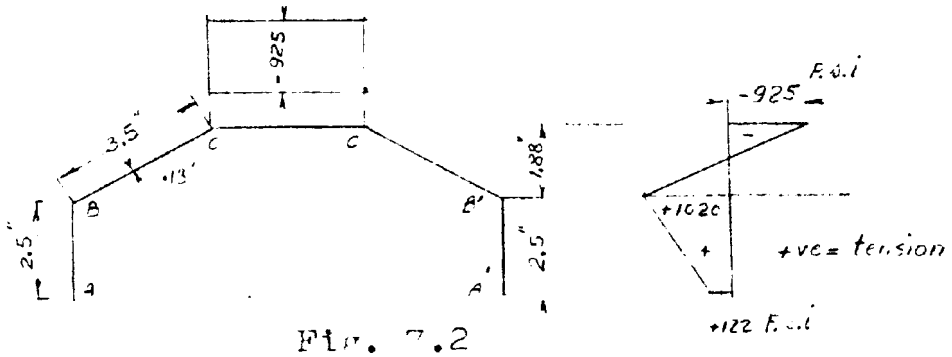

Fig. 7.2

a) Summation of longitudinal stresses:

$$\Sigma f.dA = -925 \times .455 - (925 - 1020) \times .455$$

$$+(1020 + 122) \times .325$$

$$= -421 - 421 + 465 + 332 + 40$$

$$= -842 + 837$$

The difference of $\frac{5}{842} = 0.6\%$ is apparently within the ordinary margin of error encountered in the use of the slide rule.

$\therefore \Sigma f.dA = 0$

b) Summation of moments about any axis CC', Fig. 7.2:

$$\Sigma M_{cc'} = -925 \times .455 \times \frac{1.88}{3} + 1020 \times .455 \times \frac{1.88}{3} \times 2$$

$$+1020 \times .325 \times 2.713 + 122 \times .325 \times 3.547$$

$$= -264 + 582 + 898 + 141$$

$$= +1357 \text{ lbs. inch}$$

External bending moment at middle section

$$= \frac{233.4}{2} \times \frac{35.0}{3} = +1360 \text{ lbs. inch} \qquad \text{o.k.}$$

3. CHECK OF EXPERIMENTAL STRESS DIAGRAM AT THE MIDDLE SECTION OF THE MODEL:

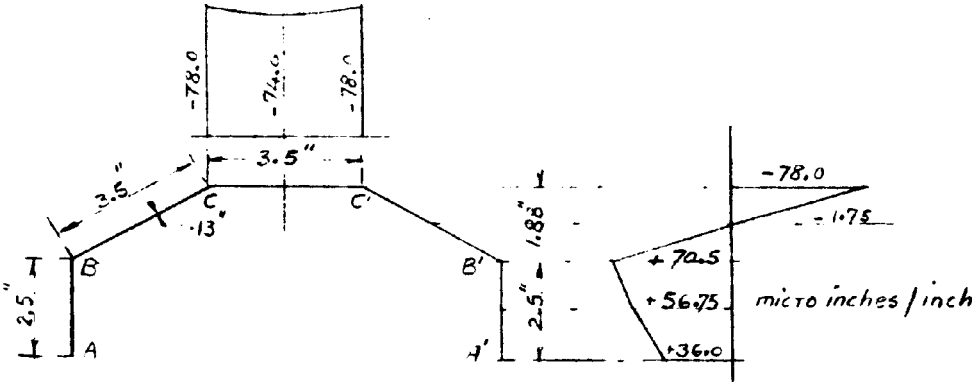

Fig. 7.3 average strain at the middle section

a) Summation of longitudinal stresses:

The unit strains e in micro-inches per inch at the middle section are given in Fig. 2a on sheet 2, Appendix I. The average of the unit strains e on both sides of the middle section are shown in Fig. 7.3 above.

$\Sigma f.dA = E\Sigma e.dA$

where $e = \frac{f}{E}$. (Hook's Law)

approximating the curve joining the measured values of strains by a parabola we get:

$$\begin{aligned}\Sigma e.dA &= -75.33 \times .455 - 78.0 \times .455 \\ &\quad + 70.5 \times .455 + 2/3 \times 2 \times .455 \times 2 \\ &\quad + 70.5 \times .325 + 36.0 \times .325 + 2/3 \times 3.5 \times .325 \times 2 \\ &= -34.25 - 35.50 + 32.10 + 1.213 + 22.92 + 11.70 + 1.516 \\ &= -69.75 + 69.449 \\ &= 0.0 \quad \text{about}\end{aligned}$$

b) Summation of moments about any axis CC', Fig. 7.3:

$\Sigma M_{cc'} = E \cdot \Sigma e \cdot dA \cdot \bar{z}$

where $\bar{z}$ = distance of elemental area from axis CC'.

$$\begin{aligned}\Sigma e \cdot dA \cdot \bar{z} &= -34.25 \times 4.38 - 35.5 \times 3.753 \\ &\quad + 32.10 \times 3.127 + 1.213 \times 3.44 \\ &\quad + 22.92 \times 2/3 \times 2.5 + 11.70 \times \frac{2.5}{3} + 1.516 \times 1.25 \\ &= -283.6 + 154.505 \\ &= 129.095\end{aligned}$$

$\therefore \Sigma M_{cc'} = 129.095 \times E$

$= 129.095 \times 10.5 \times 10^{6} \times \frac{1}{10^{6}}$

$= 1357$ lbs. inch

External Bending Moment

$= 116.7 \times \frac{35}{3}$

$= 1360$ lbs. inch o.k.